National Library of Canada

Acquisitions and Bibliographic Services Branch

395 Wellington Street
Ottawa, Ontario
K1A 0N4

Bibliothèque nationale du Canada

Direction des acquisitions et des services bibliographiques

395, rue Wellington
Ottawa (Ontario)
K1A 0N4

Your file Votre référence

Our file Notre référence

NOTICE

The quality of this microform is heavily dependent upon the quality of the original thesis submitted for microfilming. Every effort has been made to ensure the highest quality of reproduction possible.

If pages are missing, contact the university which granted the degree.

Some pages may have indistinct print especially if the original pages were typed with a poor typewriter ribbon or if the university sent us an inferior photocopy.

Reproduction in full or in part of this microform is governed by the Canadian Copyright Act, R.S.C. 1970, c. C-30, and subsequent amendments.

AVIS

La qualité de cette microforme dépend grandement de la qualité de la thèse soumise au microfilmage. Nous avons tout fait pour assurer une qualité supérieure de reproduction.

S'il manque des pages, veuillez communiquer avec l'université qui a conféré le grade.

La qualité d'impression de certaines pages peut laisser à désirer, surtout si les pages originales ont été dactylographiées à l'aide d'un ruban usé ou si l'université nous a fait parvenir une photocopie de qualité inférieure.

La reproduction, même partielle, de cette microforme est soumise à la Loi canadienne sur le droit d'auteur, SRC 1970, c. C-30, et ses amendements subséquents.

Canada

Study of Bandwidth Efficient DS-CDMA Systems

by

Jun Wang, B.Sci., M.Eng.

A thesis submitted to
the School of Graduate Studies and Research
in partial fulfillment of
the requirements for the degree of

Doctor of Philosophy

Ottawa-Carleton Institute for Electrical Engineering
Faculty of Engineering
Department of Electrical Engineering
University of Ottawa
Ottawa, Ontario, Canada, K1N 6N5

November 12, 1993

ISBN 0-612-07897-3

UNIVERSITÉ D'OTTAWA
UNIVERSITY OF OTTAWA

Dedicated to
my deceased father WANG Zhixing
and
my mother ZHAO Qingrun
for their love

Abstract

This thesis studies the modulation and coding aspects of bandwidth efficient direct-sequence CDMA systems. The novel concepts proposed and investigated are: DS-CDMA employing combined modulation schemes; MFSK/DS-CDMA employing orthogonal codes; and DS-CDMA employing permutation modulation. Under each concept, one or more schemes are developed and examined.

The first concept suggests that two or more modulation schemes can be considered together as a combined modulation in a DS-CDMA system. By combining two modulation schemes, the signal energy per symbol for a given bit energy is increased. This in turn increases the system power efficiency and also the bandwidth efficiency. By combining MFSK and MPSK, we proposed the MFSK-MPSK/DS-CDMA scheme. By combining MFSK and differential MPSK, we proposed the MFSK-DMPSK/DS-CDMA scheme.

The second concept can be thought of as an application of the first. By combining MFSK and the orthogonal PN codes, we proposed the MFSK-OC/DS-CDMA scheme. It is found in this thesis that the orthogonal code concept has many significant applications in both performance improvement and complexity reduction in DS-CDMA systems. An analysis also shows that the ideal orthogonality of the codes can be relaxed with very little performance degradation. Thus, quasi-orthogonal codes can be used in practical applications.

In the third concept, permutation modulation is applied to the DS-CDMA systems and it is proved to be a very powerful scheme in fading channels. By using the multi-tone FSK scheme, we proposed the MT-FSK/DS-CDMA system. In a fading channel, this system introduces an implicit diversity, and thus is robust in mobile environments. The concept of orthogonal codes are used here to reduce the imple-

mentation complexity. By using a simple frequency tone selection rule, we further proposed a novel scheme, nameiy OMT-FSK/DS-CDMA in which all symbols are orthogonal each other.

For the proposed schemes, performance analyses are made over AWGN and fading channels with and without FEC coding. Computer simulation is done for the MFSK-OC/DS-CDMA and MT-FSK/DS-CDMA systems.

Acknowledgements

I would like to thank Dr. Abbas Yongaçoğlu, my thesis supervisor, for his constant support, enthusiastic encouragement, constructive advice and valuable guidance over the whole period of my graduate study. I thank him not only for teaching me the knowledge and problem solving ability, but also for helping me to develop scientific attitude. I would also like to thank him for his many useful suggestions, comments and corrections in the writing of the thesis.

I would like to express my sincere appreciation to Dr. J-Y. Chouinard, Dr. W. Steenaart, Dr. M.S. El-Tanany and Dr. M. Lecours for their many helpful suggestions, critism, and constructive comments.

Finally, I would like to thank the Natural Sciences and Engineering Research Council which provided financial support for most parts of this study under a strategic grant (STR-0100720).

Contents

List of Figures

List of Tables

Acronyms

AO/LSE	Auto-Optimal Least-Sidelobe-Energy
AWGN	Additive White Gaussian Noise
BPF	Band-Pass Filter
BER	Bit Error Rate
BIB	Balanced Incomplete Block design
BPSK (PSK)	Binary Phase Shift Keying
CCD	Charge-Coupled Device
CDMA	Code Division Multiple Access
CDRA	Code Division Random Access
DBPSK (DPSK)	Differential Binary Phase Shift Keying
DMPSK	Differential M-ary Phase Shift Keying
DS	Direct Sequence
DS-CDMA	Direct Sequence CDMA
DS-SS	Direct Sequence SS
FDMA	Frequency Division Multiple Access
FEC	Forward Error Correction
FH	Frequency Hopping
FH-CDMA	Frequency Hopping CDMA
FH-SS	Frequency Hopping SS
FSK	Frequency Shift Keying
FSK-PM	FSK Permutation Modulation
ISI	Inter-Symbol Interference
LOS	Line Of Sight
MAI	Multiple-Access Interference
MF	Matched Filter
MFSK	M-ary Frequency Shift Keying
MFSK/DS-CDMA	DS-CDMA employing M-ary Frequency Shift Keying
MFSK-DMPSK/DS-CDMA	DS-CDMA employing combined MFSK and DMPSK
MFSK-MPSK/DS-CDMA	DS-CDMA employing combined MFSK and MPSK
MFSK-OC/DS-CDMA	MFSK/DS-CDMA employing Orthogonal Codes
MPSK	M-ary Phase Shift Keying
MSDD	Multiple Symbol Differential Detection

Nomenclature

α	Roll-off factor for the raised cosine filter
β_d	The number of paths having a Hamming distance d in a convolutional scheme
γ_b, $\frac{E_b}{N_0}$	Bit energy to noise spectral density ratio
γ_b', $\frac{E_b}{N_0'}$	Bit energy to effective noise (including MAI) spectral density ratio
$\bar{\gamma}_b$	Average bit energy to noise spectral density ratio
$\bar{\gamma}_b'$	Average bit energy to effective noise (including MAI) spectral density ratio
γ_{bm}	Equivalent bit energy to MAI ratio
γ_s, $\frac{E_s}{N_0}$	Signal energy per symbol to noise spectral density ratio
γ_s', $\frac{E_s}{N_0'}$	The effective symbol energy to noise spectral density (including MAI) ratio
$\bar{\gamma}_s$	The average symbol energy to noise spectral density ratio
$\bar{\gamma}_s'$	The effective average symbol energy to noise spectral density (including MAI) ratio
γ_{sm}	The equivalent symbol energy to the MAI ratio
$\delta(\cdot,\cdot)$	Kronecker function
Δ	The half of the frequency separation between adjacent frequency tones
ζ	A noise component in simulation for MFSK-OC/DS-CDMA
η	Bandwidth efficiency in b/s/Hz
η_∞	The asymptotic bandwidth efficiency in b/s/Hz
η_{nor}	Normalized bandwidth efficiency (η/η_∞)
θ	The phase introduced by modulator or channel
θ_k	The phase of the kth user introduced by modulator or channel
κ	Rician parameter (K-factor)
λ	The number of symbols containing a distinct pair of tones (in MT-FSK); cross-correlation coeficient
λ_{m_c}	Cross-correlation coeficient
μ	Chip waveform coefficient
ρ	Fading random variable
σ^2, σ_i^2	Variances of random variables; also used as parameters

MSK	Minimum Shift Keying
MSK/DS-CDMA	DS-CDMA employing Minimum Shift Keying
MT-FSK	Multiple Tone FSK
MT-FSK/DS-CDMA	DS-CDMA employing MT-FSK modulation
OMT-FSK	Orthogonal Multiple Tone FSK
OMT-FSK/DS-CDMA	DS-CDMA employing OMT-FSK modulation
PCN	Personal Communication Networks
PM	Permutation Modulation
PN	Pseudo Noise
PSK/DS-CDMA	DS-CDMA employing Phase Shift Keying
QAM	Quadrature Amplitude Modulation
QPSK	Quaternary Phase Shift Keying
RS	Reed-Solomon codes
SAW	Surface Acoustic Wave
SNR	Signal to Noise Ratio
SS	Spread Spectrum
SSMA	Spread Spectrum Multiple Access
TDMA	Time Division Multiple Access
UHF	Ultra-High Frequency
VHF	Very-High Frequency

τ_k	Channel time delay for the kth user signal
ϕ_i	Signal phase
$\Psi(t)$, $\psi(t)$	Chip waveform shaping pulses
a_i^k	The ith chip value of PN sequence signal for the kth user
$a_k(t)$	PN sequence signal for the kth user
b	The total number of distinct symbols (in MT-FSK)
b_j^k	The kth user data at jth timing interval
$b_j^{k,f}$	The jth value of the frequency tone signal for the kth user
$b_j^{k,p}$	The jth value of the phase signal for the kth user
$b_k(t)$	Binary data signal to be transmitted from the kth user
$\hat{b}_k(t)$	Estimated data at the receiver for the kth user
$b_{k,f}(t)$	MFSK modulator input signal for the kth user used in MFSK-MPSK/DS-CDMA and MFSK-OC/DS-CDMA
$b_{k,p}(t)$	MPSK modulator input signal for the kth user used in MFSK-MPSK/DS-CDMA
c	Number of orthogonal codes used in MT-FSK for complexity reduction
$D_{i,j}$	Desired signal component
d_i^k	The ith value of the nonbinary signal for the kth user in MFSK-OC/DS-CDMA
$d_k(t)$	Nonbinary data signal for the kth user in MFSK-OC/DS-CDMA
E_b	Bit energy
E_c	Chip energy
E_s	Symbol energy
f_c	Carrier frequency
${}_1F_1(\cdot,\cdot;\cdot)$	Confluent hypergeometric function
G_i	$= I_i + \zeta$ in simulation for MFSK-OC/DS-CDMA
I_i	MAI component in simulation for MFSK-OC/DS-CDMA
I_k	The MAI component for the kth user
$I_n(\cdot)$	The Bessel function of nth order of first kind
k	The number of bits per symbol; information digits in block coding
K	The total number of simultaneous users
M	The total number of symbols in an M-ary modulation scheme
M_c	The number of orthogonal codes used in MFSK-OC/DS-CDMA
M_f	The number of frequency tones used in MFSK-MPSK/DS-CDMA and MFSK-OC/DS-CDMA
M_p	The number of phases used in MFSK-MPSK/DS-CDMA
n	Code length in block coding
$n(t)$	Thermal noise signal
N	PN sequence length
N_0	One-sided thermal noise power spectral density
$N_{i,j}$	Noise power spectral densities
N_0'	Total noise power spectral density (including MAI)

$p(\cdot)$	Probability density function
P_2	Pairwise probability of error
P	Transmission power
$p_\tau(t)$	A pulse signal with unity amplitude and duration τ
P_b	Probability of bit error
P_C	Probability of correct decision
P_{Cf}	Probability of correct decision for MFSK
P_{Cp}	Probability of correct decision for MPSK
P_f	The symbol error rate for MFSK part in MFSK-PSK/DS-CDMA
P_M	Probability of symbol error for nonbinary systems
P_p	The symbol error rate for MPSK part in MFSK-PSK/DS-CDMA
P_s	Probability of symbol error
P_T	Total noise power
$Q(\cdot)$	Q-function
$Q(\cdot,\cdot)$	The generalized Q-function
r	The number of symbols containing a distinct tone (in MT-FSK)
$r(t)$	The received signal
R_b	Information bit rate
R_c	Chip rate
$r_k(t)$	The received signal for the kth user
r_c	FEC code rate
R_s	Symbol rate
s	A parameter representing the constant component in a Rician distribution
$s_k(t)$	Transmitted signal for the kth user
S_i	Signal component in simulation for MFSK-OC/DS-CDMA
t	Time variable; error correcting ability in RS codes
T_b	Bit duration ($= 1/R_b$)
T_c	Chip duration ($= 1/R_c$)
T_s	Symbol duration ($= 1/R_s$)
U, U_i, $U_{i,j}$	Decision variables
$u_k(t)$	Baseband transmitted signal for the kth user
v	The total number of frequency tones (in MT-FSK)
v_c	The total number of frequency tones (in MT-FSK) when c codes are used
$v_k(t)$	Received baseband signal of the fading output for the kth user
W	Total signal bandwidth
w	The number of tones selected for a symbol (in MT-FSK)
$w_k(t)$	The received baseband signal for the kth user
$y(t)$	Channel output signal (in the absence of noise)

Chapter 1

Introduction

1.1 Motivation

Developing more efficient modulation/multiple access systems is a very active research area in mobile communications fields, namely mobile satellite communication [1-3], digital cellular radio [4-8], and personal communication networks (PCN)[1] [9-13].

In digital communications systems, there are three basic multiple access schemes: frequency division multiple access (FDMA), time division multiple access (TDMA), and code division multiple access (CDMA). One of the key issues in selecting the multiple access schemes is the system capacity they can offer. In various studies, the capacities of FDMA, TDMA and CDMA systems have been compared. CDMA is mutual interference limited [14]. By properly controlling the mutual interference, the capacity of a CDMA system can be increased. For digital voice communication applications, it is shown that by taking advantage of voice activity factor and sectorization in a frequency reuse system, CDMA can offer greater capacity than FDMA and TDMA [2, 5, 13]. CDMA is an application of spread spectrum techniques, and is also called spread spectrum multiple access (SSMA). It is well known that spread spectrum (SS) signals can mitigate the multipath effects, and thus, make CDMA more robust in the mobile radio environment.

In the mobile communication field, especially in VHF/UHF band applications,

[1]PCN "is suitable for the wide-spread low-power tetherless access needed to support small shirt-pocket personal communications. In contrast, cellular radio is well suited to providing the vehicular communications functions" [10].

the available bandwidth is still very limited [15, 16]. Thus, how to use the bandwidth more efficiently is a big challenge for mobile communications. The system bandwidth efficiency can be enhanced by employing different techniques. From a network point of view, efficient CDMA protocols achieve large throughput, and thus, increase the system capacity [17, 18, 19]. Another way of improving CDMA capacity is to design efficient modulation/coding schemes which are suitable for CDMA applications. In this thesis, we are trying to explore this second possibility.

A large number of modulation techniques have been investigated for use in direct sequence (DS) CDMA applications. The two popular techniques are PSK and MFSK. The resultant CDMA systems are PSK/DS-CDMA and MFSK/DS-CDMA respectively. We have focused on MFSK because it is a very power efficient modulation scheme for large M. When M is very large, the Shannon limit of -1.6 dB for errorless transmission is approached [20, 21]. The disadvantage of MFSK is that it is not bandwidth efficient. This is a disadvantage when a single user at a time utilizes the channel. When many users utilize the channel simultaneously, as is the case in CDMA systems, then the bandwidth efficiency should be considered in terms of b/s/Hz. Therefore, in an SS system, minimizing the bandwidth is of no concern since one intends to spread the bandwidth anyway. By combining the advantages of MFSK modulation scheme and SS technique, we may obtain more power efficient CDMA systems.

In an SS system, the system bandwidth is largely spread and the bandwidth efficiency is low. In a CDMA system, the bandwidth efficiency is defined as the information bit rate divided by the total bandwidth and multiplied by the total number of simultaneous users, as will be discussed in more detail in Section 2.2. It is well known that the bandwidth efficiency and power efficiency in a DS-CDMA system are closely related. This argument will be addressed many times in this thesis. Thus, a powerful DS-CDMA system always implies a bandwidth efficient system.

In this thesis, we propose three DS-CDMA systems. All the systems use MFSK as a baseline modulation scheme. In each of the proposed systems, some new concepts have been introduced to add to the existing systems. System performance is analyzed and compared with the existing systems. For the system evaluation criteria, this thesis

is mainly concerned with the bit error rate (BER) and the bandwidth efficiency. In DS-CDMA systems, these two performances are closely related. So our focus is to find power efficient schemes. Since all the proposed systems employ nonbinary modulation schemes, nonbinary FEC coding is correspondingly considered.

1.2 Contributions of This Thesis

The objective of this thesis is to define and examine bandwidth efficient DS-CDMA systems. Based on the study of existing DS-CDMA systems, we propose three new DS-CDMA systems. With the introduction of the new concepts, system bandwidth efficiency is improved with respect to the existing DS-CDMA systems which mainly refer to the PSK/DS-CDMA and the MFSK/DS-CDMA. In conventional DS-CDMA systems, only a few modulation schemes are considered. With the new schemes presented in this thesis, more options are provided for the development of efficient CDMA techniques.

The three proposed systems are:

(1) DS-CDMA employing combined modulation schemes;

(2) MFSK/DS-CDMA employing orthogonal codes;

(3) DS-CDMA employing permutation modulation.

To summarize, this thesis makes the following contributions:

(1) The concept of DS-CDMA employing combined modulation schemes is proposed. In conventional DS-CDMA systems, such as PSK/DS-CDMA and MFSK/DS-CDMA, a single modulation scheme is employed. By combining two or more modulation schemes, for a given bit energy the resultant symbol energy is increased, and thus, a better symbol error rate performance can be achieved. For the combined modulation scheme, the symbol error rate is determined by the least powerful individual modulation scheme. So a proper selection of modulation combination is essential

for power efficiency. In a DS-CDMA system, unlike in a narrowband system, the bandwidth efficiency is closely related to its power efficiency. In fact, the asymptotic bandwidth efficiency is inversely proportional to the required SNR per bit for a specified BER. Thus, the application of the combined modulation concept may result in a bandwidth efficient DS-CDMA system. By combining the MFSK and MPSK modulation schemes, we propose a novel system, namely MFSK-MPSK/DS-CDMA. This system is analyzed over an AWGN channel. Results show that it achieves a better performance than BPSK/DS-CDMA and MFSK/DS-CDMA. (Chapter 3)

(2) Due to implementation considerations, a combination of MFSK and differential MPSK is more feasible than the combination of MFSK and coherent MPSK in a practical situation. So we further propose the MFSK-DMPSK/DS-CDMA scheme. Its performance over AWGN and fading channels is analyzed. An algorithm is described for the implementation of MFSK-DBPSK/DS-CDMA. It is shown that better BER performance and higher bandwidth efficiency are obtained in comparison to DPSK/DS-CDMA and MFSK/DS-CDMA. In addition, FEC coding is considered for the proposed DS-CDMA system. (Chapter 3)

(3) An MFSK/DS-CDMA system employing orthogonal codes (OC) is proposed. This scheme can be thought of as an application of the combined modulation concept. By combining the MFSK and the orthogonal code modulation, we proposed the MFSK-OC/DS-CDMA scheme. The performance of the system over AWGN and fading channels is analyzed. The orthogonal code can be equivalent to a frequency tone. Thus, the number of frequency tones can be reduced by using orthogonal codes. Moreover, nonbinary FEC coding is considered for the scheme. It is also found in this thesis that the orthogonal code concept has many significant applications in both performance improvement and complexity reduction in a DS-CDMA system. (Chapter 4)

(4) An analysis shows that the restriction of ideal orthogonality of the codes can be partially removed, and thus, some quasi-orthogonal codes can be used in practical applications. This extends the application of the orthogonal code concept. (Chapter 4)

(5) Monte Carlo simulation is done to assist the theoretical analysis. We design a simple simulation structure for the MFSK-OC/DS-CDMA scheme. (Chapter 5)

(6) The concept of permutation modulation is used for a DS-CDMA system. By using the MT-FSK scheme, we propose the MT-FSK/DS-CDMA scheme. In a fading channel, this system introduces implicit diversity, and thus, is robust in mobile environments. The system performance is evaluated over AWGN and fading channels. Particularly, an analysis for the BER performance over a Rician fading channel is presented. FEC coding is also considered. Computer simulation for the MT-FSK/DS-CDMA system is performed. (Chapter 6)

(7) By using a simple frequency tone selection rule, we further propose a novel permutation modulation scheme, namely orthogonal MT-FSK (OMT-FSK). The corresponding DS-CDMA system is OMT-FSK/DS-CDMA. This system is analyzed over AWGN and fading channels. Compared to the MT-FSK/DS-CDMA, its performance is degraded a little in an AWGN channel but improved a lot in a fading channel. Thus, it is feasible in a mobile environment. (Chapter 6)

(8) With the introduction of orthogonal codes to the MT-FSK/DS-CDMA system, implementation complexity can be greatly reduced. The total number of frequency tones decreases as orthogonal codes are used. The reduction in size of the total number of frequency tones is derived and a complexity comparison is performed. (Chapter 6)

1.3 Organization of This Thesis

In this Chapter 1, the motivation and contributions of this thesis have been discussed. The remainder of this thesis is organized as follows.

Chapter 2 presents the research background and literature survey. The CDMA technology is reviewed in Section 2.1. The issue of bandwidth efficiency is discussed in Section 2.2. A general system model is described in Section 2.3.

In Chapter 3, DS-CDMA employing combined modulation is studied. Analyses are performed to obtain the bit error rate performance and the bandwidth efficiency in an AWGN channel. Section 3.1 introduces the background of this system concept. Section 3.2 describes the system model. Section 3.3 obtains the system performance over an AWGN channel and discusses numerical results. Section 3.4 examines the relationship between the effective SNR and the multiple-access interference (MAI). Section 3.5 modifies the system by considering differential detection instead of coherent detection of PSK signals. Section 3.6 discusses the effects of FEC coding. Section 3.7 summarizes the findings of this chapter.

Chapter 4 studies the MFSK/DS-CDMA systems using orthogonal codes. Section 4.1 introduces the idea. Section 4.2 describes the system model. Section 4.3 analyzes the system performance over an AWGN channel. A simple analysis and a detailed derivation are presented. Both methods use a Gaussian approximation for the MAI. The case when the PN codes are not ideally orthogonal is also studied. Calculation results are presented. Section 4.4 analyzes the system performance over fading channels. Two types of fading, namely, Rayleigh fading and Rician fading are considered. Section 4.5 discusses the FEC coded case. Section 4.6 gives the summary of the chapter.

Chapter 5 discusses a computer simulation approach for the MFSK-OC/DS-CDMA system analysis. In Section 5.1, the simulation question is overviewed. In Section 5.2, a simulation model is described. In Section 5.3, simulation results are presented and discussed. A summary is given in Section 5.4.

Chapter 6 studies the DS-CDMA system employing permutation modulation. In Section 6.1, the concept of permutation modulation is reviewed. In Section 6.2,

two permutation modulation schemes are described. In Section 6.3, a model for the DS-CDMA system using permutation modulation is described. In Section 6.4, performance analysis is carried out. In Section 6.5, a proposed scheme named as orthogonal multi-tone permutation modulation is analyzed. In Section 6.6 orthogonal codes are considered to reduce the system complexity. FEC coding is considered in Section 6.7. In Section 6.8, a Monte Carlo simulation of an MT-FSK scheme is described. Section 6.9 gives the summary of our findings on DS-CDMA systems with permutation modulation.

Chapter 7 presents the conclusions of this thesis and suggests further studies in the related field.

In this thesis, some detailed derivations for equations are put in Appendices. In Appendix A, derivations for the BER expressions of DPSK and MFSK over a frequency non-selective slow Rician fading channel are given. In Appendix B, two Gaussian approximations for the MAI are described and compared. In Appendix C, a derivation for the variance of the MAI component is given. In Appendix D, an alternative analysis method for MFSK/DS-CDMA systems is presented and compared with the one used in the Chapter 4. Appendix E gives the probability of error of nonbinary codes for orthogonal nonbinary modulation schemes over fading channels. In Appendix F, the balanced incomplete block (BIB) design for the MT-FSK scheme is described briefly. In Appendix G, the derivation for the probability of error of MT-FSK over a Rician fading channel is presented.

Chapter 2

Background and Literature Survey

2.1 Overview of CDMA Technology

2.1.1 Spread Spectrum Techniques

CDMA being an application of SS techniques, we first briefly review these techniques. There are two basic SS techniques. The first one is termed as direct sequence (DS). In a DS-SS system, the baseband signal is spread by a DS pseudo-noise (PN) sequence in the transmitter. The PN sequence is also called PN code. It usually has a much higher rate than the symbol rate. The resultant system bandwidth is much higher than the symbol bandwidth. In the receiver, the same PN sequence is used to despread the received signal as a reference[1]. The ratio of the PN code rate to the symbol rate is defined as the processing gain, as well as the spreading factor. If each data symbol contains a PN sequence of length N, the processing gain equals N.

Another SS technique is called frequency hopping (FH). In a FH-SS system, the signal carrier frequency hops periodically to different frequency cells according to a PN sequence pattern. In contrast to the DS system, where the spreading code is used one bit at a time, the spreading code here is used k bits at a time to choose one of the 2^k frequency tones. In the receiver, the hopped signal is dehopped by the same PN code. The processing gain is equal to the number of hopping points (2^k). Each of the two techniques, DS and FH, has strong and weak points. For example, a DS-SS

[1]Despreading a DS-SS signal without knowledge of the PN sequence (known as blind despreading) can be accomplished [22]. This technique is, however, not applicable to a CDMA system.

system is generally simpler than an FH-SS system, while an FH-SS system is more robust than a DS-SS system against near-far effects. Selection of one over the other is dependent only on the requirements and the particularities of a given application. In this thesis, only DS-SS scheme is considered.

The early development of SS techniques was due to military applications, in which various intentional interference (jamming) needed to be countered. Many works in the literature have contributed to the design and analyses of SS systems for various in-band interferences over various channels [23]. Since the late 70s, more and more efforts have been made for the commercial use of SS techniques. In recent years, SS techniques have been widely considered for cellular radio, mobile satellite communications and personal communications networks. It is interesting to note that the original purpose of employing SS techniques was to obtain a better system performance in a jamming environment with a sacrifice of bandwidth, while the current motivation for considering SS techniques is to achieve a larger bandwidth efficiency.

For the SS system design, an important parameter is the processing gain. The processing gain is obtained via the correlator (matched filter) in the receiver, where the signal energy is accumulated and the interference is spread. Thus, SS systems are effective against narrowband and pulse jamming. For wideband interference, e.g., an additive white Gaussian noise (AWGN), however, the processing gain cannot be obtained. In a multiple-access application, the unintended transmission is called multiple access interference (MAI). In the SS receiver, the MAI remains spread, and only the intended signal is despread. Thus, the processing gain provides a multiple-access capability which makes CDMA applicable. In a frequency selective multipath channel, if the time delay of the multipath signal is more than a chip interval, the multipath signal will be reduced to an equivalent amount of wideband noise (well approximated by a white Gaussian noise). If the time delay of the multipath signal is less than a chip interval, as in a frequency nonselective multipath channel, the multipath signal will be partially mitigated according to the auto-correlation of the PN sequence. In a narrowband system, the delay spread due to multipath causes inter-symbol interference (ISI). In an SS system, strictly speaking, the ISI still exists. However, it will be much reduced due to the processing gain. Thus, no equalizer

is required in the CDMA system [4]. Moreover, a Rake diversity receiver can be employed to further accumulate the diffused energy in a frequency selective multipath channel [24, 25]. This is the advantage of using SS techniques over fading channels. Another advantage of SS techniques is the convenience of employing FEC coding. The system does not need a further increase in bandwidth to accommodate coding. There is no effective processing gain loss due to coding [26].

A DS-SS system can be identified by its bit modulation scheme and its chip modulation scheme. Various bit modulation schemes can be used, e.g., BPSK, QPSK and MSK. The PSK/DS-SS scheme is popular in practical systems. In this scheme, the binary bit sequence is multiplied by a higher chip rate PN sequence, and the chip modulation is also PSK. The bit sequence can be transmitted directly (coherent PSK/DS-SS system) or differentially coded (DPSK/DS-SS system). An alternative chip modulation scheme is binary FSK in which the chip chooses one of two frequency tones. However, this chip modulation scheme does not yield optimal jamming performance. Another DS-SS scheme is MFSK/DS-SS [27, 28] in which the data sequence is MFSK modulated. Each of the M frequency tones is spread by a PN sequence. The chip modulation is PSK. Since the bit modulation (MFSK) is usually noncoherent, the PSK spreading signal is despread and the envelope detected in the receiver. This scheme is used as a baseline scheme in this thesis.

In the SS receiver, the key component is the PN matched filter. It can be implemented using a digital circuit, a surface acoustic wave (SAW) device or a charge-coupled device (CCD). Due to the rapid development of integrated circuit technology, higher spreading factor, small size and low-cost implementation become possible [29].

2.1.2 CDMA Systems

In a CDMA system, several users transmit signals simultaneously within the same channel. Each user is identified by a distinct signature sequence. The signature sequence is usually a PN sequence as in an SS system. Corresponding to the two basic spread spectrum techniques, there are DS-CDMA, FH-CDMA and hybrid CDMA systems. We give a brief review for the DS-CDMA systems.

There are two types of DS-CDMA systems, i.e., sequence synchronous and se-

quence asynchronous. In a sequence synchronous system, all the users transmit with their sequence period time-aligned. This condition is difficult to maintain in most applications, particularly in a mobile environment. In a sequence asynchronous system no attempt is made to align the sequence period. This type of DS-CDMA is assumed in this thesis. Depending on the different bit modulation schemes employed, the DS-CDMA systems can be classified as BPSK/DS-CDMA, QPSK/DS-CDMA, MSK/DS-CDMA, MFSK/DS-CDMA, and etc.

In CDMA systems, in comparison to FDMA and TDMA systems, the MAI is present in addition to AWGN and fading. For the performance analysis of DS-CDMA systems, much effort has been spent in the evaluation of the MAI. In [41], Pursley obtained a BER expression using a Gaussian approximation for asynchronous BPSK/DS-CDMA systems with random signature sequences over an AWGN channel. In terms of the effective bit energy to the noise spectral density ratio γ_b', the BER expression for BPSK/DS-CDMA can be written as [41]

$$P_b = Q\left(\sqrt{2\gamma_b'}\right) \tag{2.1}$$

where the Q-function is defined as

$$Q(x) = \frac{1}{\sqrt{2\pi}} \int_x^\infty \exp(-\frac{x^2}{2}) \mathrm{d}x, \tag{2.2}$$

and γ_b' is simply approximated by

$$\gamma_b' = \left[(\gamma_b)^{-1} + \left(\frac{3N}{2(K-1)} \right)^{-1} \right]^{-1}. \tag{2.3}$$

In the above equation, K is the total number of simultaneous users, N is the PN sequence length, and $\gamma_b = E_b/N_0$ is the bit energy to noise spectral density ratio. This expression gives a convenient evaluation method for the BER performance of BPSK/DS-CDMA systems over AWGN channels. In [42], Viterbi gave a similar result using a simple argument. The exact evaluation of the MAI is very difficult. Some approximate BER performance analyses have been proposed. The characteristic-function method was used in [33]. This method was further employed to analyze DS-CDMA systems over fading channels [31] and binary/quaternary DS/CDMA systems

with random signature sequences [34]. The amount of calculations needed for this method is proportional to KN^2, which is not suitable for large K and N. For non-coherent detection, because of the nonlinearity, the characteristic-function method is not applicable. The method of moments was used in [35, 36, 37] to analyze a PSK/DS-CDMA systems. The disadvantage of these approaches is that the computational complexity is exponentially dependent on the number of system users K. Techniques employing upper and lower bounds on the BER have also been discussed in [38, 39, 40].

The Gaussian approximation is very attractive for its simplicity. Unfortunately, that approximation is not generally accurate enough. In [43, 44], it was shown that the Gaussian approximation agrees with the exact result for a large number of simultaneous users (say $K > 10$), conforming with the central limit theorem, but gives optimistic results when K is small. An improved Gaussian approximation with good accuracy was presented in [43]. Based on [43], a further simplified expression was derived in [45]. This expression is

$$\begin{aligned} P_b \simeq \; & \tfrac{2}{3}Q\left[\left(\tfrac{K-1}{3N}+\tfrac{N_0}{2E_b}\right)^{-1/2}\right]+\tfrac{1}{6}Q\left[\left(\tfrac{(K-1)(N/3)+\sqrt{3}\sigma}{N^2}+\tfrac{N_0}{2E_b}\right)^{-1/2}\right] \\ & +\tfrac{1}{6}Q\left[\left(\tfrac{(K-1)(N/3)-\sqrt{3}\sigma}{N^2}+\tfrac{N_0}{2E_b}\right)^{-1/2}\right], \end{aligned} \tag{2.4}$$

where

$$\sigma^2=(K-1)\left[N^2\frac{23}{360}+N\left(\frac{1}{20}+\frac{K-2}{36}\right)-\frac{1}{20}-\frac{K-2}{36}\right]. \tag{2.5}$$

The BER expression given above is for a coherent BPSK/DS-CDMA system over an AWGN channel. However, it will be shown later that the result can be used in the analysis of other DS-CDMA systems.

In addition to the binary PSK/DS-CDMA system, the QPSK/DS-CDMA system is also widely studied. In [53], a general form of the DS-SS signal is expressed in terms of data waveform and chip spreading. Consequently, four different signals result, namely, biphase spread/BPSK data, quadriphase spread/BPSK data, biphase spread/QPSK data, and quadriphase spread/QPSK data. It is shown that quadriphase chip spreading provides a 2-3 dB better performance than binary chip spreading against tone jamming. In the presence of AWGN and the MAI, however,

the theoretical performance remains the same. In [54], the two quadriphase chip spreading signals with BPSK and QPSK data are called balanced and dual-channel QPSK SS signals respectively. In [34], the performance of QPSK/DS-CDMA over AWGN channel with random signature sequences is shown to have the same Gaussian approximation as PSK/DS-CDMA has in (2.3). In the case of QPSK/DS-CDMA, the parameter N in (2.3) should be the ratio of chip rate over bit rate. To keep the same system bandwidth and bit rate, the PN sequence length in QPSK/DS-CDMA is twice as that in PSK/DS-CDMA.

Another well known system is MSK/DS-CDMA. The smooth phase transitions of MSK signal yields desirable spectral characteristics. The MSK/DS-CDMA can be realized as a special form of QPSK/DS-CDMA [33]. In [55], the BER performance of MSK/DS-CDMA over an AWGN channel with random signature sequences is again Gaussian approximated. In (2.3), the term $\frac{3N}{2(K-1)}$ acts as the equivalent bit energy to MAI ratio. For convenience, we denote this term as γ_{bm}. For the MSK/DS-CDMA scheme [55], $\gamma_{bm} = 6\pi^2 N/[(15+2\pi^2)(K-1)] \simeq 1.7N/(K-1)$, which is a little greater than that in PSK/DS-CDMA. However, γ_{bm} is related to the chip waveform. For convenience, we rewrite it as $\gamma_{bm} = \mu\frac{N}{K-1}$, where μ is related to the chip waveform. For a rectangular chip waveform, we have $\mu = 2/3$. Since a sine chip waveform is assumed in [55], thus $\mu = 6\pi^2/(15+2\pi^2)$. If a sine chip waveform is used for the PSK/DS-CDMA or QPSK/DS-CDMA, the same result will be obtained.

The binary and quaternary PSK/DS-CDMA systems have been extensively analyzed in the literature. In contrast, there are limited papers about the MFSK/DS-CDMA scheme. Geraniotis analyzed the MFSK/DS-CDMA over AWGN and specular multipath fading channels [30, 28]. In [32], Ha analyzed sequence asynchronous MFSK/DS-CDMA by considering an overlay of the adjacent tone symbols. It was shown in [30] that the SNR expression of noncoherent MFSK/DS-CDMA over an AWGN channel is Gaussian approximated as

$$\gamma_b' = 9\left[(\gamma_b)^{-1} + \left(\frac{3MN}{2(K-1)\log_2 M}\right)^{-1}\right]^{-1}, \tag{2.6}$$

where N is the number of chips per symbol interval. We can see that $\frac{MN}{\log_2 M} = \frac{MR_c}{R_b} =$

$\frac{W}{R_b}$ (a raised-cosine filter with a roll-off factor of 0 is assumed). Thus, a more general expression for (2.3) is

$$\gamma_b' \simeq \left[(\gamma_b)^{-1} + \left(\mu \frac{W/R_b}{K-1}\right)^{-1}\right]^{-1}. \tag{2.7}$$

All the equations given above are for asynchronous DS-CDMA systems. For synchronous DS-CDMA systems, the SNR term has a similar expression, and the factor μ takes the value of 1. Thus, synchronous DS-CDMA systems are inferior to asynchronous DS-CDMA systems. The reason is that in finding the BER expression of an asynchronous DS-CDMA system, due to the different time delay for different users, extra randomness and averaging are involved. Thus, a better performance is expected.

It should be noted that the above conclusion is valid when random signature sequences are assumed. For deterministic sequences, e.g., AO/LSE m-sequences [56], the synchronous DS-CDMA systems are apparently superior to asynchronous DS-CDMA systems [34].

In fading channels, the performance of DS-CDMA systems is poor [27, 28, 37]. Techniques for improving the system performance are diversity and FEC coding [46, 25]. However, FEC coded DS-CDMA systems are not often discussed in detail in the literature. One of the reason is that a FEC coded DS-CDMA system can be analyzed much like a corresponding narrowband system. This will be discussed in Section 3.6.

PN sequence selection is very important in a CDMA system design. The main specifications are auto-correlation, cross-correlation and available number of sequences. A good survey on the correlation properties for various PN sequences is given in [47]. Gold sequences are popular in practical applications. For the system performance analysis, random signature sequences are often used as a convenient tool [34]. For asynchronous systems, employing Gold sequences or random sequences results in the same performance. For synchronous systems, employing Gold sequences results in much better performance than employing random sequences. In [48], a DS-CDMA system using long PN sequences is discussed. The long PN sequences behave much like random signature sequences. Some complex polyphase sequences are reported to have excellent auto-correlation and cross-correlation properties [49, 50, 51]; but their

implementation is complex. In [52], a CDMA system using polyphase sequences is analyzed. However, the improvement of complex PN sequences over Gold sequences is shown to be small.

In addition to the analytical method, the system performance can be also obtained through Monte Carlo simulations. Due to the high chip rate of SS systems, however, a complete simulation for a CDMA system is much time consuming. Equivalent narrowband system simulation can be used in some cases [25].

In addition to the conventional detection methods, new DS-CDMA detection techniques such as a neural network method are being introduced [57].

For commercial use, the development of CDMA is mainly for capacity reasons. By using CDMA for voice communication, the voice activity can be fully used. Thus, capacity can be increased three times. Some other advantages of CDMA were listed in [4] for cellular radio.

2.2 Bandwidth Efficiency

2.2.1 Concept of Bandwidth Efficiency

Bandwidth efficiency is one of the main performance evaluation criteria of a communication system. In this thesis, we consider the bandwidth efficiency based on a specified bit error rate and a specified bit energy to noise spectral density ratio.

For a digital modulation scheme, the bandwidth efficiency is measured in bits per second per Hertz

$$\eta = \frac{R_b}{W} \quad \text{b/s/Hz} \tag{2.8}$$

where R_b is the information bit rate in bits/sec, and W is the total channel bandwidth occupied by the system in Hz. In a multiple access system, the channel is shared by all system users. Assuming that the total number of simultaneous users is K and all users transmit at the same bit rate, the bandwidth efficiency expression is modified as

$$\eta = \frac{KR_b}{W} \quad \text{b/s/Hz.} \tag{2.9}$$

Correspondingly, the power efficiency is defined as the bit energy to noise spectral

density ratio E_b/N_0 required to achieve a specified bit error rate P_b, say 10^{-5}. The bandwidth efficiency and the power efficiency can be traded off with each other. This is especially true for CDMA systems.

Bandwidth efficiency improvement can be considered from three different aspects, i.e., network protocols, channel filters, and modulation schemes.

In a multiple access network, random access techniques (also called contention techniques) are often used for packet radio transmission [58, 59]. A popular contention protocol is ALOHA. The efficiency of the protocols is evaluated by the *throughput* of the network which is defined as the total rate of data being transmitted between stations (users). The throughput is usually normalized to be expressed as a fraction of network capacity. The network capacity is the maximum possible total transmission rate. It is determined by the *physical link* and *data link* layers, i.e., the channel state and modulation/coding schemes. CDMA is widely considered in packet switching networks [60-64]. In this case, CDMA is, in essence, code division random access (CDRA) [17, 18]. By improving the network throughput, the overall system bandwidth efficiency can be increased. This issue, however, is not the objective of this thesis.

In a bandlimited channel, the maximum information transmission rate (without inter-symbol interference) is limited by the Nyquist rate [65]. However, achieving the Nyquist rate requires an ideal bandpass filter which is not physically realizable. To design band limited signals for no inter-symbol interference (ISI), a convenient approach is to use a raised cosine filter with a roll-off parameter α (ranging from 0 to 1). Smaller α results in a greater bandwidth efficiency. An important topic is to increase the bandwidth efficiency while maintaining the no-ISI condition. This topic is not considered in this thesis. Instead, we assume that $\alpha = 0$ which corresponds to the ideal bandpass filter. Thus, the channel bandwidth required for a binary signal is equal to the rate of the signal. For a practical filter, the obtained value of bandwidth efficiency can be easily modified by dividing it by $(1 + \alpha)$.

Another means of improving the bandwidth efficiency is to find efficient modulation schemes. Modulation schemes can be divided into two classes: bandwidth efficient and power efficient. Usually a bandwidth efficient scheme is not power ef-

ficient, and vice versa. In [66], for a narrowband system over an AWGN channel, a modulation scheme is defined as power efficient if an $E_b/N_0 < 14$ dB is sufficient to obtain a BER of 10^{-8}; a modulation scheme is defined as spectrally efficient (bandwidth efficient) if it has a transmission efficiency greater than 2 b/s/Hz. Based on this definition, MPSK and QAM are bandwidth efficient schemes while MFSK is a power efficient scheme. In a DS-CDMA system, however, the conclusion may be reversed. It will be shown below that a power efficient CDMA system is also bandwidth efficient. Let us recall that the objective of this thesis is in fact to explore bandwidth efficient DS-CDMA systems.

2.2.2 Bandwidth Efficiency of CDMA Systems

In [4], it is said that the bandwidth efficiencies of FDMA, TDMA and CDMA systems are identical in the ideal case. This is true when a special modulation scheme is assumed. For example, when binary PSK is assumed, the bandwidth efficiencies of FDMA, TDMA and CDMA systems are the same and equal to the bandwidth efficiency of BPSK. A simple argument is given below. The bandwidth efficiency of BPSK is 1 b/s/Hz. For an FDMA system with no guard bands, the system with K users corresponds to K independent narrowband systems. Thus, its bandwidth efficiency is 1 b/s/Hz. In a TDMA system without guard time between time frames or slots, with a bandwidth KW, one transmission needs only $1/K$ time interval compared to the narrowband system. Thus the bandwidth efficiency is unchanged. In such a DS-CDMA system, the underlying assumption is that all the PN sequences are orthogonal. With total bandwidth KW, the spreading factor is K, and the total number of orthogonal PN sequences available is K. Thus for a synchronous system, no MAI is present. Then a bandwidth efficiency of 1 b/s/Hz can be achieved. If a different modulation scheme is used, the results may change.

Clearly most of these assumptions are not valid in a practical system. For example, in most CDMA applications code orthogonality and the associated synchronization cannot be achieved. Thus the MAI exists, and the bandwidth efficiency of a CDMA system is limited by the MAI. Similarly, various overheads, imperfections, impairments and channel conditions limit the capacity of practical FDMA and TDMA

systems to values below what is expected with the assumptions of ideal conditions.

In a narrowband system, the bandwidth efficiency and the power efficiency cannot be traded off easily. For example, the bandwidth efficiency of noncoherent MFSK is $\log_2 M/M$. Even with a very large SNR, its bandwidth efficiency remains the same. In a DS-CDMA system, however, the bandwidth efficiency and the power efficiency are related to each other. From equations (2.3) and (2.9), the bandwidth efficiency can be written as

$$\eta = \frac{KR_b}{W} \simeq \frac{3}{2}\frac{\gamma_b - \gamma_b'}{\gamma_b \gamma_b'} \quad \text{b/s/Hz.} \tag{2.10}$$

The bandwidth efficiency of a DS-CDMA system is directly related to the given bit energy to noise spectral density ratio (γ_b) and the required bit energy to noise spectral density ratio (γ_b') for a specified BER. When $\gamma_b \to \infty$, we have the asymptotic bandwidth efficiency

$$\eta_\infty = \frac{3}{2}\frac{1}{\gamma_b'} \quad \text{b/s/Hz.} \tag{2.11}$$

The asymptotic bandwidth efficiency is inversely proportional to the required bit energy to noise spectral density ratio. Thus, it is clear that a power efficient DS-CDMA system is also bandwidth efficient.

The expression of bandwidth efficiency is derived for a BPSK signal over an AWGN channel. We will demonstrate that the same expression holds for MFSK signals. In general, if the standard Gaussian approximation (2.3) is valid, then the expression of bandwidth efficiency holds. If K is not large, the modified Gaussian approximation applies. The expression of bandwidth efficiency needs a modification. However, in most systems of interests, K is not small; so the above expression of the bandwidth efficiency is valid.

2.3 System Model

In this thesis, we study three different DS-CDMA systems. The transmitter and receiver structure are different for each system. In this section we describe a general system model, later the specifics of each system are pointed out.

2.3.1 General System Model

The CDMA system model that we consider is shown in Fig. 2.1 for K users. Since in a mobile environment all the users transmit independently and randomly, the synchronous reception from all users is difficult to achieve. So we will consider only asynchronous transmissions. We are assuming homogeneous users, which also implies perfect power control. For the PN sequence, random signature sequences are assumed. We concentrate on communication performance rather than on acquisition and tracking performance, so that the performance measures of interest are bit error rate, signal-to-noise ratio, and bandwidth efficiency.

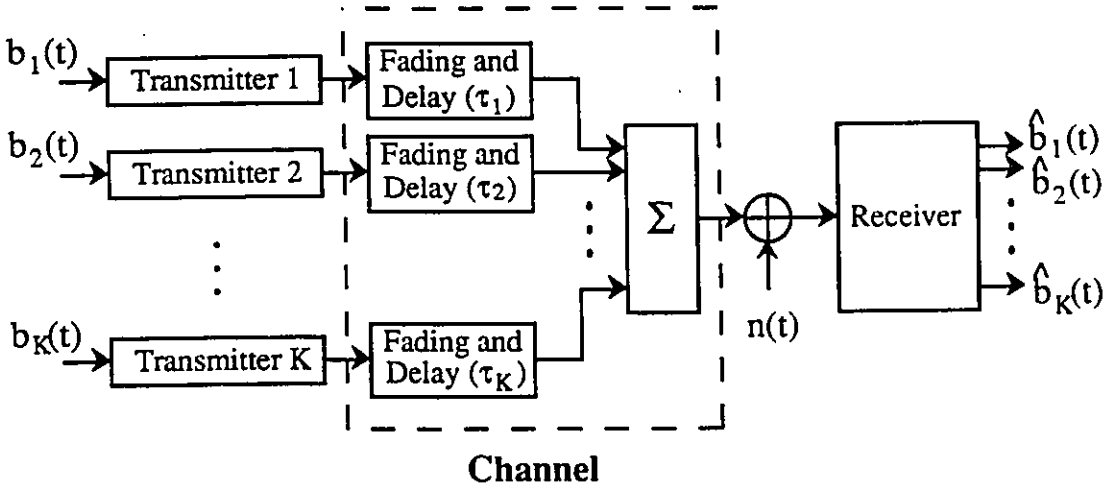

Figure 2.1 : A general CDMA system model.

In Fig. 2.1, $b_k(t)$ is the data to be transmitted by the kth user, and $\hat{b}_k(t)$ is the estimated data at the receiver. For a desired signal, all the other $(K-1)$ transmissions act as interference. The kth user's transmitted signal experiences time delay (τ_k), fading, multiple-access interference, and corruption by additive Gaussian noise. The receiver can be a central station which receives all the incoming signals simultaneously or a single receiver which receives only one intended signal. The former case corresponds to a star network, and the latter case corresponds to a distributed network. For the star network, the central station has K parallel receivers corresponding

to the K users. In either case, the performance is determined for a single receiver.

2.3.2 Mobile Communications Environments

One of the main characteristics of mobile environment is multipath fading. Depending on the amplitude distribution of the received signal the fading can be classified as, for example, Rayleigh, Rician, or log-normal. Depending on the channel coherence bandwidth (relative to the signal bandwidth), the fading can be classified as frequency selective or frequency nonselective. Depending on the Doppler spread or the fading rate (relative to the signalling interval), the fading can be classified as slow fading or fast fading. Real channels are very complicated. Generally, the cellular radio is modeled as Rayleigh fading with a delay spread of about 3 micro-seconds in urban areas [4]; while the land mobile satellite channel is modeled as Rician fading [2]. For indoor wireless radio, the multipath Rayleigh fading channel model is employed for office building [67], and the multipath Rician fading channel model is employed for factory environment [68, 69].

In this thesis, we consider frequency nonselective slow Rayleigh and Rician fading channels. These channel conditions are widely seen in practical mobile environments. For frequency selective channels, some diversity techniques can be used. For instance, significant diversity gain is achieved using a Rake receiver [25]; and a frequency diversity is obtained in an MT-FSK/DS-CDMA system as will be studied in Chapter 6. In all these cases, the system analysis can be usually performed based on the frequency nonselective fading model.

For the system analysis, the BER of coherent PSK, differential PSK and noncoherent MFSK will be used. Here we recall some well known results. The BER performance of these schemes over AWGN and Rayleigh fading channels are given in close forms [75]. A Rician fading model is more general. The Rician probability density function (pdf) is

$$p(\rho) = \frac{\rho}{\sigma^2} \exp\left[-\frac{\rho^2 + s^2}{2\sigma^2}\right] I_0\left(\frac{\rho s}{\sigma^2}\right) \quad \rho \geq 0. \tag{2.12}$$

This distribution is used to describe the amplitude of a constant signal plus a noise term. In the above expression, s represents the constant signal, and σ^2 represents the

variance of the noise term. The Rician channel is specified by the Rician parameter[2] (κ). With a normalized (unit mean-squared value) amplitude, the pdf of a Rician distribution can be expressed as [70]

$$p(\rho) = 2\rho(1+\kappa)\exp[-\kappa - \rho^2(1+\kappa)]I_0\left(2\rho\sqrt{\kappa(1+\kappa)}\right) \quad \rho \geq 0. \tag{2.13}$$

By direct comparison, we can obtain the relationships between κ and s and σ^2. The situation with $\kappa = 0$ corresponds to a Rayleigh fading channel and $\kappa \to \infty$ corresponds to an AWGN channel. Using these distributions, the derivation of the symbol error rates of differential PSK and noncoherent MFSK are given in Appendix A.

[2]The Rician parameter is defined as the ratio of the power in the LOS component to that in the diffuse component. It is commonly referred as the K-factor. Since we already used K for the number of simultaneous users, to avoid confusion we shall denote the conventional K-factor as κ.

Chapter 3

DS-CDMA Employing Combined Modulation Schemes

3.1 Introduction

In most previous studies, the modulation scheme used in a DS-CDMA system is a simple one; it varies only the frequency or the phase, but not both. By using a combined modulation scheme in a DS-CDMA system, an extra advantage can be obtained. In this chapter, we focus on considering a combined scheme which employs both MFSK and MPSK. However, this concept can be extended to other potential combination schemes. In the next chapter, *orthogonal codes* will be considered jointly with MFSK, which is also a combined scheme. In Chapter 6, *permutation modulation* is considered for a DS-CDMA system. It can also be considered jointly with the schemes discussed in this and in the next chapters.

DS-CDMA systems can employ either PSK or MFSK modulations. The resultant systems are called PSK/DS-CDMA and MFSK/DS-CDMA respectively. PSK/DS-CDMA has been widely considered in practical systems with PSK scheme both coherent and differentially detected. While for MFSK/DS-CDMA systems, only noncoherent detection is used. In [30] Geraniotis analyzed the performance of synchronous and asynchronous MFSK/DS-CDMA systems using both deterministic and random signature sequences. It was shown that MFSK/DS-CDMA achieves a better performance than PSK/DS-CDMA. In [31] he further analyzed the performance of MFSK/DS-CDMA systems over Rician fading channels. In [32] Ha analyzed a sequence asyn-

chronous MFSK/DS-CDMA system. He mentioned that by properly selecting the frequency spacing and the PN chip rate, the power spectral density of an MFSK SS signal can be shaped to resemble white noise. This in effect increases the SS signal equivalent noise bandwidth and in turn reduces the effect of interuser interference. Ha's method will be discussed in Appendix D.

In [71], we compared the capacities of MFSK/DS-CDMA and PSK/DS-CDMA systems. To achieve a specified BER (say 10^{-5}), if FEC coding is not used, the required effective SNR per bit (E_b/N_0') for MFSK/DS-CDMA is less than that for PSK/DS-CDMA. Thus MFSK/DS-CDMA offers larger capacity. For some FEC coded cases, the value of E_b/N_0' for MFSK/DS-CDMA is larger than that for PSK/DS-CDMA and the advantage of the MFSK/DS-CDMA system disappears. In [72], we further considered the capacity of MFSK/DS-CDMA systems along with the code acquisition.

Based on the study of MFSK/DS-SS system, we propose a new scheme — MFSK-MPSK/DS-CDMA. This system uses noncoherent MFSK and coherent MPSK modulation. Each of the frequency tones (in MFSK) is phase modulated and spread by the PN code. In this way, the total system bandwidth efficiency can be increased. In [73], we considered a special case of this system, namely MFSK-BPSK/DS-CDMA.

The contributions of this chapter are

(1) Presentation of MFSK-MPSK/DS-CDMA.

(2) By combining MFSK and differential MPSK modulation schemes, we propose another novel system, namely MFSK-DMPSK/DS-CDMA, which is more practical to implement.

(3) An algorithm is described for the implementation of MFSK-DBPSK/DS-CDMA.

(4) The FEC coded MFSK-DBPSK/DS-CDMA system is discussed.

In Section 3.2, we describe the system model. In Section 3.3, MFSK-MPSK/DS-CDMA is analyzed over an AWGN channel and results are discussed. In Section

3.4, the relationship between SNR and MAI is discussed. In Section 3.5, the MFSK-DBPSK/DS-CDMA system is analyzed for AWGN and fading channels. In Section 3.6, FEC coded MFSK-DBPSK/DS-CDMA is discussed. Finally in Section 3.7, a summary is given.

3.2 System Model

3.2.1 Transmitter Model

The general system model was described in Section 2.3. In the MFSK-MPSK/DS-CDMA system, we are interested in the combination of MFSK and MPSK schemes. The parameter M in MFSK and in MPSK may be different. For clarification, we use M_f to denote the number of tones in MFSK and M_p to denote the number of phases in MPSK. The block diagram of the kth transmitter is shown in Fig. 3.1.

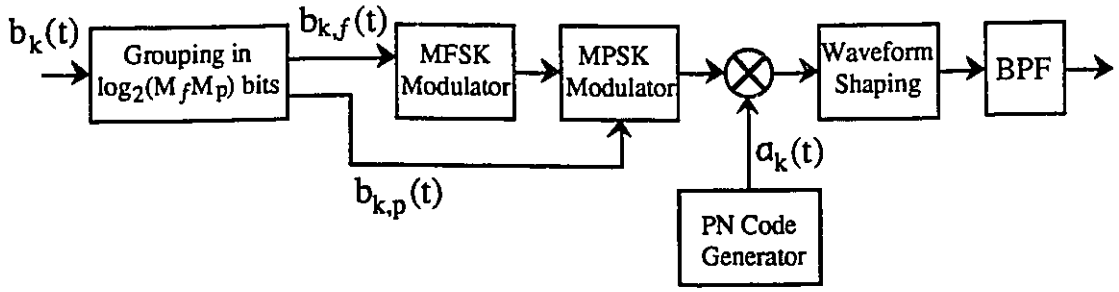

Figure 3.1 : Block diagram of the transmitter of MFSK-MPSK/DS-CDMA.

The kth user's information signal $b_k(t)$ is a stream of binary rectangular pulses of duration T_b

$$b_k(t) = \sum_{j=-\infty}^{\infty} b_j^k p_{T_b}(t - jT_b), \tag{3.1}$$

where b_j^k represents the kth user data at jth timing interval, taking values $+1$ or -1 with equal probability, and

$$p_\tau(t) = \begin{cases} 1, & 0 \le t < \tau, \\ 0, & \text{otherwise.} \end{cases} \tag{3.2}$$

Here we are not considering FEC coding. The bit stream is first grouped in $\log_2(M_f M_p)$ bits in which $\log_2 M_f$ bits are used to choose one of the M_f frequency tones in the MFSK modulator, and $\log_2 M_p$ bits choose one of the M_p phases for each frequency tone selected in the MPSK modulator. The two signals $b_{k,f}(t)$ and $b_{k,p}(t)$ can be expressed respectively as

$$b_{k,f}(t) = \sum_{j=-\infty}^{\infty} b_j^{k,f} p_{T_s}(t - jT_s), \tag{3.3}$$

and

$$b_{k,p}(t) = \sum_{j=-\infty}^{\infty} b_j^{k,p} p_{T_s}(t - jT_s), \tag{3.4}$$

where the symbol interval $T_s = T_b/\log_2(M_f M_p)$, $b_j^{k,f}$ takes the values ± 1, ± 3, $\cdots$, $\pm(M_f - 1)$, and $b_j^{k,p}$ takes the values 0, 1, $\cdots$, $M_p - 1$. The resultant signal is MFSK/MPSK modulated. It is further spread by a PN sequence

$$a_k(t) = \sum_{i=-\infty}^{\infty} a_i^k p_{T_c}(t - iT_c) \tag{3.5}$$

where a_i^k is the ith chip of the PN sequence for the kth user. We assume that the PN sequence has a period of $N = T_s/T_c$. That is, there is one period of PN sequence per symbol. The spread signal is waveform shaped in $\Psi(t) = \psi(s)$ for $s = t \pmod{T_c}$, where $\psi(s)$ is a chip waveform of duration T_c, and $T_c^{-1}\int_0^{T_c} \psi^2(s)ds = 1$. We assume a rectangular chip waveform. Thus $\psi(s) = p_{T_c}(t)$. Finally, the signal is bandpass filtered and ready for transmission.

The kth $(1 \le k \le K)$ transmitted signal can be expressed as

$$s_k(t) = \mathrm{Re}\{u_k(t)\exp(j2\pi f_c t)\} \tag{3.6}$$

where f_c is the carrier frequency and $u_k(t)$ is the kth baseband signal

$$u_k(t) = \sqrt{2E_b/T_b}\Psi(t)a_k(t)\exp\left[j2\pi(b_{f,k}(t)\Delta + b_{p,k}(t)/M_p)t + j\theta_k(t)\right]. \tag{3.7}$$

In the expression E_b/T_b is the power of the transmitted signal, $\theta_k(t)$ is the phase introduced by the kth user's modulator, and Δ is the half of the frequency spacing between adjacent tones.

The bit rate is $R_b = 1/T_b$. The symbol rate is $R_s = R_b/\log_2(M_f M_p)$; the symbol energy is $E_s = \log_2(M_f M_p)E_b$. The PN chip rate is $R_c = NR_s$; the chip energy is $E_c = E_s/N$. The bit energy to noise spectral density ratio is $\gamma_b = E_b/N_0$, and the symbol energy to noise spectral density ratio is $\gamma_s = E_s/N_0$. Assuming that a raised cosine filter with a roll-off factor α is used, then the total bandwidth W is

$$W = (1+\alpha)M_f R_c = (1+\alpha)M_f N R_s = \frac{(1+\alpha)M_f N R_b}{\log_2(M_f M_p)}. \tag{3.8}$$

In our discussion, we assume that $\alpha = 0$. When $M_f = 1$ and $M_p = 2$, the system reduces to a conventional PSK/DS-CDMA system. When $M_p = 1$, the system reduces to an MFSK/DS-CDMA system. The spectral occupancy of the signal is shown in Fig. 3.2; the spectral shape centered around each tone f_i ($i = 1, \cdots, M_f$) may in fact be different from the one illustrated in the figure.

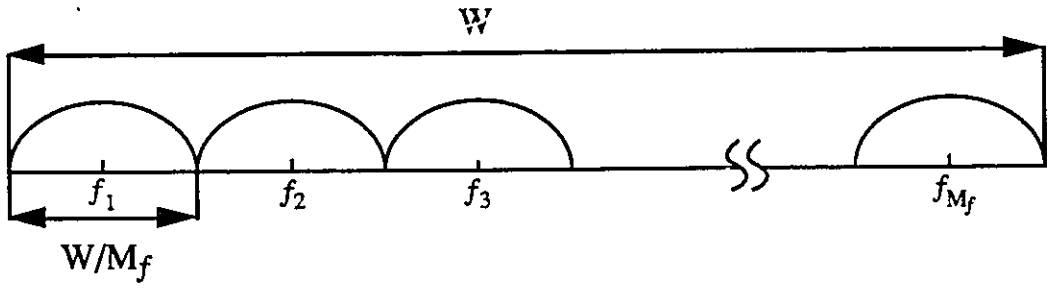

Figure 3.2 : An illustration for the spectral occupancy of an MFSK-MPSK/DS-CDMA signal.

3.2.2 Channel Model

In an asynchronous system, the signal at the input of a particular receiver (in the absence of noise) is

$$y(t) = \sum_{k=1}^{K} s_k(t - \tau_k) \tag{3.9}$$

where τ_k with $1 \leq k \leq K$ denotes the time delays along the communications links between the K transmitters and the receiver. If fine (at the chip level) synchronization

is possible between the different transmitters, then we would replace (3.9) by

$$y(t) = \sum_{k=1}^{K} s_k(t), \tag{3.10}$$

which characterizes synchronous systems. Assuming that we restrict our attention to the receiver matched to the ith transmitted signal, τ_k and θ_k are independent and uniformly distributed in $[0, T_c]$ and $[0, 2\pi]$, respectively. We also assume that the data stream, time delays, and phase angles associated with different transmitted signals are mutually independent.

The signal $y(t)$ given by (3.9) is further corrupted by additive Gaussian noise $n(t)$ of (two-sided) spectral density $N_0/2$; therefore the received signal $r(t)$ is given by

$$r(t) = y(t) + n(t). \tag{3.11}$$

3.2.3 Receiver Model

The block diagram of the receiver is shown in Fig. 3.3-(a). There are M_f branches corresponding to each one of the M_f frequency tones. Each branch consists of a matched filter (MF) which has two outputs. One of the outputs corresponds to the MPSK demodulator, another output comes from the square-law detector. A matched filter is shown in Fig. 3.3-(b). The received signal is first bandpass filtered, and then spread by multiplying with a PN code reference $a_k(t)$. The resultant signal goes to a conventional MPSK demodulator [75]. Assume that the sampling output from upper branch is X and the one from lower branch is Y. Then $(X + jY)$ is used for the MPSK decision, and $(X^2 + Y^2)$ is used for the MFSK decision.

In the decision unit. The M_f outputs from square-law detectors are first compared. The largest one is chosen and the corresponding MPSK output is selected.

For the coherent detection of MPSK, perfect carrier synchronization is assumed. In this case, MFSK can also be demodulated coherently. For comparison purposes, analysis for noncoherent MFSK will be done in next section. In fact, the carrier synchronization is difficult in practice. We just assume that it can be realized somehow. For instance, a pilot tone can be transmitted to assist the carrier synchronization. Further discussion of this topic is given in Section 3.5.

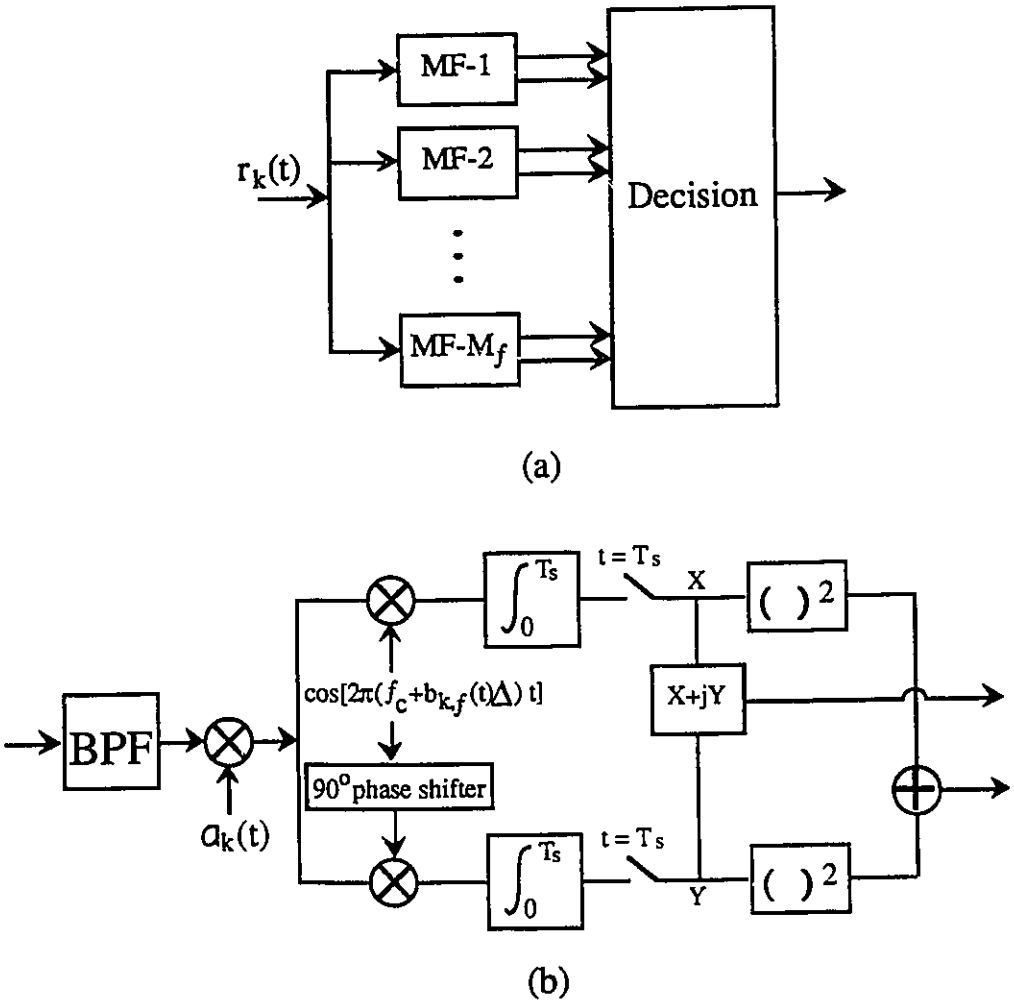

Figure 3.3 : Block diagram of the receiver of MFSK-MPSK/DS-CDMA. (a) Receiver structure; (b) Structure of a matched filter (MF).

3.3 Performance of MFSK-MPSK/DS-CDMA over an AWGN Channel

3.3.1 Analysis

In this section, we give two types of analyses for the bit error rate performance and bandwidth efficiency. The first simple analysis is suggested by Viterbi [42], and the second method is used by Pursley [41]. Both methods use the Gaussian approximation for the MAI. We avoid using the exact but complex analysis methods as in [33] and [37]. Our argument is that, for large number of simultaneous users, the Gaussian approximation is accurate. Even for a small number of simultaneous users, the improved Gaussian approximation methods [43, 45] can be shown to give very good approximations. The advantage of the Gaussian approximation method lies in its simplicity. It also lends itself to a clear physical interpretation.

3.3.1.1 Bandwidth Efficiency

The total number of interfering transmissions is $K-1$, all transmitting randomly. Each transmitted tone will be interfered by $(K-1)/M_f$ other transmissions on the average. If $(K-1)/M_f$ is large, from the central limit theorem [74], the MAI can be well approximated by an equivalent Gaussian noise. The total noise power is the sum of thermal noise power plus the mutual interference power. Assume that the one-sided bandwidth is W, for an individual frequency tone, the occupied bandwidth is W/M_f, the effective noise and MAI power is

$$N_0\frac{W}{M_f}+\frac{K-1}{M_f}E_sR_s. \tag{3.12}$$

The total noise power spectral density is

$$N_0^{'}=\frac{N_0\frac{W}{M_f}+\frac{K-1}{M_f}E_sR_s}{\frac{W}{M_f}}=N_0+\frac{(K-1)E_s}{W/R_s}. \tag{3.13}$$

The symbol energy to the effective noise spectral density ratio is

$$\gamma_s^{'}=\frac{E_s}{N_0^{'}}=\frac{\gamma_s}{1+\frac{K-1}{\frac{W}{R_s}}\gamma_s}=\frac{\log_2(M_fM_p)\gamma_b}{1+\frac{K-1}{\frac{W}{R_b}}\gamma_b}, \tag{3.14}$$

and the bit energy to the effective noise spectral density ratio is

$$\gamma_b' = \frac{E_b}{N_0'} = \frac{\gamma_b}{1 + \frac{K-1}{\frac{W}{R_b}}\gamma_b}. \tag{3.15}$$

From (3.8), W/R_b can be expressed as ($\alpha = 0$)

$$\frac{W}{R_b} = \frac{M_f N}{\log_2(M_f M_p)}. \tag{3.16}$$

For a specified BER, depending on the modulation/detection technique used, there is a corresponding SNR per bit γ_b'. We can obtain K from (3.14)

$$K = \frac{W}{R_b}\frac{(\gamma_b - \gamma_b')}{\gamma_b\gamma_b'} + 1 \simeq \frac{W}{R_b}\frac{(\gamma_b - \gamma_b')}{\gamma_b\gamma_b'}. \tag{3.17}$$

The system bandwidth efficiency is:

$$\eta = \frac{KR_b}{W} = \frac{\gamma_b - \gamma_b'}{\gamma_b\gamma_b'}. \tag{3.18}$$

Now we consider the result given by Pursley [41]. In Section 3.2, we gave the signal expression at the input of the receiver. Based on that expression, we can perform the demodulation operation and get the expression of BER performance. In arriving at the statistics of the output of the matched filter, the main term of interest is the mutual interference. The *characteristic-function method* and the *series-expansion method* can be used to perform the analysis [33, 30]. However, these methods require extensive calculations and are valid only for small K. For large K, instead, a Gaussian approximation method can be used, i.e., the interference term is approximated with a Gaussian random variable having the same second-order moments. This Gaussian approximation method gives an equivalent signal to noise ratio. In [41], Pursley gave the result for asynchronous PSK/DS-CDMA system with random signature sequences and found

$$\gamma_b' = \left[\gamma_b^{-1} + \left(\frac{3W/R_b}{2(K-1)}\right)^{-1}\right]^{-1}. \tag{3.19}$$

In [30], Geraniotis gave the same result for noncoherent MFSK/DS-CDMA system. This result can also be used for MFSK-MPSK/DS-CDMA systems. Comparing (3.19) with (3.14), we see that the latter is more conservative.

Using (3.19), the bandwidth efficiency is

$$\eta = \frac{KR_b}{W} = \frac{3}{2}\frac{\gamma_b - \gamma_b'}{\gamma_b\gamma_b'} \div \frac{R_b}{W} \simeq \frac{3}{2}\frac{\gamma_b - \gamma_b'}{\gamma_b\gamma_b'}. \tag{3.20}$$

As $\gamma_b = \infty$, we have the asymptotic bandwidth efficiency

$$\eta_\infty = \frac{3}{2\gamma_b'}. \tag{3.21}$$

Equations (3.19)–(3.21) will be used for the performance evaluation.

3.3.1.2 BER Performance

In the receiver, we need to make decisions in two stages. One is the noncoherent MFSK detection. The other one is the coherent MPSK detection. Assume that the probability of error of the first stage decision (MFSK) is P_f, and the probability of error of the second stage decision (MPSK) is P_p. Since the two decision variables are obtained from the same received signal, so they are not independent. Assume the probabilities of correct decision of MFSK and MPSK are P_{Cf} and P_{Cp} respectively, and the probability of correct decision of MPSK conditioned on the correct decision of MFSK is $P_{Cp}(p|f)$, then we have

$$P_C = P_{Cf}P_{Cp}(p|f) \geq P_{Cf}P_{Cp}. \tag{3.22}$$

The overall probability of symbol error is

$$P_s = 1 - P_C \leq 1 - (1 - P_f)(1 - P_p) = P_f + P_p - P_fP_p \simeq P_f + P_p. \tag{3.23}$$

For noncoherent MFSK, P_f is found as [75]

$$P_f = \sum_{n=1}^{M_f-1} (-1)^{n+1} \binom{M_f - 1}{n} \frac{1}{n+1} e^{-\gamma_s' n/(n+1)} \tag{3.24}$$

where $\gamma_s' = E_s/N_0'$ is given in (3.14). For coherent MPSK P_p is found as [75] (for $\gamma_s' \gg 1$)

$$P_p = Q\left(\sqrt{2\gamma_s'}\sin\frac{\pi}{M_p}\right). \tag{3.25}$$

Next we consider converting the probability of symbol error into an equivalent probability of bit error. For MFSK, the bit error rate is multiplication of the symbol

error rate and a factor $\frac{2^{\lfloor \log_2(M_f)/2 \rfloor}}{2^{\log_2(M_f)}-1}$; while for MPSK the bit error rate is multiplication of the symbol error rate and a factor $1/\log_2(M_p)$ [75]. In the MFSK-MPSK scheme, there are totally $M = M_f M_p$ symbols, each containing $\log_2(M)$ bits. For each distinct tone, there are M_p different phases. Assume Gray code is used in the mapping. Thus, those symbols with the same tone have $\log_2 M_f$ bits in common. For simplicity, assume a symbol with all "0"" bits is transmitted. From (3.23), we see that symbol error rate is composed of two terms, P_f and P_p, and P_s is determined by the larger one of the two terms. If $P_f \gg P_p$, when error occurs, the transmitted symbol is mostly error detected as other $(M_f - 1)$ tones equally, and with one of M_p phases equally, i.e., the transmitted symbol would be detected as one of other $M_p(M_f - 1)$ symbols. In those $M_p(M_f - 1)$ symbols, the total number of bits is $M_p(M_f - 1)\log_2(M)$. The total number of "1" bits in all symbols is $M\log_2(M)/2$; and within the same tone as the transmitted symbol, the total number of "1" bits is $M_p \log_2(M_p)/2$. Thus, the total number of "1" bits in those $M_p(M_f - 1)$ symbols is $M\log_2(M)/2 - M_p\log_2(M_p)/2$. The bit error rate is

$$P_b^f = \frac{\text{number of "1" bits in } M_p(M_f-1) \text{ symbols}}{\text{total number of bits in } M_p(M_f-1) \text{ symbols}} = \frac{M\log_2(M)/2 - M_p\log_2(M_p)/2}{M_p(M_f-1)\log_2(M)} P_s. \tag{3.26}$$

If $P_p \gg P_f$, and when error occurs, the bit error rate can be approximated as

$$P_b^p = \frac{1}{\log_2 M} P_s. \tag{3.27}$$

In general, we have

$$P_b = P_b^f + P_b^p = \frac{M\log_2(M)/2 - M_p\log_2(M_p)/2}{M_p(M_f-1)\log_2(M)} P_s + \frac{1}{\log_2(M)} P_s. \tag{3.28}$$

When $M_p = 1$, we have $P_b^p = 0$, and

$$P_b = \frac{M_f/2}{M_f - 1} P_s, \tag{3.29}$$

and when $M_f = 1$, we have $P_b^f = 0$, and

$$P_b = \frac{1}{\log_2 M_p} P_s. \tag{3.30}$$

For the same P_s, we have $P_b^f \simeq= \frac{1}{2}P_s$. So for $M > 4$, $P_b^f > P_b^p$. As a conservative consideration, treating all symbols as orthogonal, we have the following expression for the performance evaluation:

$$P_b \simeq \frac{2^{[\log_2(M_f M_p)/2]}}{2^{\log_2(M_f M_p)} - 1} P_s. \tag{3.31}$$

3.3.2 Numerical Results and Discussions

In this section, we present numerical results of BER performance and bandwidth efficiency evaluation of the MFSK-MPSK/DS-CDMA system. The results are obtained by using (3.23)-(3.31) for BER performance and (3.20) and (3.21) for bandwidth efficiency. We also compare these results with the ones for MFSK/DS-CDMA and PSK/DS-CDMA systems.

The BER performance of the system for M_f = 2, 4, 8, 16, 32 and M_p = 2, 4, 8, 16, 32 are given in Figs. 3.4–3.8 respectively. In these and subsequent tables, the best performance in each column is shown in boldface.

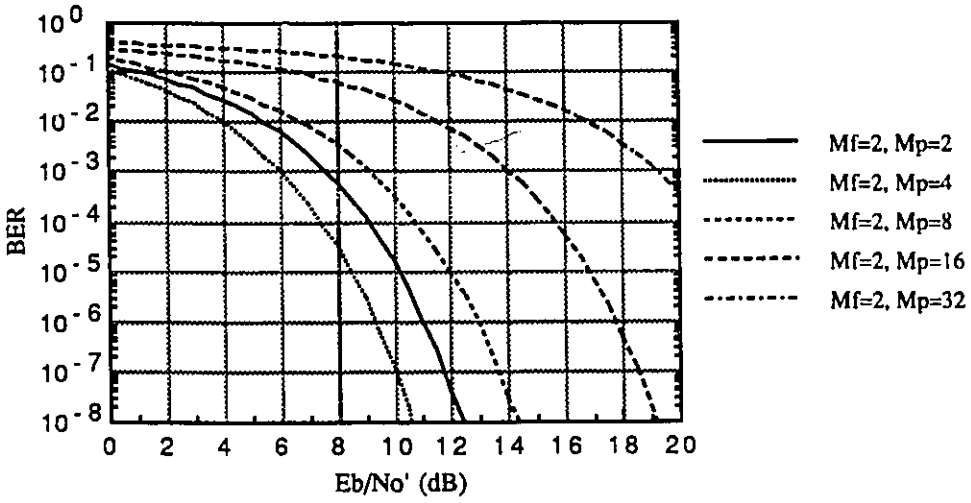

Figure 3.4 : BER performance of MFSK-MPSK/DS-CDMA for M_f = 2 and M_p = 2, 4, 8, 16, 32.

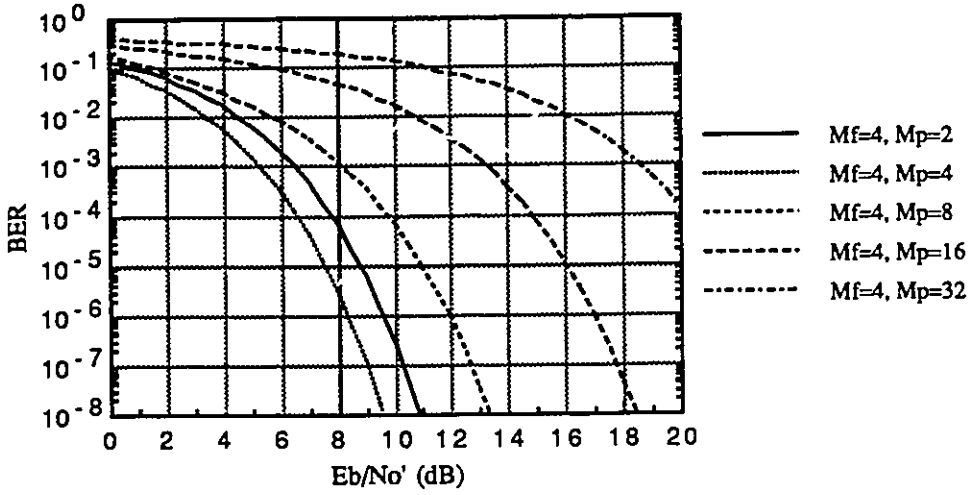

Figure 3.5 : BER performance of MFSK-MPSK/DS-CDMA for $M_f = 4$ and $M_p = 2, 4, 8, 16, 32$.

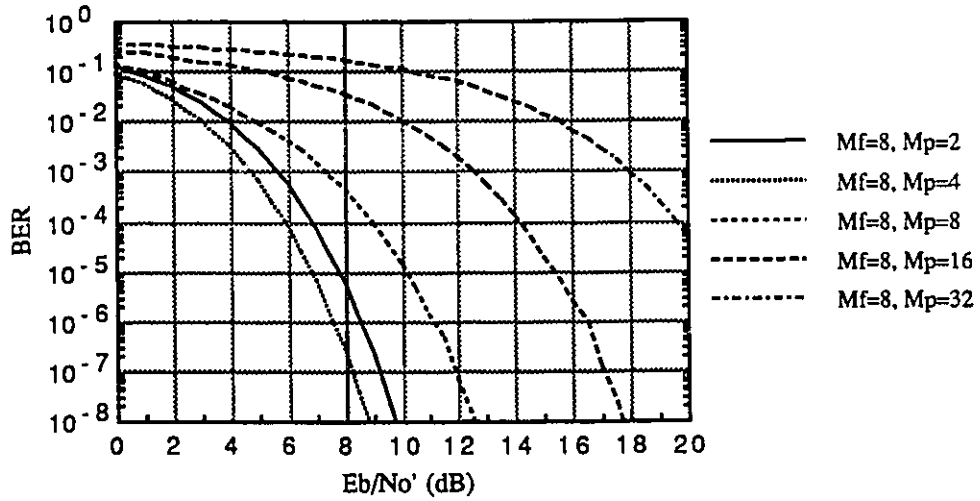

Figure 3.6 : BER performance of MFSK-MPSK/DS-CDMA for $M_f = 8$ and $M_p = 2, 4, 8, 16, 32$.

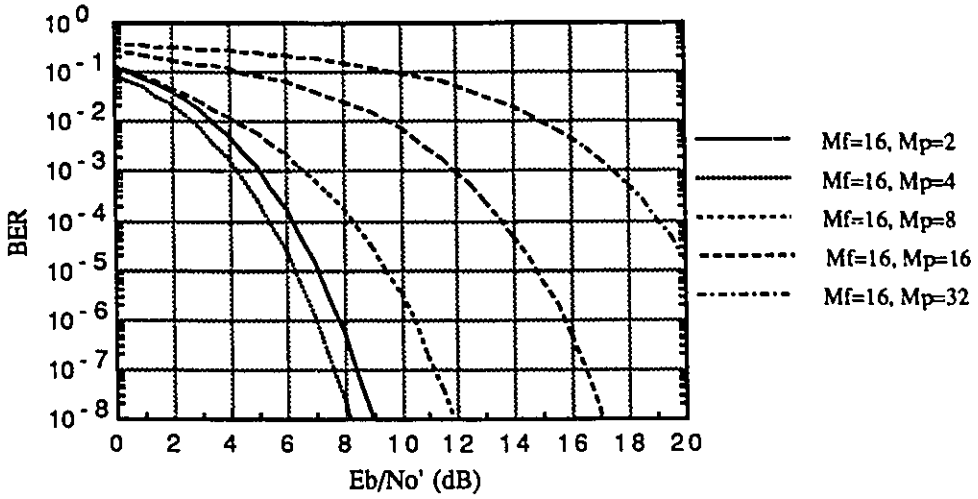

Figure 3.7 : BER performance of MFSK-MPSK/DS-CDMA for $M_f = 16$ and $M_p = 2, 4, 8, 16, 32$.

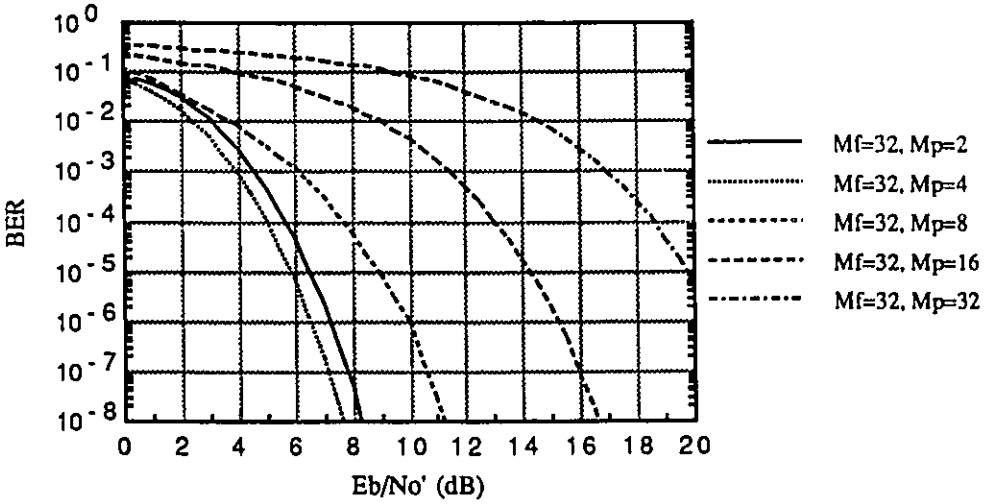

Figure 3.8 : BER performance of MFSK-MPSK/DS-CDMA for $M_f = 32$ and $M_p = 2, 4, 8, 16, 32$.

For BER values of 10^{-3} and 10^{-5}, the required bit energy to noise density ratio (in dB) is given in Table 3.1 and Table 3.2 respectively. The entries for $M_p = 1$ correspond to MFSK/DS-CDMA systems, and the entries for $M_f = 1$ correspond to MPSK/DS-CDMA systems.

Table 3.1 : The required SNR per bit γ_b' (in dB) for a BER of 10^{-3} for MFSK-MPSK/DS-CDMA systems in an AWGN channel.

	$M_f = 1$	$M_f = 2$	$M_f = 4$	$M_f = 8$	$M_f = 16$	$M_f = 32$
$M_p = 1$		10.9	8.3	6.9	6.0	5.4
$M_p = 2$	**6.8**	7.6	6.5	5.6	5.0	4.6
$M_p = 4$	7.0	**6.0**	**5.2**	**4.7**	**4.3**	**3.9**
$M_p = 8$	10.5	9.1	8.1	7.3	6.6	6.1
$M_p = 16$	15.0	14.0	13.2	12.5	11.9	11.4
$M_p = 32$	20.0	19.2	18.5	17.9	17.4	16.9

Table 3.2 : The required SNR per bit γ_b' (in dB) for a BER of 10^{-5} for MFSK-MPSK/DS-CDMA systems in an AWGN channel.

	$M_f = 1$	$M_f = 2$	$M_f = 4$	$M_f = 8$	$M_f = 16$	$M_f = 32$
$M_p = 1$		13.3	10.6	9.1	8.0	7.3
$M_p = 2$	**9.6**	10.1	8.7	7.8	7.1	6.5
$M_p = 4$	9.7	**8.4**	**7.5**	**6.8**	**6.3**	**5.8**
$M_p = 8$	13.2	11.9	10.9	10.1	9.5	8.9
$M_p = 16$	17.8	16.8	16.0	15.3	14.7	14.2
$M_p = 32$	22.8	22.0	21.3	20.7	20.2	19.7

From Figs. 3.4–3.8 and Tables 3.1–3.2, we have a few observations. For a fixed M_p, the system performance is better when M_f is larger. This is due to the power efficiency property of MFSK modulation scheme. For a fixed M_f (except $M_f = 1$), the system performance is best when $M_p = 4$ and becomes worse for increased value of M_p. For $M_p > 4$, MPSK is less power-efficient than MFSK, and the probability of symbol error contributed by MPSK (the P_p term in (3.23)) is greater than that of MFSK (the P_f term in (3.23)); then the overall probability of symbol error is determined by MPSK,

which results in a worse performance. The reason that MFSK-QPSK/DS-CDMA performs better than MFSK-BPSK/DS-CDMA can be explained as follows. For all the MFSK-MPSK/DS-CDMA considered, the MFSK part performs worse than BPSK or QPSK and thus determines the overall probability of error. For a given SNR per bit, the combination of QPSK and MFSK has a larger SNR per symbol than that of BPSK and MFSK and thus obtains better performance. It is well known that in narrowband systems, MSFK with large M_f is more powerful than both BPSK and QPSK. However, in the MFSK-MPSK combination schemes, BPSK or QPSK parts have much more gain in SNR per symbol than MFSK has for a given SNR per bit, and thus the overall performance is determined by MFSK part. As an example, we consider a combination scheme with $M_f = 16$ and $M_p = 2$. For a given SNR per bit γ_b, the SNR per symbol for BPSK part is $\gamma_s = \log_2(M_f M_p)\gamma_b = 6\gamma_b$ (comparing that $\gamma_s = \gamma_b$ in a single BPSK scheme), and the SNR per symbol for 32FSK part is $\gamma_s = \log_2(M_f M_p)\gamma_b = 6\gamma_b$ (comparing that $\gamma_s = 5\gamma_b$ in a single 32FSK scheme). Thus, BPSK part has a gain over 32FSK by $\frac{6/1}{6/5} = 5$ (7 dB).

It is noted that for $M_f = 1$, the BER performance of BPSK/DS-CDMA and QPSK/DS-CDMA are basically the same (the former is a little better), and equal to the BER performance of BPSK and QPSK in narrowband systems. However, since the bandwidth efficiency in a CDMA system is inversely proportional to the BER performance, contrary to nonspread systems, BPSK/DS-CDMA and QPSK/DS-CDMA have the same bandwidth efficiency. While in narrowband systems, the bandwidth efficiency of QPSK is twice that of BPSK. This result highlights the difference of bandwidth efficiency concept between the narrowband systems and the DS-CDMA systems.

Next we give a more quantitative argument for the bandwidth efficiency of MFSK-MPSK/DS-CDMA schemes. Suppose that for a specified value of BER, the required SNRs per bit are $\gamma_{bp}^{(1)}$ for MPSK and $\gamma_{bf}^{(1)}$ for MFSK; correspondingly, the required SNRs per symbol are $\gamma_{sp}^{(1)} = \gamma_{bp}^{(1)} \log_2 M_p$ and $\gamma_{sf}^{(1)} = \gamma_{bf}^{(1)} \log_2 M_f$ respectively. For the combined MFSK-MPSK scheme, to have the same SNR per symbol $\gamma_s^{(2)} = \gamma_{sp}^{(1)} = \gamma_{sf}^{(1)}$, the required SNR per bit is $\gamma_b^{(2)} = \gamma_s^{(2)} / \log_2(M_p M_f)$. Thus, the gain (in dB) obtained

by employing the combined scheme is

$$G_p = 10\log_{10}\left(\frac{\gamma_{bp}^{(1)}}{\gamma_b^{(2)}}\right) = 10\log_{10}\left(\frac{\log_2(M_pM_f)}{\log_2 M_p}\right) \tag{3.32}$$

over the MPSK scheme, and

$$G_f = 10\log_{10}\left(\frac{\gamma_{bf}^{(1)}}{\gamma_b^{(2)}}\right) = 10\log_{10}\left(\frac{\log_2(M_pM_f)}{\log_2 M_f}\right) \tag{3.33}$$

over the MFSK scheme. For example, to achieve a BER of 10^{-3}, $\gamma_b = 7.3$ dB for QPSK and $\gamma_b = 10.9$ dB for 2FSK are required. Using 2FSK-QPSK scheme, we have $G_p = 10\log_{10}\left(\frac{\log_2(2\cdot4)}{\log_2 4}\right) = 1.76$ dB, and $G_f = 10\log_{10}\left(\frac{\log_2(2\cdot4)}{\log_2 2}\right) = 4.77$ dB. Then the required γ_b is $7.3 - 1.76 = 5.54$ (dB) for QPSK and $10.9 - 4.77 = 6.13$ (dB) for FSK. This explains the result of 6.0 dB ($\simeq$ 6.13 dB) for $M_f = 2$ and $M_p = 4$ given in Table 3.1.

Next, we compare the bandwidth efficiency of MFSK-MPSK/DS-CDMA with PSK/DS-CDMA and MFSK/DS-CDMA. For PSK/DS-CDMA system, the bandwidth efficiency can also be expressed by (3.20). The plots of bandwidth efficiency with respect to bit energy to effective noise spectral density ratio for a BER of 10^{-5} are given in Figs. 3.9 and 3.10 for MFSK-BPSK/DS-CDMA and MFSK-QPSK/DS-CDMA respectively. We see that all the schemes except BFSK-BPSK/DS-CDMA perform better than PSK/DS-CDMA. In fact, this can be seen from the required bit energy to noise spectral density ratio. For PSK, $\gamma_b' = 6.8$ dB for a BER of 10^{-3} and $\gamma_b' = 9.6$ dB for a BER of 10^{-5}. Compared to Tables 3.1 and 3.2, all the MFSK-BPSK/DS-CDMA and MFSK-QPSK/DS-CDMA except BFSK-BPSK/DS-CDMA are superior to BPSK/DS-CDMA. The asymptotic bandwidth efficiencies for a BER of 10^{-3} and a BER of 10^{-5} are given in Tables 3.3 and 3.4 respectively.

From Figs. 3.9 and 3.10, Tables 3.3 and 3.4, we see that the overall spectral efficiency is low. In narrowband systems employing MPSK, a spectral efficiency close to $\log_2 M$ b/s/Hz can be reached. This relatively lower bandwidth efficiency in a CDMA system is because of the existence of the MAI . For an uncoded PSK/DS-CDMA system, by choosing the system bandwidth W to be NR_b where N is the PN sequence length, the equation (2.2) becomes $\eta = K/N$. In an ideal case, i.e., when all

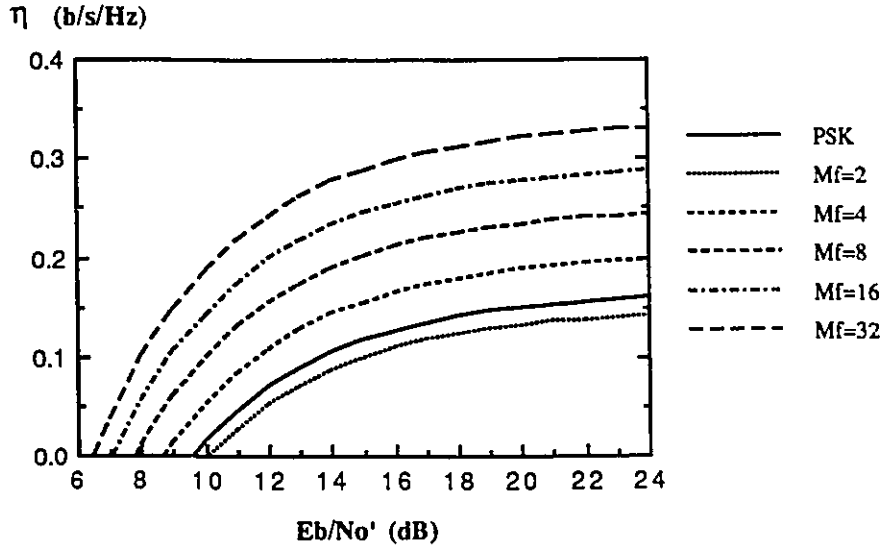

Figure 3.9 : Bandwidth efficiency η vs. E_b/N_0' for MFSK-BPSK/DS-CDMA systems at a BER of 10^{-5}.

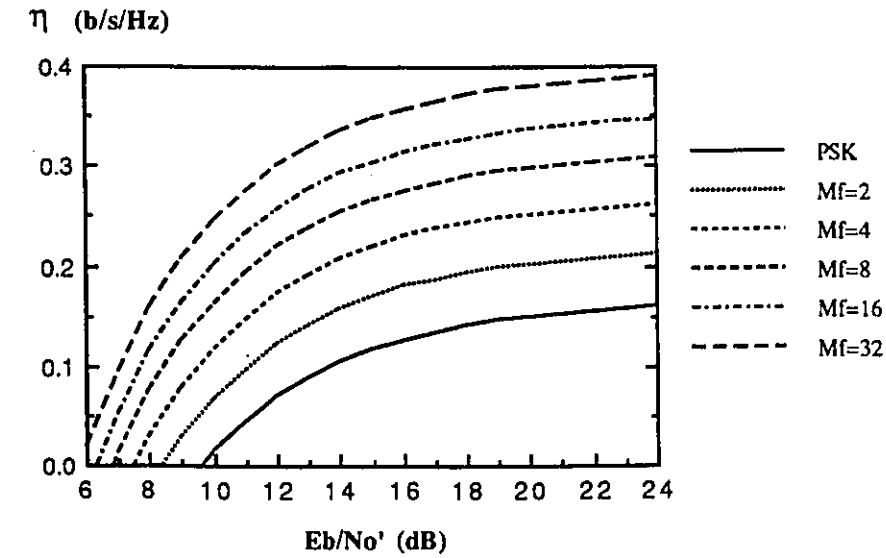

Figure 3.10 : Bandwidth efficiency η vs. E_b/N_0' for MFSK-QPSK/DS-CDMA systems at a BER of 10^{-5}.

Table 3.3 : The asymptotic bandwidth efficiency η_∞ (in b/s/Hz) of MFSK-MPSK/DS-CDMA for a BER of 10^{-3} in an AWGN channel.

	$M_f = 1$	$M_f = 2$	$M_f = 4$	$M_f = 8$	$M_f = 16$	$M_f = 32$
$M_p = 1$		0.122	0.222	0.306	0.377	0.433
$M_p = 2$	**0.313**	0.261	0.336	0.404	0.464	0.520
$M_p = 4$	0.299	**0.377**	**0.453**	**0.508**	**0.557**	**0.611**
$M_p = 8$	0.134	0.185	0.232	0.279	0.328	0.368
$M_p = 16$	0.047	0.060	0.072	0.084	0.097	0.109
$M_p = 32$	0.015	0.018	0.021	0.024	0.027	0.031

Table 3.4 : The asymptotic bandwidth efficiency η_∞ (in b/s/Hz) of MFSK-MPSK/DS-CDMA for a BER of of 10^{-5} in an AWGN channel.

	$M_f = 1$	$M_f = 2$	$M_f = 4$	$M_f = 8$	$M_f = 16$	$M_f = 32$
$M_p = 1$		0.070	0.131	0.185	0.238	0.279
$M_p = 2$	**0.164**	0.143	0.198	0.249	0.292	0.336
$M_p = 4$	0.161	**0.217**	**0.267**	**0.313**	**0.352**	**0.395**
$M_p = 8$	0.072	0.097	0.122	0.147	0.168	0.193
$M_p = 16$	0.025	0.031	0.038	0.044	0.051	0.057
$M_p = 32$	0.008	0.009	0.011	0.013	0.014	0.016

the PN codes are synchronized and orthogonal to each other, the MAI is zero. The maximum number of PN codes in the ideal case is N. Thus a bandwidth efficiency of 1 b/s/Hz can be reached. In this case, the system performance depends only on the channel condition. For a specified BER performance, some amount of MAI can be tolerated by the system, thus more than N PN codes can be used to support more than N simultaneous users, and a bandwidth efficiency of greater than 1 can be reached. This gives us the idea that the selection of PN codes is very important especially for synchronized CDMA systems.

A powerful method to improve the bandwidth efficiency is to use FEC coding. In narrowband systems the use of FEC coding may result with a penalty of expanded bandwidth. In SS systems, FEC codes with shorter PN codes can be employed. The use of FEC coding does not reduce the processing gain [26]. In [71], we considered the bandwidth efficiency of PSK/DS-CDMA and MFSK/DS-CDMA with FEC coding. For MFSK/DS-CDMA scheme, nonbinary codes were used.

MFSK/DS-CDMA systems correspond to the MFSK-MPSK/DS-CDMA systems with $M_p = 1$. For MFSK-MPSK/DS-CDMA systems with $M_p = 2$ and 4, the probability of error is determined mainly by MFSK. For a specified symbol energy to noise spectral density ratio γ_s (the same symbol error rate and thus the same bit error rate can be obtained approximately), the required bit energy to noise spectral density ratio γ_b is $\gamma_s / \log_2(M_p M_f)$. So the energy improvement of MFSK-MPSK/DS-CDMA systems ($M_p = 2$ and 4) over MFSK/DS-CDMA systems is $\log_2(M_p M_f)/\log_2 M_f$. Since the asymptotic bandwidth efficiency is $1.5/\gamma_b$, the improvement in bandwidth efficiency is also $\log_2(M_p M_f)/\log_2 M_f$. The results are shown in Table 3.5 for $M_p = 2$ and 4. It can be seen that for large M_f, the improvement is small.

Table 3.5 : The bandwidth efficiency improvement ratio of MFSK-PSK/DS-CDMA over MFSK/DS-CDMA for $M_p = 2$ and 4.

	$M_f = 2$	$M_f = 4$	$M_f = 8$	$M_f = 16$	$M_f = 32$
$M_p = 2$	2	1.5	1.33	1.25	1.2
$M_p = 4$	3	2	1.67	1.5	1.4

3.4 Relationship between $E_b/N_0^{'}$ and the MAI

In the previous analysis, the BER performance is evaluated as a function of the bit energy to the effective noise spectral density ratio $\gamma_b^{'}$, which is given in (3.19). $\gamma_b^{'}$ is determined by two components, i.e., the bit energy to the noise spectral density ratio γ_b and the MAI. If we define an equivalent bit energy to the MAI ratio as

$$\gamma_{bm} \triangleq \frac{3W/R_b}{2(K-1)}, \tag{3.34}$$

then $\gamma_b^{'}$ can be written as

$$\gamma_b^{'} = [(\gamma_b)^{-1} + (\gamma_{bm})^{-1}]^{-1}. \tag{3.35}$$

For uncoded PSK/DS-CDMA, the ratio $W/R_b = N$ is the total bandwidth spreading factor, where N is the PN sequence length. Thus, γ_{bm} is determined by the PN sequence length N and the number of simultaneous users K. For MFSK-MPSK/DS-CDMA, we have $W/R_b = M_f N/\log_2(M_f M_p)$, and $\gamma_{bm} = 3M_f N/[2\log_2(M_f M_p)(K-1)]$. In this case, γ_{bm} is related to several parameters. When $M_f = 1$ and $M_p = 2$, $W/R_b = N$. Thus the MFSK-MPSK/DS-CDMA reduces to the PSK/DS-CDMA. Corresponding to the definition of γ_{bm}, the equivalent symbol energy to the MAI ratio can be defined as $\gamma_{sm} = 3M_f N/[2(K-1)]$. The symbol energy to the effective noise spectral density ratio $\gamma_s^{'}$ can be also expressed as

$$\gamma_s^{'} = [(\gamma_s)^{-1} + (\gamma_{sm})^{-1}]^{-1}. \tag{3.36}$$

As shown in the previous section, the system performance is determined by $\gamma_b^{'}$. To achieve a specified value of $\gamma_b^{'}$, both γ_b and γ_{bm} should have a greater value. The maximum value of γ_b is usually given by the system design (e.g., the link budget in a satellite communication system design). Thus for a specified value of BER, the required value of $\gamma_b^{'}$ should be less than γ_b. Otherwise, the system design would fail. Another question is the trade-off between γ_b and γ_{bm}. An unbalanced design with a big difference between these two values is not efficient. The asymptotic bandwidth efficiency considered in this thesis is only for analytical convenience. A good trade-off

for γ_b and γ_a is a balanced arrangement. If $\gamma_b = \gamma_a$, we have $\gamma_b' = \gamma_b/2$. Thus, γ_b' should be 3 dB less than γ_b.

From (3.20), to obtain a bandwidth efficiency close to η_∞, γ_b needs to be much larger than γ_b'. Dividing (3.20) by (3.21), we have the normalized bandwidth efficiency

$$\eta_{nor} \triangleq \frac{\eta}{\eta_\infty} = 1 - \frac{\gamma_b'}{\gamma_b}. \tag{3.37}$$

This relationship between η_{nor} and γ_b/γ_b' is plotted in Fig. 3.11. For example, if we need $\eta \geq 0.9\eta_\infty$, then we must have $\gamma_b \geq 10\gamma_b'$, or $\gamma_b \geq \gamma_b' + 10$ (in dB).

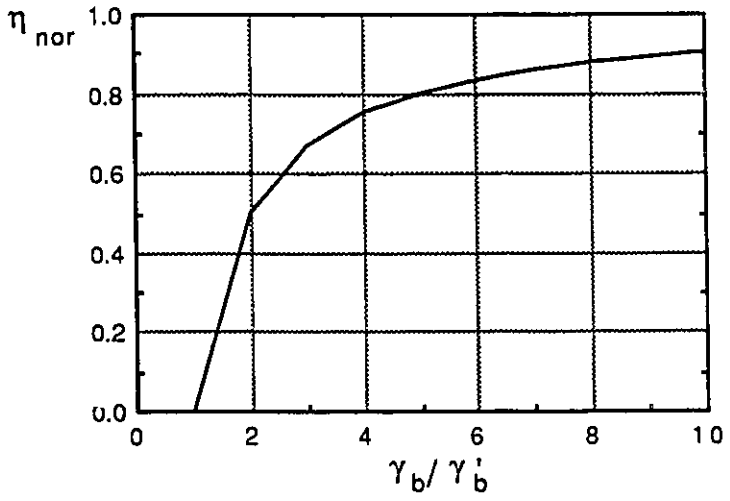

Figure 3.11 : Relationship between the normalized bandwidth efficiency η_{nor} and γ_b/γ_b'.

In our study, the PN sequence is assumed to be a random signature sequence. As mentioned in Section 2.1, for small number of simultaneous users, the Gaussian approximation is not accurate. In this case, an improved Gaussian approximation can be used. For the MFSK-MPSK/DS-CDMA system, as shown in (3.16), the parameter $W/R_b = N$ in (3.35) and (3.36) needs to be replaced by $M_f N/\log_2(M_f M_p)$. The standard and the improved Gaussian approximation methods are considered in [43]. For large K, both approximations agree with the accurate analysis. A comparison

between the two Gaussian approximations is made in Appendix B which shows the validity of using the standard Gaussian approximation in our analysis.

Due to the MAI, error floor exists in a DS-CDMA system. For $K > 1$, the value of γ_b' is limited by $3(W/R_b)/2(K-1)$. In fact, for small K, when the MAI is properly controlled, the effect of MAI can be ignored. For a large value of K, the MAI resembles noise and results in an error floor. However, what we are interested in is to achieve a specified BER. If the error floor is lower than the specified BER, then the specified BER is achievable.

3.5 MFSK-DMPSK/DS-CDMA

As shown in the previous sections, the MFSK-MPSK/DS-CDMA schemes achieve higher capacities than both MFSK/DS-CDMA and PSK/DS-CDMA schemes. However, the implementation of coherent detection of PSK is difficult. In [76], Simon and Polydoros analyzed a coherent FH FSK system, in which phase continuity from one hop to another is assumed. They mentioned that "state-of-the-art coherent frequency synthesizers will undoubtedly allow the design of such a system to be feasible in the near future". In the MFSK-MPSK/DS-CDMA systems, similar argument applies. One possible way of implementing a coherent system is to use a pilot tone as a carrier reference. If all the frequency tones are transmitted coherently, then only one reference tone can be used for coherently detecting all the M frequency tones.

To avoid the difficulty of obtaining and maintaining a carrier phase reference, an efficient method is to use differential detection. By combining the noncoherent MFSK and DMPSK schemes, we have a new system, namely MFSK-DMPSK/DS-CDMA. Since the DMPSK with large M_p is not power efficient, we will consider only $M_p = 2$ and 4. Differential detection is easily implemented for a single tone scheme. In the multi-tone scheme as in the case of MFSK, however, there is a question of finding the relative pair of tones. In our proposed system, an algorithm is presented in the following subsection.

3.5.1 Detection of MFSK-DPSK/DS-CDMA Signals

When $M_f = 1$, the proposed system reduces to the DPSK/DS-CDMA. For a DPSK/DS-CDMA system, the differential detector is shown in Fig. 3.12 [30]. We see that there are two main branches of which one employs a delay of T_s seconds. For each branch, there are two sub-branches which are the I and Q-channels. The four outputs are denoted as U_I, U_Q, U_{dI} and U_{dQ} respectively. Based on these output samples, decisions can be made. A brief description of the decision process is as follows (see [78, 79] for detail). Assume that two successively transmitted signals are $a_k(t)\cos(2\pi f_c t + \phi_0)$ and $a_k(t)\cos(2\pi f_c t + \phi_1)$, where ϕ_i (i=0, 1) takes 0 and π, and the difference between the successive phases represents the information. In the U_I branch, the received signal (interference and noise free) is first multiplied with a local reference:

$$a_k(t)\cos(2\pi f_c t + \phi_1)a_k(t)\cos(2\pi f_c t) = a_k^2(t)\frac{1}{2}[\cos(4\pi f_c t + \phi_1) + \cos(\phi_1)]. \quad (3.38)$$

The squaring operation of the PN sequence $a_k(t)$ indicates despreading. After integration (equivalent to low pass filtering) and sampling, we have

$$U_I = \frac{1}{2}\cos(\phi_1). \quad (3.39)$$

Similarly, we have

$$U_Q = -\frac{1}{2}\sin(\phi_1), \quad (3.40)$$

$$U_{dI} = \frac{1}{2}\cos(\phi_0), \quad (3.41)$$

and

$$U_{dQ} = -\frac{1}{2}\sin(\phi_0). \quad (3.42)$$

Then, we have the decision variable

$$U \triangleq 4(U_I U_{dI} + U_Q U_{dQ}) = [\cos(\phi_1)\cos(\phi_0) + \sin(\phi_1)\sin(\phi_0)] = \cos(\phi_1 - \phi_0). \quad (3.43)$$

When $\phi_1 = \phi_0$, $U = 1$; when $\phi_1 \neq \phi_0$, $U = 0$. The above discussion demonstrated the detection principle.

Using this single tone DPSK detector, we can build a receiver for the MFSK-DPSK/DS-CDMA scheme. As will be shown later, the performance of MFSK-DPSK/DS-CDMA systems for $M_p = 2$ and 4 are almost the same in an AWGN

channel. In a fading channel, $M_p = 2$, i.e., DBPSK performs better, hence we focus on describing the structure for the MFSK-DBPSK/DS-CDMA system.

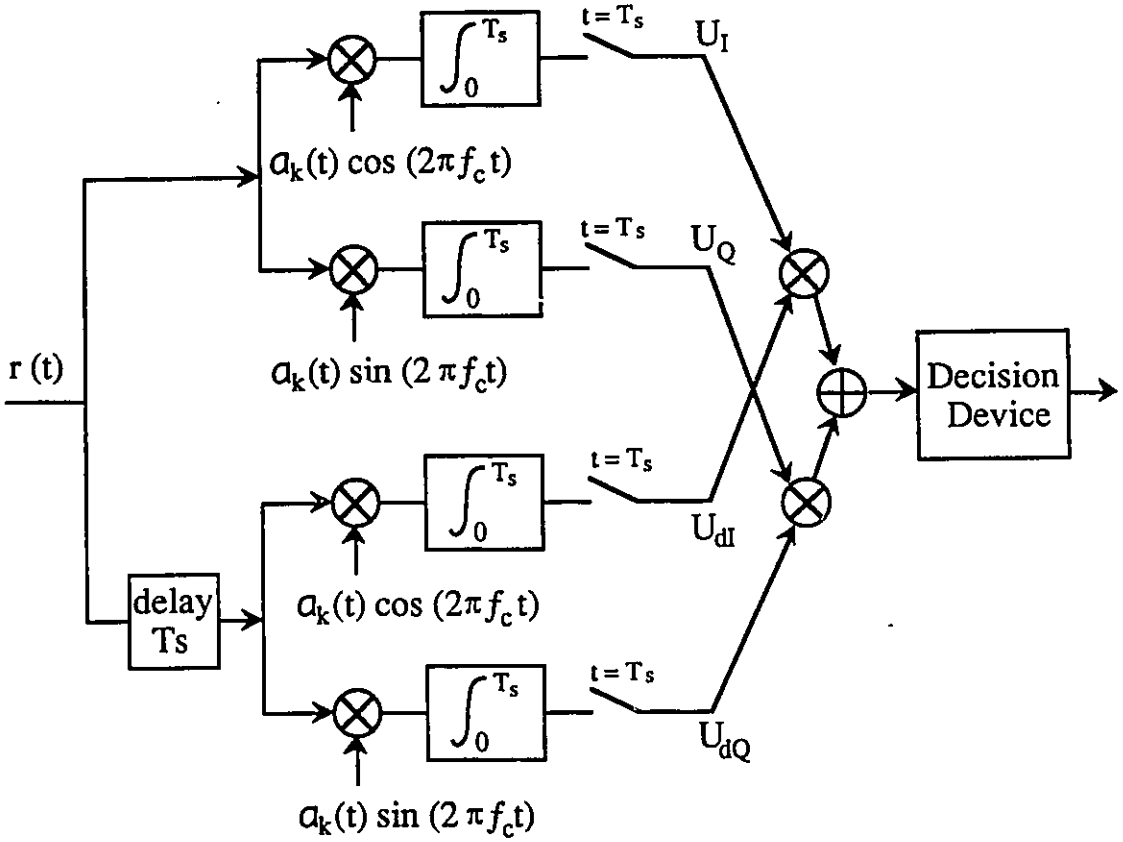

Figure 3.12 : Structure of the DPSK detector in a DPSK/DS-CDMA system.

The transmitter of the MFSK-DPSK/DS-CDMA scheme is shown in Fig. 3.13-(a). It is similar to the transmitter structure of MFSK-MPSK/DS-CDMA. The difference is in the DPSK modulator which employs a differential encoder. The receiver of the MFSK-DPSK/DS-CDMA scheme is shown in Fig. 3.13-(b). There are M_f matched filters (MF) corresponding to the M_f frequency tones. Each matched filter is composed of the upper branches in Fig. 3.12, (yielding U_I and U_Q) with the frequency corresponding to one of the M_f tones. The two outputs from each matched filter are the sampled values from I-channel and Q-channel respectively, and are denoted

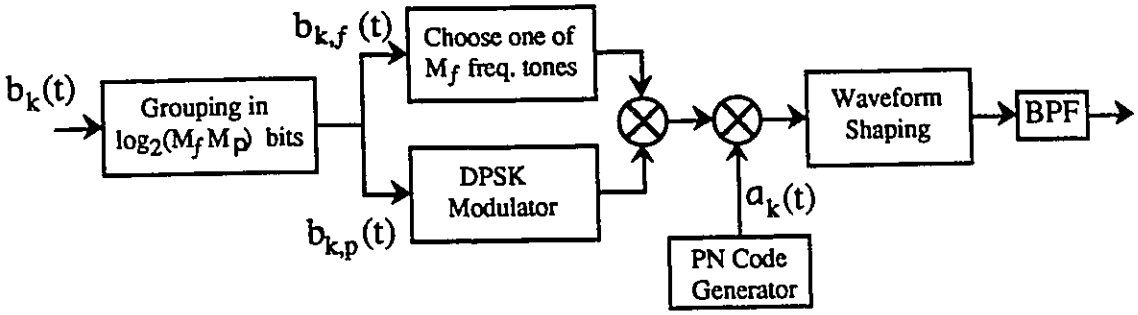

(a)

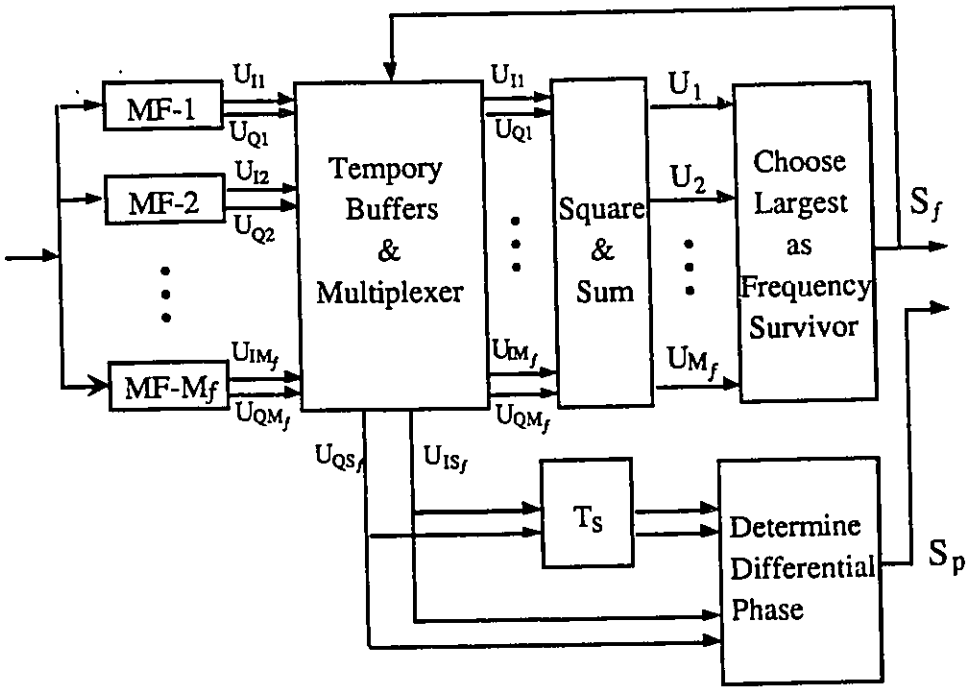

(b)

Figure 3.13 : Block diagram of the MFSK-DPSK/DS-CDMA system. (a) Transmitter; (b) Receiver.

as U_{Im} and U_{Qm} $(m = 1, 2, \cdots, M_f)$. The algorithm performing the symbol decision works as follows:

(1) The $2M_f$ inputs (from M_f matched filters) are saved in $2M_f$ temporary buffers which can be accessed by the survivor tone. These data are kept for only one symbol interval.

(2) Squared sum operations are performed on each pair of I and Q inputs: $U_m^2 = U_{Im}^2 + U_{Qm}^2$, $(m = 1, 2, \cdots, M_f)$. Thus, there are M_f outputs corresponding to M_f matched filters.

(3) The M_f data U_m^2, $(m = 1, 2, \cdots, M_f)$ are compared and the largest one is chosen as the survivor S_f.

(4) The survivor S_f is used to select a pair of data U_{IS_f} and U_{QS_f} in the temporary buffers. Using also the one-symbol delayed pair of data, the differential phase is determined as shown in Fig. 3.12. The result is denoted as S_p.

(5) The MFSK decision S_f and the differential detection output S_p together form the symbol decision.

In the above algorithm, all the operations are in baseband and can be done by using DSP circuits.

3.5.2 Performance over an AWGN Channel

The BER performance and bandwidth efficiency of this system can be analyzed in a similar manner to that of MFSK-MPSK/DS-CDMA systems. Since the scheme for large M_p is not power efficient, we only consider this scheme for $M_p = 2$ and 4. For the calculation of the probability of symbol error, (3.23) can be used. Now P_p is given by

$$P_p = \frac{1}{2} e^{-\gamma_s'} \tag{3.44}$$

for $M_p = 2$ [75]. For DQPSK, the BER is given by [75]

$$P_b^{(1)} = Q(a,b) - \frac{1}{2} I_0(ab) \exp[-\frac{1}{2}(a^2+b^2)], \tag{3.45}$$

where $Q(\cdot,\cdot)$ is the generalized Q function [75], and

$$a = \sqrt{2\gamma_b'(1-\frac{1}{\sqrt{2}})}, \tag{3.46}$$

$$b = \sqrt{2\gamma_b'(1+\frac{1}{\sqrt{2}})}. \tag{3.47}$$

Since for QPSK, $\gamma_s' = 2\gamma_b'$, and $P_b \simeq \frac{1}{2} P_s$, thus we have

$$P_p = 2P_b^{(1)}, \tag{3.48}$$

and a and b are modified as

$$a = \sqrt{\gamma_s'(1-\frac{1}{\sqrt{2}})}, \tag{3.49}$$

and

$$b = \sqrt{\gamma_s'(1+\frac{1}{\sqrt{2}})}. \tag{3.50}$$

For BER values of 10^{-3} and 10^{-5}, the required bit energy to noise ratio (in dB) is given in Table 3.6 and Table 3.7 respectively. From these results, we see that the performance of MFSK-DMPSK/DS-CDMA is better than that of MFSK/DS-CDMA scheme ($M_p = 1$). Compared to the MFSK-MPSK/DS-CDMA systems, the performance for $M_p = 2$ is the same. This is because the performance is determined by MFSK (since the probability of error of DBPSK is lower than that of MFSK). There is no big difference between the performance of MFSK-DBPSK/DS-CDMA and MFSK-DQPSK/DS-CDMA. The latter is a little better at a BER of 10^{-3} and a little worse for a BER of 10^{-5}. The reason for this lies in the fact that the difference between DBPSK and DQPSK becomes large in lower BER range. For $M_f = 1$, we see that DBPSK/DS-CDMA is better than DQPSK/DS-CDMA. The performance difference is 1.5 dB for a BER of 10^{-3} and a little more than 2 dB for a BER of 10^{-5}.

The asymptotic bandwidth efficiencies for a BER of 10^{-3} and a BER of 10^{-5} are given in Tables 3.8 and 3.9 respectively. Since MFSK-DQPSK/DS-CDMA and MFSK-DBPSK/DS-CDMA have not much difference in performance, the less complex one, i.e., the one with BPSK is preferred.

Table 3.6 : The required SNR per bit γ_b' (in dB) for a BER of 10^{-3} for MFSK-DMPSK/DS-CDMA systems in an AWGN channel.

	$M_f = 1$	$M_f = 2$	$M_f = 4$	$M_f = 8$	$M_f = 16$	$M_f = 32$
$M_p = 1$		10.9	8.3	6.9	6.0	5.4
$M_p = 2$	**7.9**	7.6	6.5	5.7	5.1	4.6
$M_p = 4$	9.4	7.6	**6.3**	**5.5**	**4.8**	**4.3**

Table 3.7 : The required SNR per bit γ_b' (in dB) for a BER of 10^{-5} for MFSK-DMPSK/DS-CDMA systems in an AWGN channel.

	$M_f = 1$	$M_f = 2$	$M_f = 4$	$M_f = 8$	$M_f = 16$	$M_f = 32$
$M_p = 1$		13.3	10.6	9.1	8.0	7.3
$M_p = 2$	**10.4**	**10.2**	**8.8**	**7.8**	**7.1**	**6.5**
$M_p = 4$	12.7	10.3	9.0	8.0	7.2	6.6

Table 3.8 : The asymptotic bandwidth efficiency η_∞ (in b/s/Hz) of MFSK-DMPSK/DS-CDMA for a BER of 10^{-3} in an AWGN channel.

	$M_f = 1$	$M_f = 2$	$M_f = 4$	$M_f = 8$	$M_f = 16$	$M_f = 32$
$M_p = 1$		0.122	0.222	0.306	0.377	0.433
$M_p = 2$	**0.243**	0.261	0.336	0.404	0.464	0.520
$M_p = 4$	0.172	0.261	**0.352**	**0.423**	**0.497**	**0.557**

Table 3.9 : The asymptotic bandwidth efficiency η_∞ (in b/s/Hz) of MFSK-DMPSK/DS-CDMA for a BER of 10^{-5} in an AWGN channel.

	$M_f = 1$	$M_f = 2$	$M_f = 4$	$M_f = 8$	$M_f = 16$	$M_f = 32$
$M_p = 1$		0.070	0.131	0.185	0.238	0.279
$M_p = 2$	**0.137**	**0.143**	**0.198**	**0.249**	**0.292**	**0.336**
$M_p = 4$	0.081	0.140	0.189	0.238	0.286	0.328

3.5.3 Performance over Fading Channels

We consider only the MFSK-DBPSK/DS-CDMA system. The channel is assumed to be slow Rician fading, with the special case of $\kappa = 0$ corresponding to the Rayleigh fading. To determine the BER performance, we need to find the symbol error rate of DPSK and MFSK over Rician fading channels. The two symbol error rates are found in Appendix A equations(A.8) and (A.10) as

$$P_{\text{DPSK}} = \frac{1+\kappa}{2\bar{\gamma}_b + 2(1+\kappa)} \exp\left[-\frac{\kappa\bar{\gamma}_b}{\bar{\gamma}_b + (1+\kappa)}\right], \tag{3.51}$$

and

$$P_{\text{MFSK}} = \sum_{n=1}^{M-1} (-1)^{n+1} \binom{M-1}{n} \frac{1+\kappa}{n\bar{\gamma}_s + (n+1)(1+\kappa)} \exp\left[-\frac{\kappa n\bar{\gamma}_s}{n\bar{\gamma}_s + (n+1)(1+\kappa)}\right]. \tag{3.52}$$

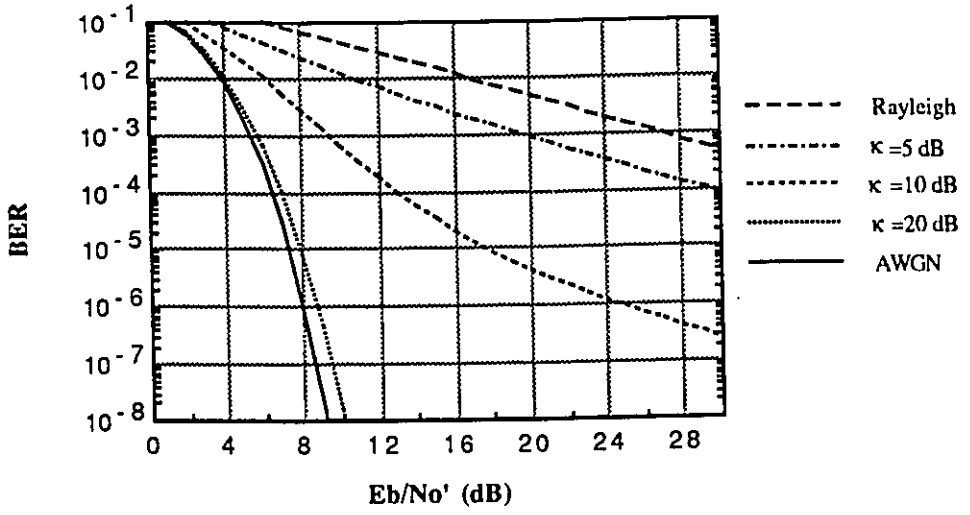

Figure 3.14 : BER performance of 16FSK-DBPSK/DS-CDMA over different channels.

In Fig. 3.14, we give the performance curve of 16FSK-DBPSK/DS-CDMA over AWGN and fading channels. We see that the performance in Rician fading is quite close to that in an AWGN channel with $\kappa = 20$ dB, and similar to that in a Rayleigh

fading with $\kappa = 5$ dB. For a typical satellite channel with $\kappa = 10$ dB, the performance curve is just in between the two extreme cases.

The system performance over a Rayleigh channel and Rician channel with $\kappa = 10$ dB for a BER of 10^{-3} are given in Tables 3.10 and 3.11 respectively. The corresponding asymptotic bandwidth efficiencies are given in Tables 3.12 and 3.13 respectively. For Rayleigh fading, the performance of MFSK-DPSK/DS-CDMA is a little better than DPSK/DS-CDMA. When M_f is small, the improvement of MFSK-DPSK/DS-CDMA over MFSK/DS-CDMA is large. When M_f is large, the improvement is very small. For Rician fading channel with $\kappa = 10$ dB (a typical parameter in satellite channel), for $M_f = 2$, the improvement of MFSK-DPSK/DS-CDMA over MFSK/DS-CDMA is about 3 dB, while for $M_f = 16$, the improvement is about 1 dB.

Table 3.10 : The required SNR per bit $\bar{\gamma}_b'$ (in dB) for a BER of 10^{-3} for MFSK-DPSK/DS-CDMA systems over a Rayleigh fading channel.

	$M_f = 1$	$M_f = 2$	$M_f = 4$	$M_f = 8$	$M_f = 16$	$M_f = 32$
$M_p = 1$	-	30.0	27.9	26.9	26.5	26.2
$M_p = 2$	27.0	27.0	26.5	26.1	25.9	25.8

Table 3.11 : The required SNR per bit $\bar{\gamma}_b'$ (in dB) for a BER of 10^{-3} for MFSK-DPSK/DS-CDMA systems over a Rician fading channel with $\kappa = 10$ dB.

	$M_f = 1$	$M_f = 2$	$M_f = 4$	$M_f = 8$	$M_f = 16$	$M_f = 32$
$M_p = 1$	-	14.2	11.8	10.6	9.9	9.4
$M_p = 2$	11.2	10.8	9.9	9.3	8.9	8.6

In Rayleigh fading channel, the bandwidth efficiency is very low. To improve the performance, FEC coding must be employed. For Rician fading (with $\kappa = 10$ dB), the bandwidth efficiency is much better.

In the tables, the entry with $M_f = 1$ and $M_p = 2$ corresponds to the differential PSK/DS-CDMA scheme. Compared to this scheme, MFSK-DPSK/DS-CDMA is a

Table 3.12 : The asymptotic bandwidth efficiency η_∞ (in b/s/Hz) of the MFSK-DPSK/DS-CDMA over a Rayleigh fading channel for a BER of 10^{-3}.

	$M_f = 1$	$M_f = 2$	$M_f = 4$	$M_f = 8$	$M_f = 16$	$M_f = 32$
$M_p = 1$	-	0.0015	0.0024	0.0031	0.0034	0.0036
$M_p = 2$	0.0030	0.0030	0.0034	0.0037	0.0039	0.0039

Table 3.13 : The asymptotic bandwidth efficiency η_∞ (in b/s/Hz) of the MFSK-MPSK/DS-CDMA over a Rician fading channel ($\kappa = 10$ dB) for a BER of 10^{-3}.

	$M_f = 1$	$M_f = 2$	$M_f = 4$	$M_f = 8$	$M_f = 16$	$M_f = 32$
$M_p = 1$	-	0.057	0.099	0.131	0.153	0.172
$M_p = 2$	0.114	0.125	0.153	0.176	0.193	0.207

little better. In Rayleigh fading channel, however, since the improvement is very small, there is no advantage in using the MFSK-DPSK/DS-CDMA. In Rician fading channel, we have two and half dB gain in using 32FSK-DPSK/DS-CDMA.

3.6 FEC Coded MFSK-DPSK/DS-CDMA

3.6.1 Concept of a Coded CDMA System

From an FEC coding point of view, an SS signal with a PN sequence of length N corresponds to a rate $1/N$ code with constraint length one. Such a code is equivalent to a repetition code which is a trivial form of coding. In practical SS systems, efficient FEC coding techniques are widely used to improve the system performance [23, 80].

Both FEC coding and PN sequence spreading expand the system bandwidth. In an SS system, however, FEC coding can be realized without further increasing the system bandwidth. The coded SS system does not reduce the overall processing gain [23, 26]. An optimum processing gain for a block coded SS system in the presence of tone and Gaussian jammers is considered in [81]. In that paper, however, the received signal is first chip-by-chip processed by an integrate-and-dump filter and

then multiplied by the PN sequence, which is not an efficient despreading method. In [80], Viterbi proposed a very low rate coding scheme in which the whole system bandwidth is spread only by FEC coding. The relationship of FEC coding and PN sequence spreading in an SS system remains to be an open issue. It is not further discussed in this thesis. In this section, some well known codes will be examined in our proposed CDMA schemes.

A typical coded DS-SS system is illustrated in Fig. 3.15. A data sequence is FEC coded, modulated, and spread by a PN sequence. In the receiver, a reverse processing is carried out. For a channel with memory, data interleaving is necessary. An interleaver after the FEC encoder and a deinterleaver before the FEC decoder should be added.

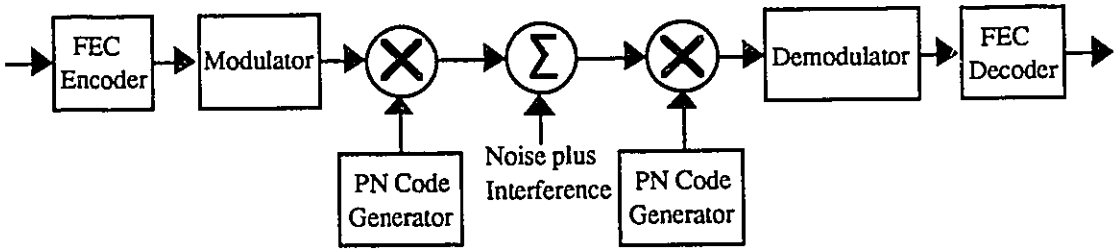

Figure 3.15 : A typical FEC coded DS-SS system.

In a coded SS system, the modulator, the PN spreader, the channel, the PN despreader and the demodulator can be considered as an equivalent modulation channel with its input coming from the FEC encoder and its output going to the FEC decoder. Thus, the implementation of the coding is not different in an SS system as in a narrowband system. It is well known that, for a system with hard decision decoding, the equivalent modulation channel (uncoded part) is equivalent to a memoryless symmetric channel. Thus, the performance of the coded system is determined by the symbol error rate before decoding. For a system with soft decision decoding, the equivalent modulation channel still applies [82]. Coming back to the coded CDMA system, our conclusion is that it can be analyzed in a similar manner to the corresponding narrowband system. The difference is in the SNR expression.

The proposed systems all employ M-ary modulation schemes. So we will consider only nonbinary coding. An important class of nonbinary block coding is Reed-Solomon coding. However, only hard decision decoding is practically available[1] for this code. Well known nonbinary convolutional codes are dual-k codes and rate-1 codes [75, 82]. In [83], two classes of nonbinary convolutional codes are studied, which are extensions of dual-k codes and rate-1 codes. Some concatenated codes are also good options.

3.6.2 Performance Evaluation

For the MFSK-DPSK/DS-CDMA scheme, the analysis is performed only for hard decision decoding. We have considered using Reed-Solomon codes and dual-k codes.

For an (n, k) Reed-Solomon code [75, 84], the parameter n can be chosen as $M-1$, where $M = M_f M_p = 2M_f$. The error correcting ability $t = (n-k)/2$, where the parameter k takes the value in [1,2, $\cdots$, $n-1$]. The code rate is $r_c = k/n$. The probability of symbol error is

$$P_s = \frac{1}{n} \sum_{i=t+1}^{n} i \binom{n}{i} p^i (1-p)^{n-i}, \tag{3.53}$$

where the probability of error for the uncoded symbol p is given by (3.23):

$$p \simeq P_f + P_p. \tag{3.54}$$

The average symbol energy to the equivalent noise spectral density ratio given by

$$\gamma_s' = r_c \log_2 M \gamma_b'. \tag{3.55}$$

For the dual-k codes with each symbol repeated r times, from the transfer function, the number of symbol errors β_d associated with a path having a Hamming distance d from the all-zero path can be expressed as [75]

$$\sum_{d=4r}^{\infty} \beta_d D^d = \frac{(2^k-1)D^{4r}}{[1-2D^r-(2^k-3)D^{2r}]^2}. \tag{3.56}$$

[1]Soft decision decoding of RS codes in general is impractical due to the high complexity of the decoding algorithm. An efficient soft decoding algorithm for simple RS codes is discussed in [87].

A dual-k code has a code rate of $1/2r$. Its free distance is $d_{free} = 4r$. The Hamming distance is referred for the M-ary ($M = 2^k$) symbol. The probability of symbol error is upper bounded by

$$P_s \leq \sum_{d=d_{free}}^{\infty} \beta_d P_2(d). \tag{3.57}$$

For hard decision decoding, the pairwise probability of error is

$$P_2(d) = \begin{cases} \sum_{i=(d+1)/2}^{d} \binom{d}{i} p^i (1-p)^{d-i}, & (d \text{ odd}), \\ \sum_{i=d/2-1}^{d} \binom{d}{i} p^i (1-p)^{d-i} + \frac{1}{2}\binom{d}{d/2} p^{d/2}(1-p)^{d/2}, & (d \text{ even}). \end{cases} \tag{3.58}$$

The probability of bit error is given by multiplying P_s by a factor $\frac{2^{k-1}}{2^k-1}$.

In Fig. 3.16, the BER performance of 16FSK-DBPSK/DS-CDMA over an AWGN channel using Reed-Solomon codes is given with error correcting capability $t = 1$, 2 and 4. For this scheme, the code length is 31. Compared to the uncoded case, the performance of coded systems improves as t increases. However, at low SNR, the improvement due to coding is not significant. At a BER of 10^{-3}, the coding gain of the coded scheme with $t = 4$ is only a little more than one dB. At low BER, the gain increases. More powerful codes with larger t can be used to further improve the system performance. However, the advantage of these codes disappears at a low SNR value.

The BER performance of 8FSK-DBPSK/DS-CDMA over a Rician fading channel (with $\kappa = 10$ dB) using Reed-Solomon codes is given in Fig. 3.17. The code length is 15. The error correcting capability t is 1, 2, 4 and 8 respectively. At a BER of 10^{-3}, using the codes with $t = 4$ and 8, the coding gain is more than 3 dBs. At a BER of 10^{-5}, the gain is up to 8 dBs.

In Fig. 3.18, we have the BER performance over a Rayleigh fading channel. The system considered is again 16FSK-DBPSK/DS-CDMA. We see that even at a BER of 10^{-3}, the coding gain is pretty large. This gain is attributable to the equivalent diversity introduced by coding.

Next we examine the effects of the dual-k codes using hard decision decoding. In Figs. 3.19, BER performance is given for $M_f = 4$, 8 and 16 over an AWGN channel.

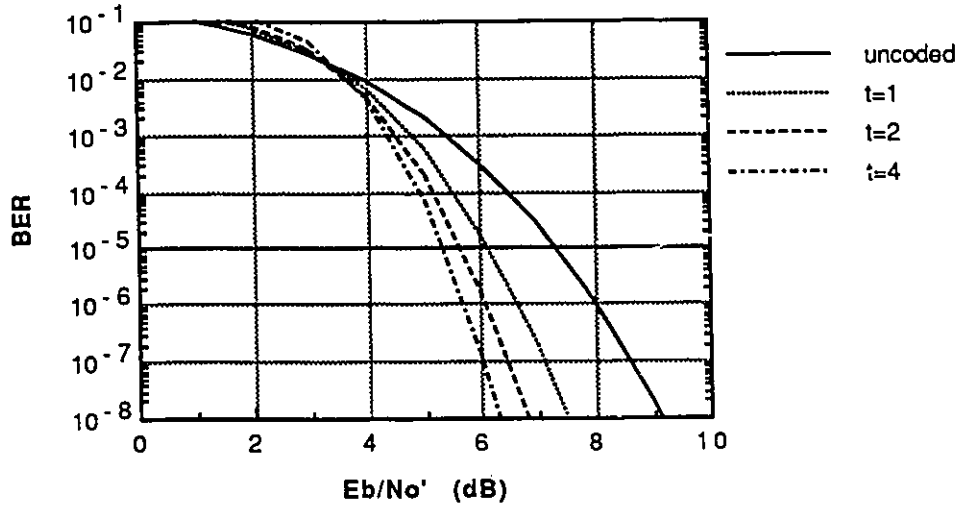

Figure 3.16 : BER performance of 16FSK-DBPSK/DS-CDMA over an AWGN channel using Reed-Solomon codes with code length 31 and error correcting capability of $t = 1$, 2 and 4 respectively.

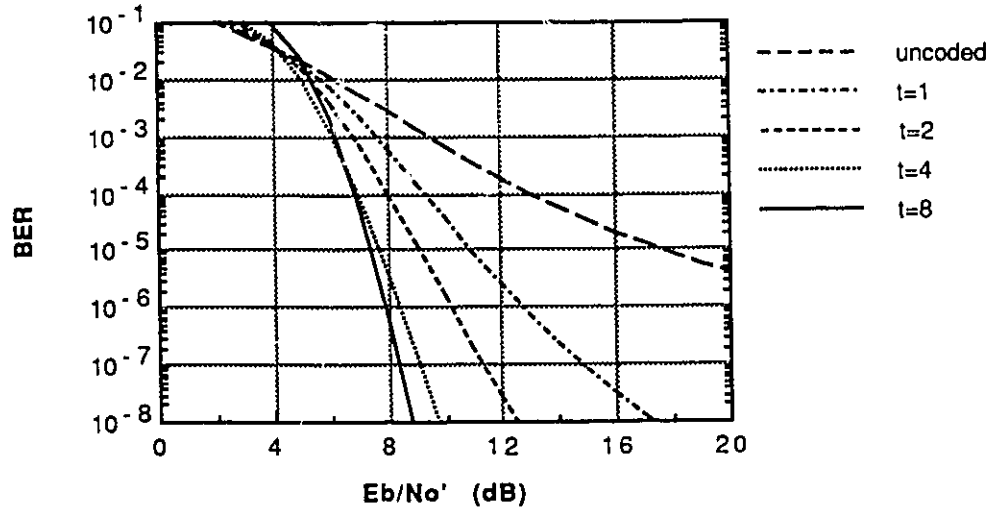

Figure 3.17 : BER performance of 8FSK-DBPSK/DS-CDMA over a Rician fading channel (κ = 10 dB) using Reed-Solomon codes with code length 15 and error correcting capability of $t = 1$, 2 and 4 respectively.

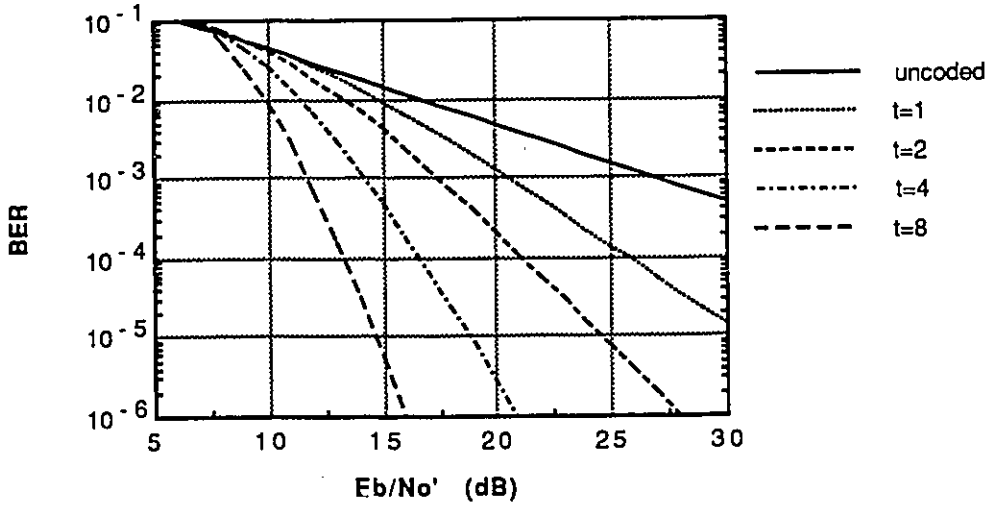

Figure 3.18 : BER performance of 16FSK-DBPSK/DS-CDMA over a Rayleigh fading channel using Reed-Solomon codes with code length 31 and error correcting capability of $t = 1$, 2 and 4 respectively.

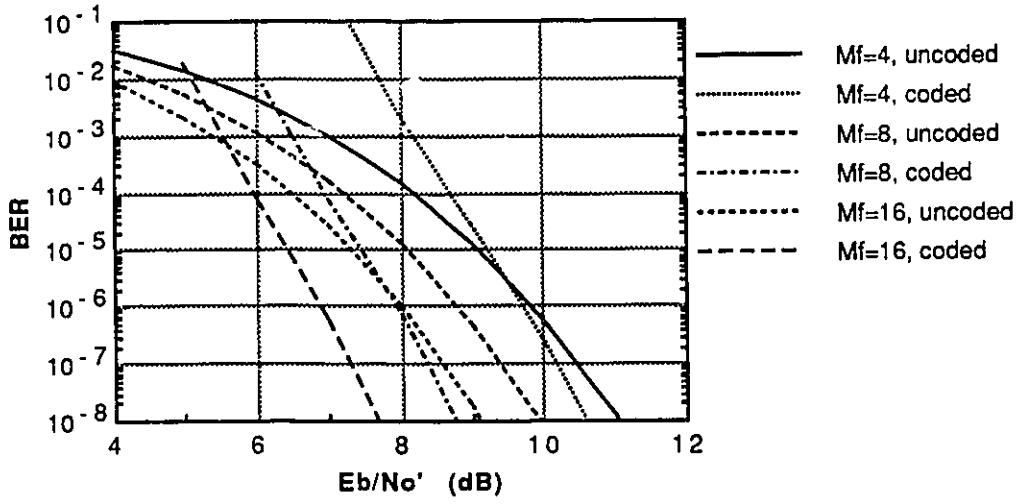

Figure 3.19 : BER performance of MFSK-DBPSK/DS-CDMA over an AWGN channel using dual-k codes with $k = 3$, 4 and 5 for $M_f = 4$, 8 and 16 respectively.

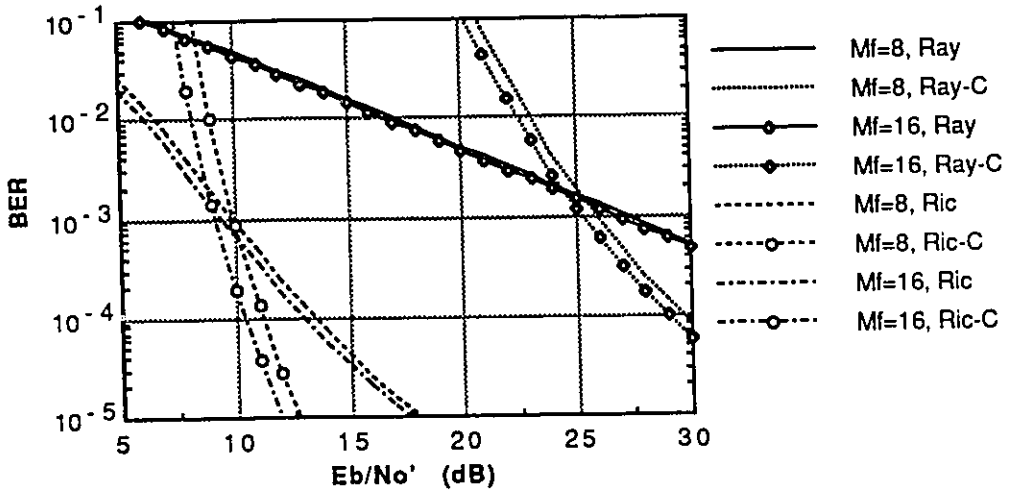

Figure 3.20 : BER performance of MFSK-DBPSK/DS-CDMA over fading channels using dual-k codes with $k = 4$ and 5 for $M_f = 8$ and 16 respectively. Ray: Rayleigh fading and no-coding; Ray-C: Rayleigh fading with coding; Ric: Rician fading ($\kappa = 10$ dB) and no-coding; Ric-C: Rician fading ($\kappa = 10$ dB) with coding.

At a BER of 10^{-3}, no coding gain is achieved. At a BER of 10^{-5}, the dual-5 code for the 16FSK-DBPSK/DS-CDMA scheme has only one dB gain. This is due to the inefficiency of the hard decision decoding. In Fig. 3.20, BER performance using dual-k codes for $M_f = 8$ and 16 over fading channels is shown. At a BER of 10^{-3}, there is no coding for both Rayleigh and Rician fading. At a lower BER, the gain becomes larger. However, compared to the Reed-Solomon codes, dual-k codes using hard decision decoding is not powerful.

Table 3.14 : The required SNR per bit $\bar{\gamma}_b'$ (in dB) and the asymptotic bandwidth efficiency η_∞ (in b/s/Hz) for a BER of 10^{-3} for the 16FSK-DBPSK/DS-CDMA system.

schemes	AWGN	Rician ($\kappa = 10$ dB)	Rayleigh
uncoded	5.5/0.423	10.0/0.15	26.8/0.0031
RS ($n = 31, t = 1$)	4.8/0.497	8.0/0.238	20.5/0.013
RS ($n = 31, t = 2$)	4.5/0.532	7.4/0.273	17.3/0.028
RS ($n = 31, t = 4$)	4.3/0.557	7.4/0.273	14.0/0.060
RS ($n = 31, t = 8$)	–	–	11.6/0.104
dual-k	5.5/0.423	9.2/0.180	25.2/0.0045

Table 3.15 : The required SNR per bit $\bar{\gamma}_b'$ (in dB) and the asymptotic bandwidth efficiency η_∞ (in b/s/Hz) for a BER of 10^{-5} for the 16FSK-DBPSK/DS-CDMA system.

schemes	AWGN	Rician ($\kappa = 10$ dB)	Rayleigh
uncoded	7.3/0.279	18.3/0.022	–
RS ($n = 31, t = 1$)	6.1/0.368	11.2/0.114	–
RS ($n = 31, t = 2$)	5.6/0.413	9.6/0.164	24.7/0.0051
RS ($n = 31, t = 4$)	5.3/0.442	9.1/0.185	18.8/0.020
RS ($n = 31, t = 8$)	–	–	14.7/0.051
dual-k	6.4/0.344	11.8/0.099	–

In Tables 3.14 and 3.15, we list the required SNR for various coded systems over AWGN and fading channels. The corresponding asymptotic bandwidth efficiencies

are also given in the same tables. The coding gains at a BER of 10^{-3} are smaller than those at a BER of 10^{-5}. The Reed-Solomon codes have large gains in Rayleigh fading channels. While the dual-k codes do not perform well.

3.7 Summary

In this Chapter we first considered MFSK-MPSK/DS-CDMA systems, in which MFSK demodulation is noncoherent and MPSK demodulation is coherent. It was shown that except for BFSK-BPSK/DS-CDMA, all the MFSK-BPSK/DS-CDMA and MFSK-QPSK/DS-CDMA perform better than the PSK/DS-CDMA system. Compared to MFSK/DS-CDMA, MFSK-MPSK/DS-CDMA has an improvement in bandwidth efficiency by a factor of $\log_2(M_p M_f)/\log_2 M_f$. For large M_f, the improvement is not significant. The primary advantage of MFSK-MPSK/DS-CDMA is to increase the effective signal energy to noise spectral density ratio for a given bit energy to noise spectral density ratio.

Secondly, we considered MFSK-DMPSK/DS-CDMA systems. Due to power efficiency of the DBPSK relative to other DMPSK systems, we focused on a system with $M_p = 2$. The performance is examined over both AWGN and fading channels. In an AWGN channel, the proposed systems have one to three dB gains over the corresponding MFSK/DS-CDMA systems. Compared to the PSK/DS-CDMA, up to 4 dB gain is achieved with large M_f, while in a Rayleigh fading channel, the gain is relatively small. Using FEC coding, system performance is greatly improved especially in a Rayleigh fading channel. Reed-Solomon codes were shown to be very powerful. The relative power inefficiency of dual-k codes lies in the hard decision decoding.

All the analyses are based on the bit energy to effective noise spectral density ratio γ_b'. In section 3.4, we discussed the relationship between γ_b' and the MAI and pointed out the validity of the Gaussian approximation.

Chapter 4

MFSK/DS-CDMA Employing Orthogonal Codes

4.1 Introduction

In conventional CDMA systems, PN codes (or PN sequences) function as user's identity signatures. Each user has a distinct PN code. Thus, multiple users can be identified and distinguished. On the other hand, a PN code can also be used to represent the data information. M_c different PN codes can represent $\log_2 M_c$ bits of information. If the number of available codes is more than the number of users, each user can use more than one code not only for its identity signature but also for its data transmission. The application of orthogonal codes to CDMA was discussed in [85] and [86]. In this chapter, we consider the orthogonal codes in MFSK/DS-CDMA systems. The resultant system is MFSK-OC/DS-CDMA. This system is characterized by two parameters: the number of frequency tones M_f and the number of orthogonal codes M_c. MFSK/DS-CDMA is a special case of MFSK-OC/DS-CDMA with $M_c = 1$.

For efficient detection, all PN codes should be orthogonal or quasi-orthogonal (having a small cross-correlation). An example of orthogonal codes is a Hadamard code in which the number of orthogonal codes is equal to the code length. However, the orthogonality of this code is retained only for synchronized reception. Since this code is not quite random, and practical systems are generally asynchronized, other PN codes with small cross-correlation (e.g., Gold-sequence) are more likely to be used. The number of Gold-sequences is equal to the length of the sequence plus 2. When

the number of simultaneous users increases in a CDMA system, MAI accumulates due to the cross-correlation between the codes (although small).

For a conventional BPSK/DS-CDMA system, assuming each bit interval contains a single PN sequence, the total number of distinct codes can be chosen as the length of the PN sequence. If the total number of simultaneous users is chosen as one eighth of the PN code length (spreading factor), then 8 codes can be used to represent 3 bit information.

The disadvantage of introducing the orthogonal codes is an increase in the MAI. Since more PN codes are used, the maximum possible value of cross-correlation will increase. By controlling the total number of PN codes, the mutual interference can be kept at an acceptable level. The major limitation of orthogonal codes is finding a large set of PN codes with a good cross-correlation property.

The contributions of this chapter can be summarized as follows:

(1) Applying the concept of orthogonal codes to the MFSK/DS-CDMA system, we propose a novel system, namely MFSK-OC/DS-CDMA.

(2) Performance with non-ideal orthogonal codes is analyzed. It is shown that the orthogonality condition can be relaxed with little overall degradation.

(3) FEC coded MFSK-OC/DS-CDMA systems are analyzed.

In Section 4.2, we will describe the system model. In Section 4.3, we analyze the system performance over an AWGN channel. In Section 4.4, we analyze the system performance over a fading channel. In Section 4.5, we consider FEC coded system over both AWGN and fading channels. Section 4.6 summarizes the conclusions of this chapter.

4.2 System Model

The transmitter block diagram for the kth user is shown in Fig. 4.1. The expression of $b_k(t)$ is given in Section 3.2:

$$b_k(t) = \sum_{j=-\infty}^{\infty} b_j^k p_{T_b}(t - jT_b). \tag{4.1}$$

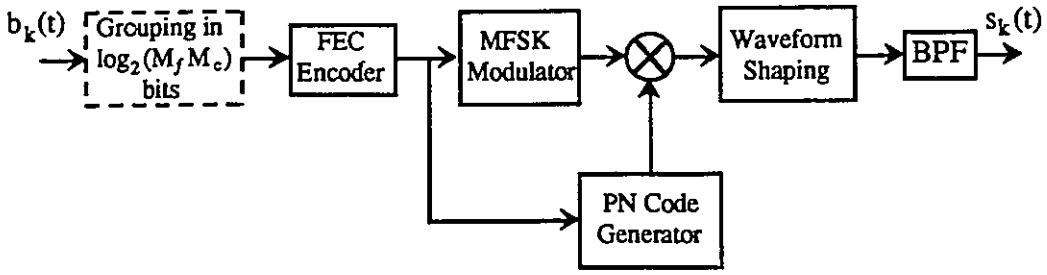

Figure 4.1 : Transmitter block diagram for the kth user in an MFSK-OC/DS-CDMA system.

The bit stream is first applied to a FEC encoder with a code rate r_c. To match to the nonbinary modulator, a nonbinary FEC code is employed. The output of the FEC encoder is an Mary symbol ($M \triangleq M_f M_c$) stream

$$d_k(t) = \sum_{i=-\infty}^{\infty} d_i^k p_{T_s}(t - iT_s), \tag{4.2}$$

where d_i^k is a random variable taking values from the set $[1, 2, \cdots, M]$ with equal probability, and T_s is the symbol duration

$$T_s = \log_2(M_f M_c) r_c T_b. \tag{4.3}$$

Each Mary symbol will be used to choose one of the M_f frequency tones and one of the M_c PN codes. The selected frequency tone is multiplied by the selected PN code. The resultant signal has a symbol rate

$$R_s = \frac{1}{T_s} = \frac{R_b}{r_c \log_2(M_f M_c)}. \tag{4.4}$$

The symbol energy is

$$E_s = r_c \log_2(M_f M_c) E_b. \tag{4.5}$$

The signal is further waveform shaped and bandpass filtered to generate the transmitted signal $s_k(t)$.

For an uncoded system, the input bit stream is grouped in $\log_2(M_f M_c)$ bits (as shown in the dashed box of Fig. 4.1) among which $\log_2 M_f$ bits are used to choose

one of the M_f frequency tones and $\log_2 M_c$ bits are used to choose one of the M_c PN codes. The equations (4.3)-(4.5) still hold with $\tau_c = 1$.

The transmitted signal for the kth user ($1 \leq k \leq K$) is

$$s_k(t) = \mathrm{Re}\{u_k(t)e^{j2\pi f_c t}\}, \tag{4.6}$$

where $u_k(t)$ is the baseband signal of the kth user

$$u_k(t) = \sqrt{2P}\Psi(t)a_k(t)\exp\left[j2\pi b_{k,f}(t)\Delta + j\theta_k(t)\right], \tag{4.7}$$

where P, $\Psi(t)$, Δ and $\theta_k(t)$ have the same meaning as described in 3.2.1. During a symbol interval, the phase $\theta_k(t)$ is assumed to be constant. In (4.7), $b_{k,f}(t)$ is defined in 3.2.1, and $a_k(t)$ is

$$a_k(t) = \sum_{i=-\infty}^{\infty} a_{i,j}^k p_{T_c}(t - iT_c), \quad j = 1, 2, \cdots, M_c, \tag{4.8}$$

where $a_{i,j}^k$ represents the ith chip of jth PN code. In our analysis, the PN codes are considered as random signature sequences. Then $a_{i,j}^k$ is treated as a random variable taking $+1$ and -1 with equal probability.

The received signal is

$$r_k(t) = \mathrm{Re}\{w_k(t)e^{j2\pi f_c t}\}, \tag{4.9}$$

where $w_k(t)$ is the equivalent baseband signal

$$w_k(t) = \sum_{i=1}^{K} v_i(t) + n_k(t), \tag{4.10}$$

where $v_k(t)$ is the output of the fading channel for an input $u_k(t)$. For an AWGN channel, we have $v_k(t) = u_k(t)$. In (4.9) $n_k(t)$ is the equivalent lowpass additive Gaussian noise having a zero mean and a power spectral density N_0.

The receiver block diagram is shown in Fig. 4.2. There are $M_f M_c$ branches, each branch is a matched filter corresponding to a specified frequency tone and a specified PN code. A branch of the receiver is shown in Fig. 4.3. It is realized in the form of a correlation receiver. The decision unit chooses the largest output from the $M_f M_c$ matched filters as the estimate. The decision output is then FEC decoded.

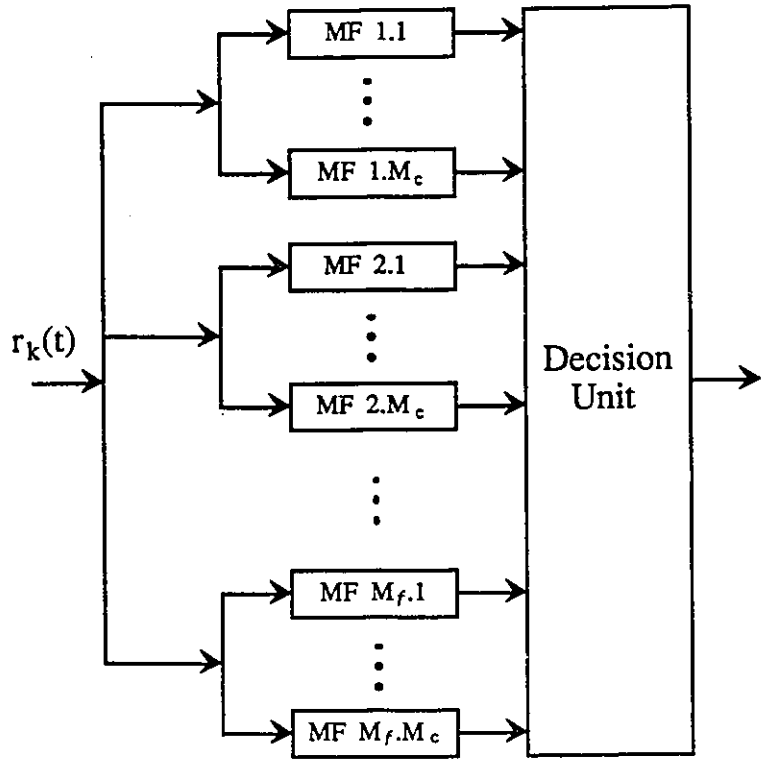

Figure 4.2 : Receiver block diagram of an MFSK-OC/DS-CDMA system.

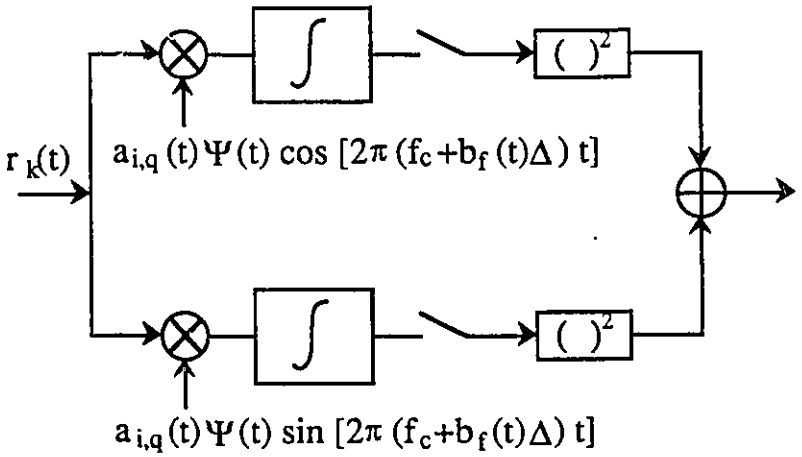

Figure 4.3 : A branch of the MFSK-OC/DS-CDMA receiver.

4.3 System Performance over an AWGN channel

In this section, we consider the system performance over AWGN channel for the uncoded case. A simple analysis is given first, and then a more detailed description follows.

4.3.1 A Simple Analysis

For the uncoded MFSK-OC/DS-CDMA system, each symbol contains $\log_2(M_f M_c)$ bits, then the effective symbol energy to noise spectral density ratio is

$$\gamma_s' = \log_2(M_f M_c)\gamma_b'. \tag{4.11}$$

If we are assuming that all the M_c PN codes employed by a user are orthogonal to each other, then all the $M_f M_c$ signals are orthogonal. Thus, the symbol error rate for noncoherent detection is similar to noncoherent MFSK

$$P_s = \sum_{n=1}^{M_f M_c - 1} (-1)^{n+1} \begin{pmatrix} M_f M_c - 1 \\ n \end{pmatrix} \frac{1}{n+1} e^{-\gamma_s' n/(n+1)}. \tag{4.12}$$

The bit error rate is

$$P_b = \frac{2^{(\log_2 M_f M_c - 1)}}{2^{(\log_2 M_f M_c)} - 1} P_s. \tag{4.13}$$

Next we determine γ_s'. We use the Gaussian approximation for the MAI [42]. The total noise power is the sum of thermal noise power plus the mutual interference power. Assume that the one-sided bandwidth is W, we have the thermal noise power $N_0 W$, and the interference power $(K-1)E_s/T_s$. The total noise power is

$$P_T = N_0 W + \frac{(K-1)E_s}{T_s}. \tag{4.14}$$

The total noise power spectral density is

$$N_0' = \frac{P_T}{W} = N_0 + \frac{(K-1)E_s}{T_s W} = N_0 + \frac{(K-1)E_s}{W/R_s}. \tag{4.15}$$

The symbol energy to the effective noise spectral density ratio is

$$\gamma_s' = \frac{E_s}{N_o'} = \frac{\frac{E_s}{N_0}}{1 + \frac{K-1}{W/R_s}\frac{E_s}{N_0}} = \frac{\gamma_s}{1 + \frac{K-1}{W/R_s}\gamma_s}. \tag{4.16}$$

The bit energy to the effective noise spectral density ratio is

$$\gamma_b' = \frac{\gamma_b}{1 + \frac{K-1}{W/R_b}\gamma_b} = \left[(\gamma_b)^{-1} + \left(\frac{W/R_b}{K-1} \right)^{-1} \right]^{-1}. \tag{4.17}$$

From (4.17), the number of simultaneous users is:

$$K = \frac{W}{R_b} \frac{(\gamma_b - \gamma_b')}{\gamma_b \gamma_b'} + 1 \simeq \frac{W}{R_b} \frac{(\gamma_b - \gamma_b')}{\gamma_b \gamma_b'} \quad (\text{for } K \gg 1). \tag{4.18}$$

The bandwidth efficiency is:

$$\eta = \frac{KR_b}{W} = \frac{\gamma_b - \gamma_b'}{\gamma_b \gamma_b'} \quad (\text{b/s/Hz}). \tag{4.19}$$

The symbol energy to the effective noise spectral density ratio can be rewritten as

$$\gamma_s' = \log_2(M_f M_c)\gamma_b' = \log_2(M_f M_c) \left[(\gamma_b)^{-1} + \left(\frac{W/R_b}{K-1} \right)^{-1} \right]^{-1}. \tag{4.20}$$

In the above equation, the three parameters W, R_b and K determine the bandwidth efficiency. For a given γ_b and bandwidth efficiency, the MFSK-OC/DS-CDMA scheme (with $M_c > 1$) has a larger effective symbol energy to the effective noise spectral density ratio than that of MFSK/DS-CDMA, and thus a better symbol error rate performance can be achieved. From (4.13), the bit error rate has only a small difference with the symbol error rate.

Recalling that $\gamma_s = \log_2(M_f M_c)\gamma_b$, the equation (4.20) can be written as

$$\gamma_s' = \left[(\gamma_s)^{-1} + \left(\frac{M_f N}{K-1} \right)^{-1} \right]^{-1}. \tag{4.21}$$

Now the second term in the bracket is not related to M_c. In fact, for different M_c, the bandwidth W will change. The asymptotic value of γ_s' is determined by the second term.

For a required BER, one can find γ_s' from (4.12) (or γ_b' from (4.13)), and for a given E_b/N_0, one can estimate the capacity using (4.19).

4.3.2 A Detailed Analysis

For the AWGN channel, the optimum receiver for the ith user computes the decision variables

$$U_{m_f,m_c} = \left| \int_0^{T_s} w_i(t) u^{(i)*}_{m_f,m_c}(t) \mathrm{d}t \right| \quad m_f = 1, 2, \cdots, M_f; \quad m_c = 1, 2, \cdots . M_c \tag{4.22}$$

and selects the signal corresponding to the largest decision variable. In the above equation, $u^{(k)}_{m_f,m_c}(t)$ is given in (4.7), and * denotes the complex conjugate operation.

To derive the probability of error, suppose that the signal $u^{(i)}_{1,1}(t)$ is transmitted. Then the equivalent lowpass received signal is

$$w_i(t) = u^{(i)}_{1,1}(t) e^{-j\phi_i} + n(t) + \sum_{k \neq i} u_k(t) e^{j\theta_k}. \tag{4.23}$$

Since the signals are detected noncoherently, the phase term $e^{-j\phi_i}$ becomes irrelevant and may be dropped from consideration. Thus

$$U_{m_f,m_c} = |D_{m_f,m_c} + N_{m_f,m_c} + \sum_{k \neq i} I_k|. \tag{4.24}$$

The desired signal D_{m_f,m_c} takes the form

$$D_{m_f,m_c} = 2E_s \delta(m_f, 1) \delta(m_c, 1) \tag{4.25}$$

where the Kronecker function $\delta(\cdot, \cdot)$ is defined by $\delta(x_1, x_2) = 0$ if $x_1 \neq x_2$ and $\delta(x, x) = 1$. The noise term

$$N_{m_f,m_c} = \int_0^{T_s} n_i(t) u^{(i)*}_{m_f,m_c}(t) \mathrm{d}t \tag{4.26}$$

has a zero mean and variance of $\sigma_N^2 = 2E_s N_0$. When K is large, the MAI $\sum_{k \neq i} I_k$ can be approximated as a Gaussian random variable. Then the sum $N_{m_f,m_c} + \sum_{k \neq i} I_k$ is also a complex-valued Gaussian random variable. From the symmetry property, the mean of the $\sum_{k \neq i} I_k$ can be assumed to be zero. Its variance for a single interferer is derived in Appendix C as

$$\mathrm{E}\{I_k^2\} = (2E_s T^{-1})^2 \frac{1}{M_f} T_s \left(2 \frac{N^2 T_c^3}{6} \right) = \frac{(2E_s)^2}{3 M_f N}. \tag{4.27}$$

The sum of N_{m_f,m_c} and $\sum_{k \neq i} I_k$ has a zero mean and a variance of

$$\sigma_m^2 = 2E_s N_0 + (2E_s)^2 (K - 1)/(3 M_f N). \tag{4.28}$$

Since all users transmit independently, the M complex-valued Gaussian random variables are mutually uncorrelated and identically distributed, and the decision variables $U_1, \cdots, U_M$ are mutually statistically independent. $U_2, \cdots, U_M$ are described statistically by a Rayleigh probability density function [75]

$$p(u_m) = \frac{u_m}{\sigma_m^2} \exp\left(-\frac{u_m^2}{2\sigma_m^2}\right) \qquad m = 2, \cdots, M, \tag{4.29}$$

and U_1 is described statistically by a Rician probability density function

$$p(u_1) = \frac{u_1}{\sigma_1^2} \exp\left(-\frac{u_1^2 + s^2}{2\sigma_1^2}\right) I_0\left(\frac{su_1}{\sigma_1^2}\right) \tag{4.30}$$

where $\sigma_1^2 = \sigma_m^2$ (for ideal orthogonal PN codes), $s = 2E_s$, and $I_0(\cdot)$ is modified Bessel function of first kind and zero-order. For simplicity, we have used U_1 for $U_{1,1}$ and U_m for the rest of U_{m_f,m_c}. The probability of a correct decision is simply the probability that U_1 exceeds all the other $\{U_m\}$. That is

$$\begin{aligned}
P_C &= Pr\left(U_2 < U_1, U_3 < U_1, \cdots, U_M < U_1\right) \\
&= \int_0^\infty Pr\left(U_2 < U_1, U_3 < U_1, \cdots, U_M < U_1 | U_1 = u_1\right) p(u_1) \mathrm{d}u_1 \\
&= \int_0^\infty \left[\Pr(U_2 < U_1 | U_1 = u_1)\right]^{M-1} p(u_1) \mathrm{d}u_1 \\
&= \int_0^\infty \left[\int_0^{u_1} p(u_m) \mathrm{d}u_m\right]^{M-1} p(u_1) \mathrm{d}u_1 \\
&= \int_0^\infty \left(1 - e^{-u_1^2/2\sigma_1^2}\right)^{M-1} p(u_1) \mathrm{d}u_1 \\
&= \sum_{n=0}^{M-1} (-1)^n \binom{M-1}{n} \int_0^\infty e^{-nu_1^2/2\sigma_m^2} \frac{u_1}{\sigma_1^2} \exp\left(-\frac{u_1^2+s^2}{2\sigma_1^2}\right) I_0\left(\frac{su_1}{\sigma_1^2}\right) \mathrm{d}u_1 \\
&= \sum_{n=0}^{M-1} \frac{(-1)^n}{n+1} \binom{M-1}{n} e^{-\frac{ns^2}{2(n+1)\sigma_m^2}} \int_0^\infty \frac{\sqrt{n+1}u_1}{\sigma_m^2} \\
&\quad \exp\left[-\frac{(\sqrt{n+1}u_1)^2 + (s/\sqrt{n+1})^2}{2\sigma_m^2}\right] I_0\left[\frac{(s/\sqrt{n+1})(\sqrt{n+1}u_1)}{\sigma_m^2}\right] \mathrm{d}(\sqrt{n+1}u_1) \\
&= \sum_{n=0}^{M-1} \frac{(-1)^n}{n+1} \binom{M-1}{n} e^{-\frac{ns^2}{2(n+1)\sigma_m^2}} \\
&= \sum_{n=0}^{M-1} \frac{(-1)^n}{n+1} \binom{M-1}{n} e^{-\frac{n\gamma_s'}{(n+1)}}.
\end{aligned} \tag{4.31}$$

In the above equation, we made use of the fact that

$$\begin{aligned}
&\int_0^\infty \frac{\sqrt{n+1}u_1}{\sigma_m^2} \exp\left[-\frac{(\sqrt{n+1}u_1)^2 + (\frac{s}{\sqrt{n+1}})^2}{2\sigma_m^2}\right] \\
&\qquad I_0\left[\frac{(\frac{s}{\sqrt{n+1}})(\sqrt{n+1}u_1)}{\sigma_m^2}\right] \mathrm{d}(\sqrt{n+1}u_1) = 1.
\end{aligned} \tag{4.32}$$

The signal energy to the effective noise spectral density ratio is

$$\gamma_s' = \frac{s^2}{2\sigma_m^2} = \left[\left(\frac{E_s}{N_0}\right)^{-1} + \left(\frac{3M_fN}{2(K-1)}\right)^{-1}\right]^{-1}. \tag{4.33}$$

The bandwidth efficiency is:

$$\eta = \frac{KR_b}{W} \simeq \frac{3}{2}\frac{\gamma_b - \gamma_b'}{\gamma_b\gamma_b'} \quad \text{(b/s/Hz)}. \tag{4.34}$$

The probability of symbol error is

$$P_M = 1 - P_C = \sum_{n=1}^{M-1}(-1)^{n+1}\begin{pmatrix} M-1 \\ n \end{pmatrix}\frac{1}{n+1}e^{-\gamma_s' n/(n+1)}. \tag{4.35}$$

The result is the same as that for noncoherent MFSK modulation [75] with M being replaced by M_fM_c. The result obtained is also the same as that obtained in (4.12), except the difference of γ_s'. The bit error rate can be obtained from (4.13). Results from the detailed analysis will be used for the performance evaluation.

In the analysis, the MAI component is evaluated using Geraniotis and Pursley's method [33, 30]. In Section 3.1, we mentioned that Ha used different approach for the MFSK/DS-CDMA system analysis. Ha's method is described in Appendix D.

4.3.3 Performance with Non-ideal PN Codes

In the above analysis, we assumed that all the PN codes employed by a user are ideally orthogonal. In fact, the cross-correlation between any two PN codes is generally not zero. In this case, (4.25) should be rewritten as

$$D_{m_f,m_c} = \begin{cases} 2E_s, & m_f = 1 \text{ and } m_c = 1, \\ 2E_s\lambda_{m_c}, & m_f = 1 \text{ and } m_c \neq 1, \\ 0, & m_f \neq 1, \end{cases} \tag{4.36}$$

where λ_{m_c} $(0 < \lambda_{m_c} < 1)$ is the cross-correlation between the first and the m_cth PN codes employed by any specific user. For each user, the received PN code is synchronized to the reference. So only one cross-correlation value is required. We further assume that all the M_c PN codes are chosen such that the cross-correlation values between any two of these codes are equal. Thus $\lambda_{m_c} = \lambda$ for $m_c = 1, 2, \cdots, M_c$. If the cross-correlation values are not equal, we choose $\lambda = \text{Max}\{\lambda_{m_c} | m_c = 1, 2, \cdots, M_c\}$

as a conservative approximation. The cross-correlation value can be either positive or negative. Thus the variable D_{m_f,m_c} (with $m_f = 1$ and $m_c \neq 1$) can be modeled as a random variable taking λ and $-\lambda$ with equal probability. For convenience, as a conservative consideration, we further approximate it using a Gaussian random variable with a zero mean and a variance of $(2\lambda E_s)^2$. Clearly, when λ is large, system performance degrades significantly. The correlation value is determined by the PN codes employed. Thus the total number of available PN codes is restricted, i.e., we cannot increase the number of orthogonal codes arbitrarily. However, for a reasonable number of PN codes, the value of λ is very small. For example, using Gold codes of length $N = 2^n - 1$, the cross-correlation takes three different values: -1, $-t_n$ and $t_n - 2$ where t_n is defined as [47]

$$t_n = \begin{cases} 2^{(n+1)/2} + 1 & n \text{ odd} \\ 2^{(n+2)/2} + 1 & n \text{ even.} \end{cases} \tag{4.37}$$

In (4.36), λ is the normalized value relative to N.

Next we analyze the effect of non-ideally orthogonal PN codes. The probabilities of U_{m_f,m_c} are given as follows

$$p(u_{m_f,m_c}) = \begin{cases} \frac{u_1}{\sigma_1^2} \exp\left(-\frac{u_1^2+s^2}{2\sigma_1^2}\right) I_0\left(\frac{su_1}{\sigma_1^2}\right) & m_f = m_c = 1, \\ \frac{u_2}{\sigma_2^2} \exp\left(-\frac{u_2^2}{2\sigma_2^2}\right) & m_f = 1, m_c \neq 1, \\ \frac{u_m}{\sigma_m^2} \exp\left(-\frac{u_m^2}{2\sigma_m^2}\right) & m \neq 1. \end{cases} \tag{4.38}$$

Again for simplicity, we used u_1, u_2 and u_m to express u_{m_f,m_c} with $(m_f = m_c = 1)$, $(m_f = 1, m_c \neq 1)$ and $(m_f \neq 1)$ respectively. In the equation, $\sigma_1^2 = \sigma_m^2$ is given by (4.28), $\sigma_2^2 = \sigma_m^2 + (2\lambda E_S)^2$ and $s = 2E_s$.

The probability of a correct decision is

$$P_C = \int_0^\infty [\Pr(U_m < U_1 | U_1 = u_1)]^{M-M_c} [\Pr(U_2 < U_1 | U_1 = u_1)]^{M_c-1} p(u_1) \mathrm{d}u_1, \tag{4.39}$$

where

$$[\Pr(U_m < U_1 | U_1 = u_1)]^{M-M_c} = \sum_{n_1=0}^{M-M_c} (-1)^{n_1} \binom{M - M_c}{n_1} e^{-n_1 u_1^2/2\sigma_m^2}, \tag{4.40}$$

and

$$[\Pr(U_2 < U_1 | U_1 = u_1)]^{M_c-1} = \sum_{n_2=0}^{M_c-1} (-1)^{n_2} \binom{M_c - 1}{n_2} e^{-n_2 u_1^2/2\sigma_2^2}. \tag{4.41}$$

Then

$$P_C = \sum_{n_1=0}^{M-M_c M_c-1} \sum_{n_2=0} (-1)^{n_1+n_2} \begin{pmatrix} M-M_c \\ n_1 \end{pmatrix} \begin{pmatrix} M_c-1 \\ n_2 \end{pmatrix} \int_0^\infty \exp\left[-\left(\frac{n_1}{\sigma_m^2}+\frac{n_2}{\sigma_2^2}\right)\frac{u_1^2}{2}\right] \frac{u_1}{\sigma_1^2} \exp\left(-\frac{u_1^2+s^2}{2\sigma_1^2}\right) I_0\left(\frac{su_1}{\sigma_1^2}\right) \mathrm{d}u_1. \tag{4.42}$$

The integral term in the above equation can be expressed as

$$\begin{aligned} & \int_0^\infty \exp\left[-\left(\frac{n_1}{\sigma_m^2}+\frac{n_2}{\sigma_2^2}\right)\frac{u_1^2}{2}\right] \frac{u_1}{\sigma_1^2} \exp\left(-\frac{u_1^2+s^2}{2\sigma_1^2}\right) I_0\left(\frac{su_1}{\sigma_1^2}\right) \mathrm{d}u_1 \\ = & \frac{1}{\sigma_1^2} \exp\left(-\frac{s^2}{2\sigma_1^2}\right) \int_0^\infty u_1 \exp\left[-\left(\frac{u_1^2}{\sigma_a^2}+\frac{u_1^2}{\sigma_1^2}\right)\frac{u_1^2}{2}\right] I_0\left(\frac{su_1}{\sigma_1^2}\right) \mathrm{d}u_1 \\ = & \frac{\sigma_b^2}{\sigma_1^2} \exp\left(-\frac{s^2}{2\sigma_1^2}\right) \exp\left(\frac{s'^2}{2\sigma_b^2}\right) \int_0^\infty \frac{u_1}{\sigma_b^2} \exp\left(-\frac{u_1^2+s'^2}{2\sigma_b^2}\right) I_0\left(\frac{s'u_1}{\sigma_c^2}\right) \mathrm{d}u_1 \\ = & \frac{\sigma_b^2}{\sigma_1^2} \exp\left[-\left(\frac{s^2}{2\sigma^2}-\frac{s'^2}{2\sigma_b^2}\right)\right], \end{aligned} \tag{4.43}$$

where

$$\sigma_a^2 \triangleq \left(\frac{n_1}{\sigma_m^2}+\frac{n_2}{\sigma_2^2}\right)^{-1} = \frac{\sigma_2^2\sigma_m^2}{n_1\sigma_2^2+n_2\sigma_m^2}, \tag{4.44}$$

$$\sigma_b^2 \triangleq \left(\frac{1}{\sigma_a^2}+\frac{1}{\sigma_1^2}\right)^{-1} = \frac{\sigma_1^2\sigma_a^2}{n_1\sigma_1^2+n_2\sigma_a^2}, \tag{4.45}$$

and

$$s' \triangleq \frac{\sigma_b^2 s}{\sigma_1^2}. \tag{4.46}$$

Setting $\sigma_1^2 = \sigma_m^2$, and $\sigma_2^2 = \sigma_2 m^2 + (2\lambda E_s)^2$, we have

$$\frac{s^2}{2\sigma_m^2} = \frac{(2E_s)^2}{2\left[2E_sN_0+\frac{(2E_s)^2(K-1)}{3M_fN}\right]} = \gamma_s', \tag{4.47}$$

$$\frac{s'^2}{2\sigma_b^2} = \frac{1}{2\sigma_b^2}\left(\frac{\sigma_b^2 s}{\sigma_m^2}\right)^2 = \frac{s^2}{2\sigma_m^2}\frac{\sigma_b^2}{\sigma_m^2} = \gamma_s'\frac{\sigma_b^2}{\sigma_m^2}, \tag{4.48}$$

and

$$\begin{aligned} \frac{\sigma_b^2}{\sigma_m^2} = & \frac{\sigma_a^2}{\sigma_m^2+\sigma_a^2} = \frac{1}{1+\frac{\sigma_m^2}{\sigma_a^2}} = \frac{1}{1+\frac{n_1\sigma_2^2+n_2\sigma_m^2}{\sigma_2^2}} \\ = & \frac{1}{1+n_1+n_2\frac{\sigma_m^2}{\sigma_2^2}} = \frac{1}{1+n_1+n_2\frac{1}{\frac{(2\lambda E_s)^2}{\sigma_m^2}}} = \frac{1}{1+n_1+n_2\frac{1}{1+2\lambda^2\gamma_s'}}. \end{aligned} \tag{4.49}$$

The probability of correct decision is

$$P_C = \sum_{n_1=0}^{M-M_c M_c-1} \sum_{n_2=0} (-1)^{n_1+n_2} \begin{pmatrix} M-M_c \\ n_1 \end{pmatrix} \begin{pmatrix} M_c-1 \\ n_2 \end{pmatrix} \frac{1}{1+n_1+n_2\frac{1}{1+2\lambda^2\gamma_s'}} \exp\left[-\gamma_s'\left(1-\frac{1}{1+n_1+n_2\frac{1}{1+2\lambda^2\gamma_s'}}\right)\right]. \tag{4.50}$$

The probability of a symbol error is

$$P_s = 1 - P_C. \tag{4.51}$$

Letting $\lambda = 0$ and $n = n_1 + n_2$, the above equation reduces to (4.35).

4.3.4 Numerical Results and Discussions

In this subsection, we consider two cases corresponding to the ideal and the non-ideal orthogonal codes respectively.

4.3.4.1 Ideal Orthogonal Codes

Comparing (4.35) to (2.16), we see that the expression of the probability of symbol error of MFSK-OC/DS-CDMA is the same as that of MFSK-MPSK/DS-CDMA. The difference is the parameter M and the relationship between the bit energy and symbol energy. In Tables 4.1 and 4.2, we give the required bit energy to the effective noise spectral density ratio for BER of 10^{-3} and 10^{-5} respectively, using (4.35) and (4.13). We see that schemes with the same product $M_f M_c$ have nearly the same performance. This can be seen clearly from (4.35), where $M = M_f M_c$, and $E_b = E_s/\log_2(M_f M_c)$. For comparison, the performance of MFSK/DS-CDMA ($M_c = 1$) is also listed in the Tables. For a fixed M_f, γ_b' decreases as M_c increases. For a fixed M_c, γ_b' decreases as M_f increases. In general, γ_b' decreases as M increases. For smaller M_f, the improvement in energy efficiency by employing the orthogonal codes is more significant. It should be noted that the same value of γ_b' in MFSK-OC/DS-CDMA and MFSK/DS-CDMA (with $M = M_f M_c$) does not correspond to the same γ_b, since γ_b' is determined by two terms as given in (4.33).

Next we examine the bandwidth efficiency of MFSK-OC/DS-CDMA systems. The system bandwidth is expressed as

$$W = M_f R_c = M_f N R_s = M_f N \frac{R_b}{\log_2 M}, \tag{4.52}$$

where $M = M_f M_c$. Thus the bandwidth efficiency is

$$\eta = \frac{K R_b}{W} = \frac{K \log_2 M}{M_f N}. \tag{4.53}$$

Table 4.1 : The required SNR per bit γ_b' (in dB) for a BER of 10^{-3} for the MFSK-OC/DS-CDMA.

	$M_f = 2$	$M_f = 4$	$M_f = 8$	$M_f = 16$	$M_f = 32$
$M_c = 1$	10.9	8.3	7.0	6.1	5.4
$M_c = 2$	8.3	7.0	6.1	5.4	4.9
$M_c = 4$	7.0	6.2	5.5	5.0	4.6
$M_c = 8$	6.2	5.5	5.1	4.7	4.3

Table 4.2 : The required SNR per bit γ_b' (in dB) for a BER of 10^{-5} for the MFSK-OC/DS-CDMA.

	$M_f = 2$	$M_f = 4$	$M_f = 8$	$M_f = 16$	$M_f = 32$
$M_c = 1$	13.3	10.6	9.1	8.1	7.3
$M_c = 2$	10.6	9.1	8.1	7.3	6.7
$M_c = 4$	9.1	8.1	7.3	6.8	6.3
$M_c = 8$	8.1	7.3	6.8	6.3	5.9

For a fair comparison, we keep the same BER performance for different systems. Consider (4.33) for a very large γ_s. We have the asymptotic value

$$\gamma_{s,\infty}' = \frac{3M_fN}{2(K-1)}. \tag{4.54}$$

The product M_fN can be expressed as

$$M_fN = \frac{2}{3}(K-1)\gamma_{s,\infty}' = \frac{2}{3}(K-1)\log_2 M\gamma_b'. \tag{4.55}$$

Substituting the above result into (4.53)

$$\eta = \frac{3K}{2(K-1)\gamma_b'} = \frac{3}{2\gamma_b'} \quad \text{for large } K. \tag{4.56}$$

This result is the same as equation (2.21). For a general case, equation (2.20) still holds

$$\eta = \frac{3}{2}\frac{\gamma_b - \gamma_b'}{\gamma_b\gamma_b'} + \frac{R_b}{W}, \tag{4.57}$$

Table 4.3 : Asymptotic bandwidth efficiency η_∞ (in b/s/Hz) of MFSK-OC/DS-CDMA systems for a BER of 10^{-3}.

	$M_f = 2$	$M_f = 4$	$M_f = 8$	$M_f = 16$	$M_f = 32$
$M_c = 1$	0.12	0.22	0.30	0.37	0.43
$M_c = 2$	0.22	0.30	0.37	0.43	0.49
$M_c = 4$	0.30	0.36	0.42	0.47	0.52
$M_c = 8$	0.36	0.42	0.46	0.51	0.56

Table 4.4 : Asymptotic bandwidth efficiency η_∞ (in b/s/Hz) of MFSK-OC/DS-CDMA systems for a BER of 10^{-5}.

	$M_f = 2$	$M_f = 4$	$M_f = 8$	$M_f = 16$	$M_f = 32$
$M_c = 1$	0.07	0.13	0.18	0.23	0.28
$M_c = 2$	0.13	0.18	0.23	0.28	0.32
$M_c = 4$	0.18	0.23	0.28	0.31	0.35
$M_c = 8$	0.23	0.28	0.31	0.35	0.39

where $R_b/W = \log_2 M/(M_f N)$ can be omitted (for $M = 32$, $M_f = 2$ and $N = 128$, R_b/W=0.02). The asymptotic bandwidth efficiency corresponding to Tables 4.1 and 4.2 are given in Tables 4.3 and 4.4 respectively.

We can give a direct explanation for the results in these two tables. From (4.54), if we keep the three parameters M_f, N and K fixed, the value of γ_s' of MFSK-OC/DS-CDMA is larger than (or equal to) that of MFSK/DS-CDMA. The bandwidth efficiency improvement factor is (using (4.53))

$$f_{\mathrm{BW}} = \frac{\eta_{\{\mathrm{MFSK-OC/DS-CDMA}\}}}{\eta_{\{\mathrm{MFSK/DS-CDMA}\}}} = \frac{\frac{K\log_2(M)}{M_f N}}{\frac{K\log_2 M_f}{M_f N}} = 1 + \frac{\log_2 M_c}{\log_2 M_f}. \tag{4.58}$$

Table 4.5 lists the values of f_{BW} for MFSK-OC/DS-CDMA with different M_f and M_c. The value of f_{BW} for MFSK/DS-CDMA systems ($M_c = 1$) is set to 1 as the reference. The bandwidth efficiency of MFSK-OC/DS-CDMA is f_{BW} times that of MFSK/DS-CDMA with the same M_f. By checking the results in Tables 4.3 and 4.4, the improvement is a little smaller than f_{BW}. For example, in Tables 4.3, the ratio

of the entry with $M_f = 2$ and $M_c = 8$ over the entry with $M_f = 2$ and $M_c = 1$ is 0.36/0.12= 3; while the corresponding value of f_{BW} given in Table 4.5 is 4. This is because the same value of γ_s' does not result in exactly the same BER performance. For a fixed value of M_f, the summation index M in (4.35) is different for different M_c. However, the bandwidth efficiency improvement factor does give a clear physical meaning.

Table 4.5 : Bandwidth efficiency improvement factor f_{BW} of MFSK-OC/DS-CDMA systems with the same γ_s'.

	$M_f = 2$	$M_f = 4$	$M_f = 8$	$M_f = 16$	$M_f = 32$
$M_c = 1$	1	1	1	1	1
$M_c = 2$	2	1.5	1.33	1.25	1.2
$M_c = 4$	3	2	1.67	1.5	1.4
$M_c = 8$	4	2.5	2	1.75	1.6

The bandwidth efficiency shown in Tables 4.3 and 4.4 are asymptotic values. To obtain the asymptotic bandwidth efficiency η_∞, a necessary condition is that the corresponding values of γ_b' are achievable. To satisfy this condition, we need that

$$\gamma_{b,\infty}' = \frac{\gamma_{s,\infty}'}{\log_2(M_f M_c)} = \frac{3M_f N}{2(K-1)\log_2(M_f M_c)} \geq \gamma_b', \tag{4.59}$$

i.e.,

$$\frac{M_f N}{(K-1)\log_2(M_f M_c)} \geq \frac{2\gamma_b'}{3} = \frac{1}{\eta_\infty}. \tag{4.60}$$

The left side of the above equation is the reciprocal of the actual bandwidth efficiency as shown in (4.53). Thus for a specified BER the realizable bandwidth efficiency should be less than the asymptotic bandwidth efficiency.

4.3.4.2 Non-ideal Orthogonal Codes

Now we consider the case of non-ideal orthogonal codes. To be specific, we consider the Gold sequence of length 127. For this code, $t_n = 17$, thus three possible cross-correlation values are -1, -17 and $+15$ respectively. Generally, we can select the PN sequences (with a shifted version) in such a way that the cross-correlation values

between every pair of the PN codes employed by a user is -1. For $M_c = 8$, it is not difficult to divide the Gold sequence of length 127 into 16 sets, which meet the requirement. For a cross-correlation value of -1, we found that the BER performance is the same (within one tenth of a dB) as that of ideal case. However, to consider the worst case, we give the calculation results for $\lambda = \frac{17}{127} = 0.134$ shown in Tables 4.6 and 4.7 for bit error rates of 10^{-3} and 10^{-5} respectively.

Table 4.6 : The required SNR per bit γ_b' (in dB) for a BER of 10^{-3} for the MFSK-OC/DS-CDMA with $\lambda = 0.134$.

	$M_f = 2$	$M_f = 4$	$M_f = 8$	$M_f = 16$	$M_f = 32$
$M_c = 1$	10.9	8.3	7.0	6.1	5.4
$M_c = 2$	9.0	7.4	6.3	5.6	5.0
$M_c = 4$	7.9	6.7	5.9	5.2	4.7
$M_c = 8$	7.3	6.3	5.6	4.9	4.4

Table 4.7 : The required SNR per bit γ_b' (in dB) for a BER of 10^{-5} for the MFSK-OC/DS-CDMA with $\lambda = 0.134$.

	$M_f = 2$	$M_f = 4$	$M_f = 8$	$M_f = 16$	$M_f = 32$
$M_c = 1$	13.3	10.6	9.1	8.1	7.3
$M_c = 2$	12.4	10.5	9.3	8.3	7.5
$M_c = 4$	11.3	10.0	9.0	8.2	7.4
$M_c = 8$	10.5	9.5	8.7	8.0	7.3

The difference with the ideal case is large for small BER (10^{-5}). The difference can be up to two dBs. So the selection of a set of PN codes is important. A direct explanation of the effect of the non-ideal codes is given as follows. In the reception, there is interference from $(K-1)$ other users. For the (M_c-1) branches which have the same frequency tone as the received signal, in addition to the MAI, there is one more interference from the desired signal. The signal to interference ratio corresponding to one interfering user (approximated as Gaussian noise) is $\gamma_1 = \frac{3M_fN}{2}$, while the signal to interference ratio due to the desired signal is $\gamma_2 = \frac{(2E_s)^2}{(2\lambda E_s)^2} = 1/\lambda^2$. For $M_f = 1$,

$\gamma_1 = 192$. For cross-correlation values 1 and 17, $\gamma_2 = 16129$ and 55.8 respectively. So for a small cross-correlation value ($\lambda = 1/N$), the effect of the non-ideal code is trivial; while for the large cross-correlation value ($\gamma_2 = 17$), the interference from the desired signal can be more severe than MAI. Fortunately, we can easily choose a set of orthogonal codes with small single cross-correlation between each pair. From now on, we will treat all the M_c orthogonal codes as ideal ones.

4.4 System Performance over Fading Channels

In this section, we consider system performance without FEC coding over frequency non-selective slow Rayleigh and Rician fading channels. For the BER evaluation, Gaussian approximation method is used.

4.4.1 Performance over a Frequency Non-selective Slow Rayleigh Fading Channel

4.4.1.1 Analysis

In this section, we determine the system performance over a slow Rayleigh fading channel. Signals are assumed to be transmitted on L diversity channels. Each diversity channel is assumed to be frequency nonselective and the fading processes on the L channels are assumed to be mutually statistically independent. The diversity can be obtained in different ways (e.g. multiple antennas). In addition, an additive white Gaussian noise corrupts each channel and all the noise processes are assumed to be mutually statistically independent. The fading is sufficiently slow so that the channel parameters (fading strength α and phase shift θ) remain constant for the duration of the signalling interval (T_s). The fading channel can be described by the following input-output relationship

$$v_k(t) = \alpha_k e^{j\theta_k} u_k(t), \tag{4.61}$$

where $\alpha_k e^{j\theta_k}$ is a complex Gaussian random variable. Its amplitude α_k is Rayleigh distributed, and its phase θ_k is uniformly distributed over $(0, 2\pi)$.

Because of the noncoherent detection, the combiner for the L diversity channels

is a squared law combiner. Its output consists of $M_f M_c$ decision variables

$$U_{m_f,m_c} = \begin{cases} U_1 = \sum_{l=1}^{L} |2E_s\alpha_i^{(l)} e^{j\theta_i^{(l)}} + \sum_{k\neq i}(\alpha_k^{(l)} e^{j\theta_k^{(l)}} I_k^{(l)}) + N_{m_f,m_c}^{(l)}|^2 & m_f = m_c = 1, \\ U_2 = \sum_{l=1}^{L} |\sum_{k}(\alpha_k^{(l)} e^{j\theta_k^{(l)}} I_k^{(l)}) + N_{m_f,m_c}^{(l)}|^2 & m_f = 1, \quad m_c \neq 1, \\ U_3 = \sum_{l=1}^{L} |\sum_{k\neq i}(\alpha_k e^{j\theta_k^{(l)}} I_k^{(l)}) + N_{m_f,m_c}^{(l)}|^2 & m_f \neq 1. \end{cases} \tag{4.62}$$

In the above equation, all the three terms $\alpha_i^{(l)} e^{j\theta_i^{(l)}}$, $\sum_{k\neq i}(\alpha_k^{(l)} e^{j\theta_k^{(l)}} I_k^{(l)})$ and $N_{m_f,m_c}^{(l)}$ are Gaussian distributed. $I_k^{(l)}$ is given in (C.1). The variables U_1, U_2 and U_3 are chi-square distributed with $2L$ degrees of freedom [75], i.e.,

$$p_{U_1}(u_1) = \frac{1}{(2\sigma_1^2)^L (L-1)!} u_1^{L-1} e^{-u_1/2\sigma_1^2}, \tag{4.63}$$

$$p_{U_2}(u_2) = \frac{1}{(2\sigma_2^2)^L (L-1)!} u_2^{L-1} e^{-u_2/2\sigma_2^2}, \tag{4.64}$$

and

$$p_{U_3}(u_3) = \frac{1}{(2\sigma_3^2)^L (L-1)!} u_3^{L-1} e^{-u_3/2\sigma_3^2}. \tag{4.65}$$

The three variances can be found as

$$\begin{aligned} \sigma_1^2 = & \ \tfrac{1}{2}\mathrm{E}\left(|2E_s\alpha_i^{(l)} e^{j\theta_i^{(l)}} + \sum_{k\neq i}(\alpha_k^{(l)} I_k) + N_{m_f,m_c}|^2 \right) \\ = & \ 2E_s N_0 \bar{\gamma}_s + (K-1)\tfrac{4E_s N_0 \bar{\gamma}_s}{3M_f N} + 2E_s N_0, \end{aligned} \tag{4.66}$$

$$\sigma_2^2 = K\frac{4E_s N_0 \bar{\gamma}_s}{3M_f N} + 2E_s N_0, \tag{4.67}$$

and

$$\sigma_3^2 = (K-1)\frac{4E_s N_0 \bar{\gamma}_s}{3M_f N} + 2E_s N_0 \tag{4.68}$$

where $\bar{\gamma}_s = \mathrm{E}\{\alpha^2\}\frac{E_s}{N_0}$.

The probability of correct decision is

$$P_C = \int_0^\infty \left[\int_0^{u_1} p(u_2)\mathrm{d}u_2\right]^{M_c-1} \left[\int_0^{u_1} p(u_3)\mathrm{d}u_3\right]^{M-M_c} p(u_1)\mathrm{d}u_1. \tag{4.69}$$

The probability of symbol error is

$$\begin{aligned} P_e = & \ 1 - P_C \\ = & \ 1 - \int_0^\infty \frac{1}{(2\sigma_1^2)^L (L-1)!} u_1^{L-1} e^{-u_1/2\sigma_1^2} \left[1 - e^{-u_1/2\sigma_2^2} \sum_{l=0}^{L-1} \frac{(u_1/2\sigma_2^2)^l}{l!}\right]^{M_c-1} \\ & \left[1 - e^{-u_1/2\sigma_3^2} \sum_{l=0}^{L-1} \frac{(u_1/2\sigma_3^2)^l}{l!}\right]^{M-M_c} \mathrm{d}u_1. \end{aligned} \tag{4.70}$$

By replacing the integrate variable $u = u_1/2\sigma_3^2$, the above equation can be rewritten as

$$\begin{aligned} P_e = & \ 1 - \int_0^\infty \frac{1}{(L-1)!} \left(\frac{\sigma_3^2}{\sigma_1^2}\right)^L u^{L-1} e^{-\frac{\sigma_3^2}{\sigma_1^2}u} \left[1 - e^{-\frac{\sigma_3^2}{\sigma_2^2}u} \sum_{l=0}^{L-1} \left(\frac{\sigma_3^2}{\sigma_2^2}\right)^l \frac{u^l}{l!}\right]^{M_c-1} \\ & \left[1 - e^{-u} \sum_{l=0}^{L-1} \frac{u^l}{l!}\right]^{M-M_c} \mathrm{d}u. \end{aligned} \tag{4.71}$$

From (4.66), (4.67) and (4.68), we have

$$\frac{\sigma_3^2}{\sigma_1^2} = \frac{(K-1)\frac{4E_sN_0\bar{\gamma}_s}{3M_fN} + 2E_sN_0}{2E_sN_0\bar{\gamma}_s + (K-1)\frac{4E_sN_0\bar{\gamma}_s}{3M_fN} + 2E_sN_0} = \frac{1}{1+\bar{\gamma}_s'}, \tag{4.72}$$

and

$$\frac{\sigma_3^2}{\sigma_2^2} = \frac{(K-1)\frac{4E_sN_0\bar{\gamma}_s}{3M_fN} + 2E_sN_0}{K\frac{4E_sN_0\bar{\gamma}_s}{3M_fN} + 2E_sN_0} = \frac{1}{1+\frac{2}{3M_fN}\bar{\gamma}_s'}, \tag{4.73}$$

where $\bar{\gamma}_s'$ is average signal energy to the equivalent noise spectral density ratio

$$\bar{\gamma}_s' = \left[\bar{\gamma}_s^{-1} + \left(\frac{3M_fN}{2(K-1)}\right)^{-1}\right]^{-1}, \tag{4.74}$$

and

$$\bar{\gamma}_s = \log_2(M_fM_c)\bar{\gamma}_b/L. \tag{4.75}$$

Substituting (4.72) and (4.73) into (4.71), we have

$$\begin{aligned} P_e = & \ 1 - \int_0^\infty \frac{1}{(1+\bar{\gamma}_s')^L (1+(L-1)!)} u^{L-1} e^{-\frac{u}{1+\bar{\gamma}_s'}} \\ & \left[1 - e^{-\frac{u}{1+\frac{2}{3M_fN}\bar{\gamma}_s'}} \sum_{l=0}^{L-1} \frac{u^l}{(1+\frac{2}{3M_fN}\bar{\gamma}_s')^l l!}\right]^{M_c-1} \left[1 - e^{-u} \sum_{l=0}^{L-1} \frac{u^l}{l!}\right]^{M-M_c} \mathrm{d}u. \end{aligned} \tag{4.76}$$

The above equation can be used for the BER calculation.

For $L = 1$, (4.70) reduces to

$$\begin{aligned} P_e &= 1 - \int_0^\infty \tfrac{1}{2\sigma_1^2} e^{-u_1/2\sigma_1^2} [1 - e^{-u_1/2\sigma_2^2}]^{M_c-1} [1 - e^{-u_1/2\sigma_3^2}]^{M-M_c} \mathrm{d}u_1 \\ &= 1 - \sum_{n_1=0}^{M-M_c} \sum_{n_2=0}^{M_c-1} (-1)^{n_1+n_2} \begin{pmatrix} M-M_c \\ n_1 \end{pmatrix} \begin{pmatrix} M_c-1 \\ n_2 \end{pmatrix} \\ &\quad \tfrac{1}{2\sigma_1^2} \int_0^\infty \exp -\tfrac{u_1}{2\sigma_1^2} - \tfrac{n_1 u_1}{2\sigma_2^2} - \tfrac{n_2 u_1}{2\sigma_3^2} \mathrm{d}u_1 \\ &= 1 - \sum_{n_1=0}^{M-M_c} \sum_{n_2=0}^{M_c-1} (-1)^{n_1+n_2} \begin{pmatrix} M-M_c \\ n_1 \end{pmatrix} \begin{pmatrix} M_c-1 \\ n_2 \end{pmatrix} \tfrac{\sigma_a^2}{\sigma_1^2}, \end{aligned} \tag{4.77}$$

where

$$\sigma_a^2 = \left(\frac{1}{\sigma_1^2} + \frac{n_1}{\sigma_2^2} + \frac{n_2}{\sigma_3^2} \right)^{-1}, \tag{4.78}$$

and

$$\begin{aligned} \tfrac{\sigma_a^2}{\sigma_1^2} &= \left(1 + \tfrac{n_1 \sigma_1^2}{\sigma_2^2} + \tfrac{n_2 \sigma_1^2}{\sigma_3^2} \right)^{-1} \\ &= \left(1 + n_1 \tfrac{1+\bar{\gamma}_s + (K-1)\frac{2\bar{\gamma}_s}{3M_f N}}{1+K\frac{2\bar{\gamma}_s}{3M_f N}} + n_2 \tfrac{1+\bar{\gamma}_s+(K-1)\frac{2\bar{\gamma}_s}{3M_f N}}{1+(K-1)\frac{2\bar{\gamma}_s}{3M_f N}} \right)^{-1}. \end{aligned} \tag{4.79}$$

If all the M_c PN codes used by a specific user are ideally orthogonal, then

$$\sigma_2^2 = \sigma_3^2 = (K-1)\frac{4E_s N_0 \bar{\gamma}_s}{3M_f N} + 2E_s N_0, \tag{4.80}$$

and

$$\begin{aligned} P_e &= \sum_{n=1}^{M_f M_c - 1} (-1)^{n+1} \begin{pmatrix} M_f M_c - 1 \\ n \end{pmatrix} \tfrac{1}{1+n\frac{\sigma_1^2}{\sigma_2^2}} \\ &= \sum_{n=1}^{M_f M_c - 1} (-1)^{n+1} \begin{pmatrix} M_f M_c - 1 \\ n \end{pmatrix} \tfrac{1}{1+n+n\bar{\gamma}_s'}. \end{aligned} \tag{4.81}$$

4.4.1.2 Numerical Results and Discussions

As in Chapter 2, the analysis can be performed in two steps. The first step is to examine the BER as a function of $\bar{\gamma}_b'$ using (4.81). The second step is to examine the relationship between $\bar{\gamma}_b'$ and the MAI term as given in (4.74) and (4.75). The second relationship is the same as that described in Chapter 2.

From (4.81), we see that for the ideal orthogonal codes, the BER performance of the system with parameters M_f and M_c is the same as that of MFSK/DS-CDMA with $M = M_f M_c$. This result is the same as the discussion for AWGN channel in Section 3.3.4. Thus, the BER performance as a function of $\bar{\gamma}_b'$ is the same as that

in narrowband MFSK system with $M = M_f M_c$ [75]. We know that in conventional MFSK system, the performance is better than BPSK in AWGN channel for $M \geq 8$. While in Rayleigh fading channel, BPSK performs better than MFSK. The same result holds for the comparison between MFSK-OC/DS-CDMA and PSK/DS-CDMA.

For non-ideal orthogonal codes, the intended signal acts as interference to $M_c - 1$ decision branches which have the same frequency tone as the intended signal. Thus, the overall performance will be degraded. In Figs. 4.4 and 4.5, the BER performance is illustrated for $M_f = 8$, $M_c = 2$ and $M_f = 8$, $M_c = 4$ respectively. For both cases, the PN sequence length is $N = 15$. Diversity $L = 1$, 2 and 4 are included. Larger diversity brings significant advantage. Compared with the performance using ideal orthogonal codes, the non-ideal orthogonal codes have an obvious degradation. We notice that when number of diversity increases, the degradation becomes smaller. The PN sequence length also affects the performance. In Figs. 4.4 and 4.5, the BER performance for the same systems is illustrated with PN sequence length $N = 63$. Compared with the ideal Orthogonal codes, much smaller degradation is observed than using $N = 15$. The effects of L and N can be explained from (4.73). With larger N and L (thus smaller $\bar{\gamma}_s{}'$), the term σ_3^2/σ_2^2 is close to unity, which corresponds the ideal case. Otherwise, worse performance occurs.

In the analysis, the effect of the signal on the same tone branches is treated as an MAI user. In fact, by properly choosing the PN codes, much better correlation properties can be obtained, and the resultant performance will be very close to the ideal case. As for the relationship between $\bar{\gamma}_b{}'$ and the MAI, the discussion in Section 3.5 also applies.

4.4.2 Performance over a Frequency Non-selective Slow Rician Fading Channel

4.4.2.1 Analysis

The frequency non-selective Rician fading channel is described by the following input-output relationship

$$v_k(t) = \rho u_k(t) \tag{4.82}$$

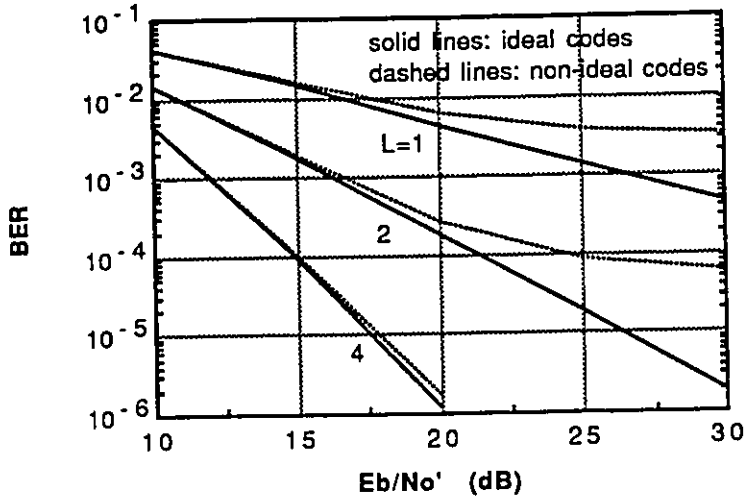

Figure 4.4 : BER performance of MFSK-OC/DS-CDMA systems with $M_f = 8$ and $M_c = 2$ over a Rayleigh fading channel using diversity $L = 1$, 2 and 4, and PN sequence length $L = 15$.

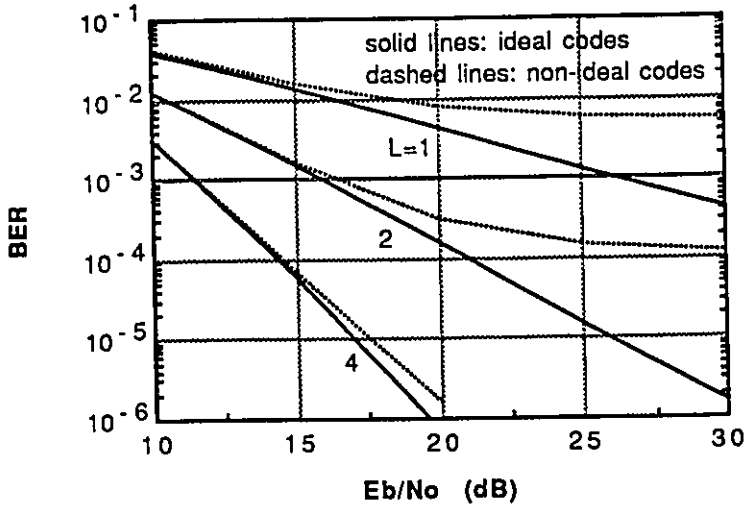

Figure 4.5 : BER performance of MFSK-OC/DS-CDMA systems with $M_f = 8$ and $M_c = 4$ over a Rayleigh fading channel using diversity $L = 1$, 2 and 4, and PN sequence length $L = 15$.

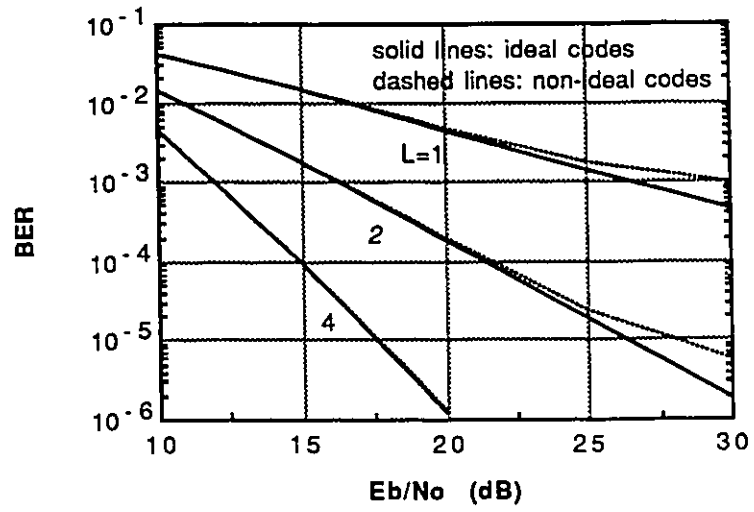

Figure 4.6 : BER performance of MFSK-OC/DS-CDMA systems with $M_f = 8$ and $M_c = 2$ over a Rayleigh fading channel using diversity $L = 1$, 2 and 4, and PN sequence length $L = 63$.

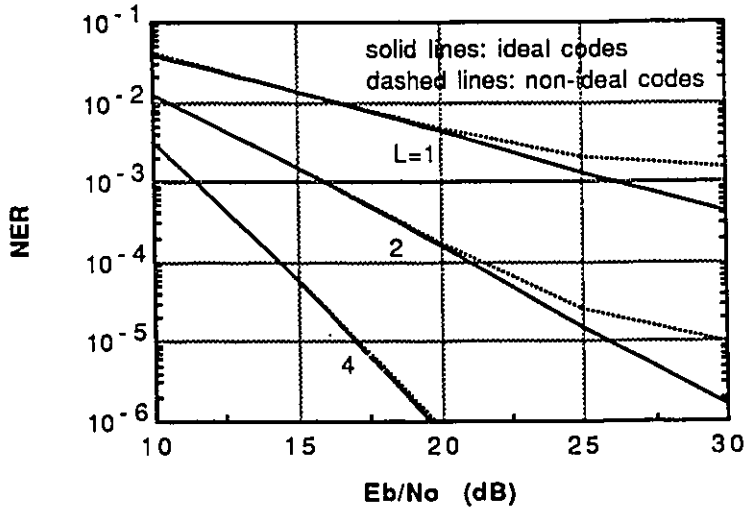

Figure 4.7 : BER performance of MFSK-OC/DS-CDMA systems with $M_f = 8$ and $M_c = 4$ over a Rayleigh fading channel using diversity $L = 1$, 2 and 4, and PN sequence length $L = 63$.

for $lT_c \le t < (l+1)T_c$, where ρ is random variable with Rician distribution as given in (2.12). The decision variables are

$$U_{m_f,m_c} = \begin{cases} |2E_s\rho + \sum_{k\neq i}\rho I_{k,i} + \zeta| & m_f = m_c = 1, \\ |\sum_{k}\rho I_{k,i} + \zeta| & \text{otherwise}, \end{cases} \tag{4.83}$$

where ζ represents AWGN component. Again we use the Gaussian approximation for the MAI component. The mean and variance of the MAI plus noise are

$$\mu_{m_f,m_c} = \mathrm{E}\{\sum_{k}\rho I_{k,i} + \zeta\} = 0, \tag{4.84}$$

and

$$\begin{aligned} \sigma^2 = & \ \mathrm{E}\{\sum_{k\neq i}\rho I_{k,i} + \zeta\}^2 \\ = & \ \sum_{k\neq i}\mathrm{E}\{\rho^2\}\mathrm{E}\{I_{k,i}^2\} + \mathrm{E}\{\zeta^2\} \\ = & \ (K-1)\tfrac{(2E_s)^2}{3M_fN} + 2E_sN_0. \end{aligned} \tag{4.85}$$

The average symbol energy to the effective noise spectral density ratio is given in (4.74). Using (A.10), we have the following result

$$P_{\mathrm{MFSK}} = \sum_{n=1}^{M-1}(-1)^{n+1}\binom{M-1}{n}\frac{1+\kappa}{n\bar{\gamma_s'} + (n+1)(1+\kappa)}\exp\left[-\frac{\kappa n\bar{\gamma_s'}}{n\bar{\gamma_s'} + (n+1)(1+\kappa)}\right]. \tag{4.86}$$

4.4.2.2 Numerical Results and Discussions

In Fig. 4.8, we give the BER performance of MFSK-OC/DS-CDMA over a Rician fading channel with $\kappa = 10$ dB. From this figure the following two observations can be made. As M increases, the performance improves; the difference in performance is large at high and moderate BERs and diminishes at low BERs. In Fig. 4.9, we present the BER curves of MFSK-OC/DS-CDMA with different M for different channel: AWGN, Rayleigh fading, and Rician fading with $\kappa = 20$ dB, 10 dB and 5 dB. Here $M = M_fM_c$. The more severe the fading, the smaller the difference between large M and small M. So in severe fading environment, the advantage obtained by increasing M is very limited.

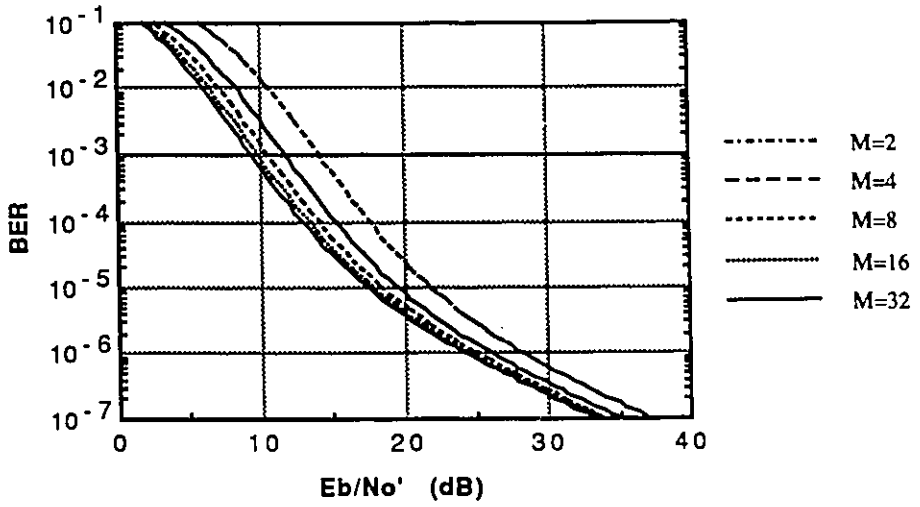

Figure 4.8 : BER performance of MFSK-OC/DS-CDMA systems over a Rician fading channel with $\kappa = 10$ dB.

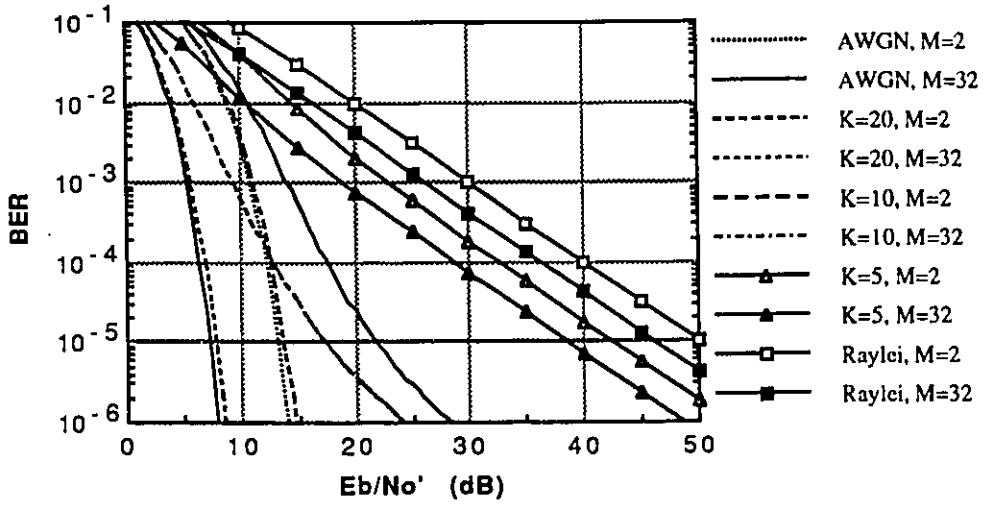

Figure 4.9 : BER performance of MFSK-OC/DS-CDMA systems over different channels.

4.5 Performance of an FEC Coded System over a Frequency Non-selective Slow Rayleigh Fading Channel

From the previous results about the uncoded system, we see that the bandwidth efficiency is very low. In this subsection, we consider the system performance employing both block and convolutional codes. Generally, both binary and nonbinary codes can be used. For binary code, $\log_2 M$ coded bits are grouped to be transmitted as one of the channel symbol. In this case, the length of the block code is better chosen as a multiple of $\log_2 M$. The block diagram of the system is shown in Fig. 4.10-(a). More natural way of implementating coding is using nonbinary codes for the nonbinary modulation scheme. For the Mary modulation scheme, a $\log_2 M$-ary code can be employed. The block diagram of the nonbinary coded system is shown in Fig. 4.10-(b).

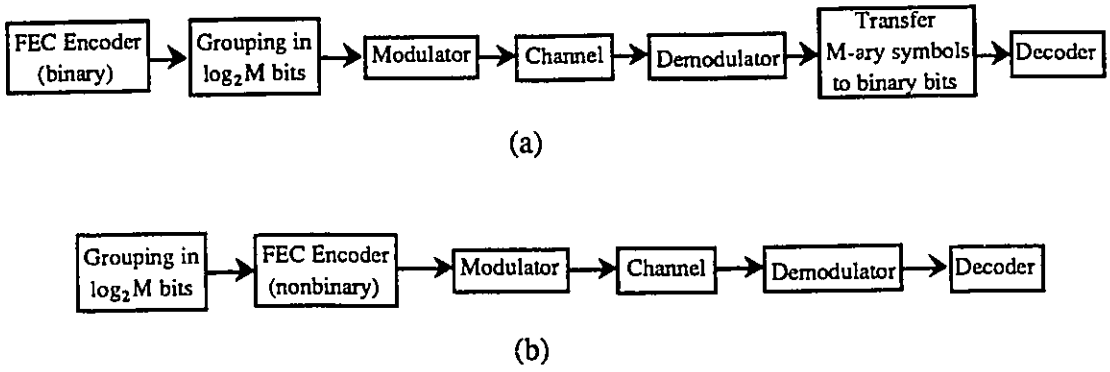

Figure 4.10 : Block diagram of an FEC coded MFSK-OC/DS-CDMA system. (a) A system with binary coding; (b) A system with nonbinary coding.

Now we consider the BER performance of Reed-Solomon codes and dual-k codes. Reed-Solomon codes are hard decision decoded, while dual-k codes are soft decision decoded. A detailed derivation for the performance of soft decision decoding is given in Appendix E.

4.5.1 Performance of Reed-Solomon Codes

The expression for the performance of Reed-Solomon codes was given in Section 3.6. The BER performance using hard decision RS code over a Rayleigh fading channel is shown in Fig. 4.11. With FEC coding, the performance is improved significantly. When M $(= M_f M_c)$ is large, a large error correcting ability t is possible. From Fig. 4.11, the BER performance is mostly determined by the parameter t. This shows the advantage of using the combined MFSK and orthogonal code scheme which achieves large M.

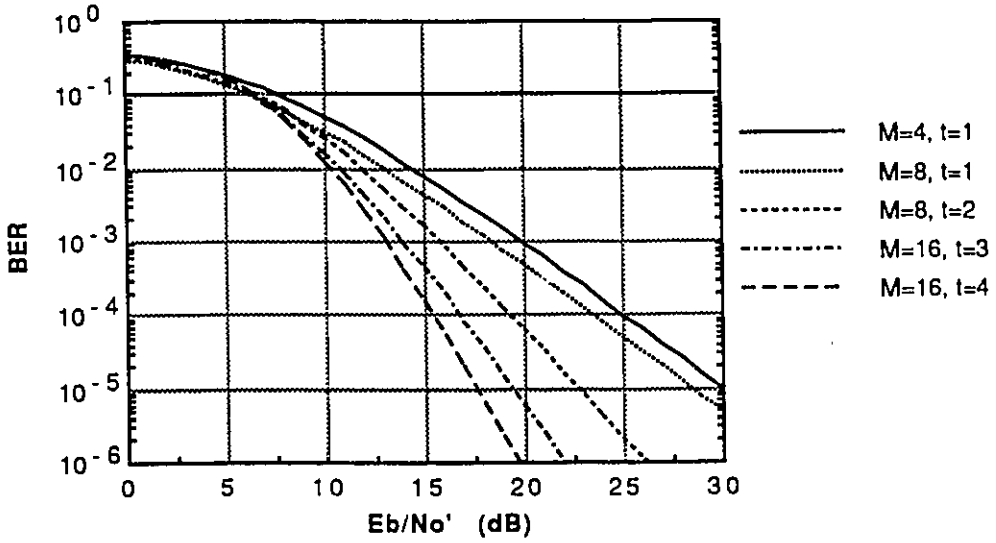

Figure 4.11 : Performance of MFSK-OC/DS-CDMA systems using RS codes over a Rayleigh fading channel.

In Table 4.8, we list the required γ_b' and the asymptotic bandwidth efficiency at a BER of 10^{-3}. Recalling that (Section 3.5.3) the bandwidth efficiency for the uncoded system in a Rayleigh fading channel is in the order of 10^{-4}, the coded system is much better.

Table 4.8 : The required SNR per bit γ_b' (in dB) for a BER of 10^{-3} and the asymptotic bandwidth efficiency (in b/s/Hz) over a Rayleigh fading channel using RS codes (code length $n = M - 1$)

	$M = 4, t = 1$	$M = 8, t = 1$	$M = 8, t = 2$	$M = 16, t = 3$	$M = 16, t = 4$
γ_b'	19.8	18.4	15.8	14.0	13.0
η	0.016	0.022	0.039	0.060	0.075

4.5.2 Performance of Dual-k Codes

For the nonbinary convolutional code, dual-k code, since soft decision decoding can be employed, a better performance can be achieved. For $M = 8$, $M = 16$ and $M = 32$, the performance using dual-3, dual-4 and dual-5 codes are shown in Fig. 4.12. The results for a BER of 10^{-3} is listed in Table 4.9. A better performance is observed compared with RS codes.

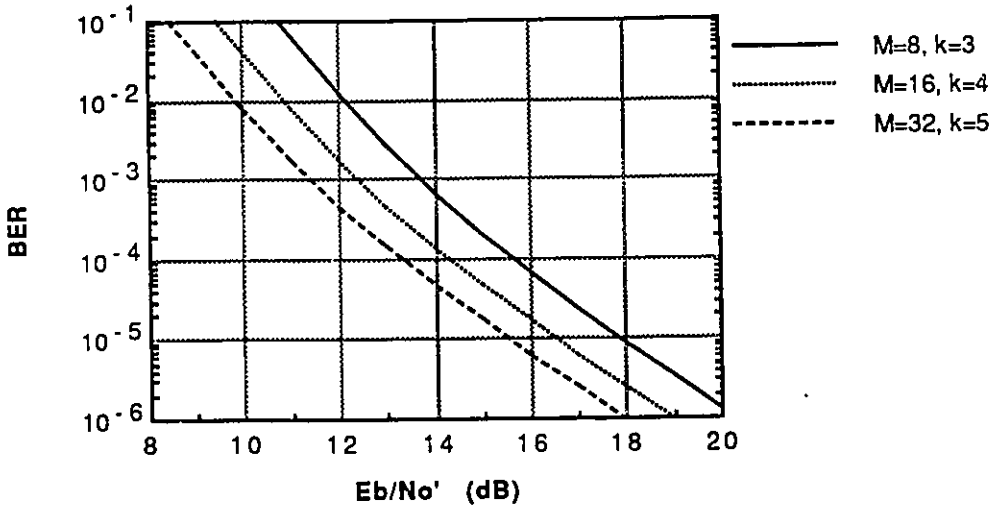

Figure 4.12 : Performance of MFSK-OC/DS-CDMA systems using dual-k codes over a Rayleigh fading channel.

Table 4.9 : The required SNR per bit γ_b' (in dB) for a BER of 10^{-3} and the asymptotic bandwidth efficiency (in b/s/Hz) over a Rayleigh fading channel using dual-k codes.

	$M = 8,\ k = 3$	$M = 16,\ k = 4$	$M = 32,\ k = 5$
γ_b'	13.6	12.4	11.4
η	0.065	0.086	0.11

4.6 Summary

In this chapter, we applied the concept of orthogonal codes to the MFSK/DS-CDMA system. It is shown that the resultant system (MFSK-OC/DS-CDMA) is equivalent to the MFSK/DS-CDMA systems with $M = M_f M_c$. For a fixed M_f, the proposed system is better than MFSK/DS-CDMA. With the introduction of orthogonal codes, the system complexity can be reduced. System performance over AWGN and fading channels were examined. The effects of FEC coding were also considered. Orthogonal codes can be easily realized in practical situations. We analyzed the system performance using practical PN codes which are not orthogonal. It was shown that some PN codes (e.g., Gold codes) with good correlation property can be used with very small degradation.

Chapter 5

Simulation Studies of MFSK-OC/DS-CDMA Systems

5.1 Introduction

The purpose of this chapter is to describe the simulation work we have performed to verify and extend the analysis given in Chapter 4. For SS systems, direct simulation is very inefficient. To simulate an SS system with a spreading factor N, the simulation time is at least N times that of a corresponding narrowband system. For many narrowband system simulations, a linear channel model can be used which allows using one sample per symbol. In SS systems, for the MAI component, simple one sample per chip simulation method is not enough. In an asynchronous system, the MAI term from each interferer has a time delay which is uniformly distributed in a chip period. The one sample per chip simulation method ignores the delay effect. In addition, in coherent detection systems, the carrier synchronization is achieved only for the desired signal. The one sample per chip simulation method assumes a coherent summation for the MAI chips, thus much more effort should be made to get accurate simulation results. In many cases, however, we do not need to simulate the whole SS system. Usually an equivalent narrowband system model can be used [25]. We performed our simulations by taking such considerations into account.

In this thesis, the baseline signal employed is MFSK. For MFSK system simulation, a lot of frequency manipulations are required. Thus the simulation for MFSK scheme is not efficient. Based on the orthogonality of MFSK signals, we propose

a simple simulation model for MFSK scheme simulation. For the MFSK-OC/DS-CDMA system, we use Gaussian approximation for the MAI components. Thus we can focus our effort on the new system concept.

In Section 5.2, a simulation model for MFSK is described. Then the model is modified for MFSK-OC/DS-CDMA system. In Section 5.3, simulation results are discussed and compared with the analytical results. Section 5.4 summarizes the conclusions of this chapter.

5.2 Simulation Model

5.2.1 Simulation Model for MFSK

For the MFSK scheme, M distinct symbols have M distinct frequency tones. To represent a frequency tone in simulation, one needs multiple samples for each symbol period. The resultant simulation model would be complex and time consuming. It is well known that the frequency tones of MFSK modulation are orthogonal if the frequency spacing between adjacent tones is a multiple of $1/2T_s$ for coherent detection and a multiple of $1/T_s$ for noncoherent detection. We consider only noncoherent detection. When orthogonality is satisfied, there is no interference between different frequency tones. We can view these M frequency tones as M independent channels. A simulation model based on this consideration is given in Fig. 5.1. The "binary data generator" produces a stream of random binary data taking "0" and "1" with equal probability. Then the binary data is grouped in every $\log_2 M$ bits, which represent one of the M MFSK symbols (one of the M frequency tones). In the simulation program, we are not doing any frequency domain operation. Each of the M symbols is identified by two index values: (1) a constant float value representing the symbol energy which is the same for all the M symbols; (2) an integer value representing one of the M symbols. The symbol passes through a fading channel and AWGN channel; these channels affect only the first index value. In the fading channel operation, there is no difference for different symbols. For the AWGN channel, we consider M branches. During each symbol period, only one of the paths contains the signal. Other paths contain only the noise components. In the ideal MFSK scheme, the M symbols

are orthogonal to each other. The noise components in the M paths are assumed to be statistically independent. In the decision unit, all the M branch outputs are compared in absolute value and the largest is chosen as the decision. The selected symbol is converted to binary data, and the error rate is determined in the "error count".

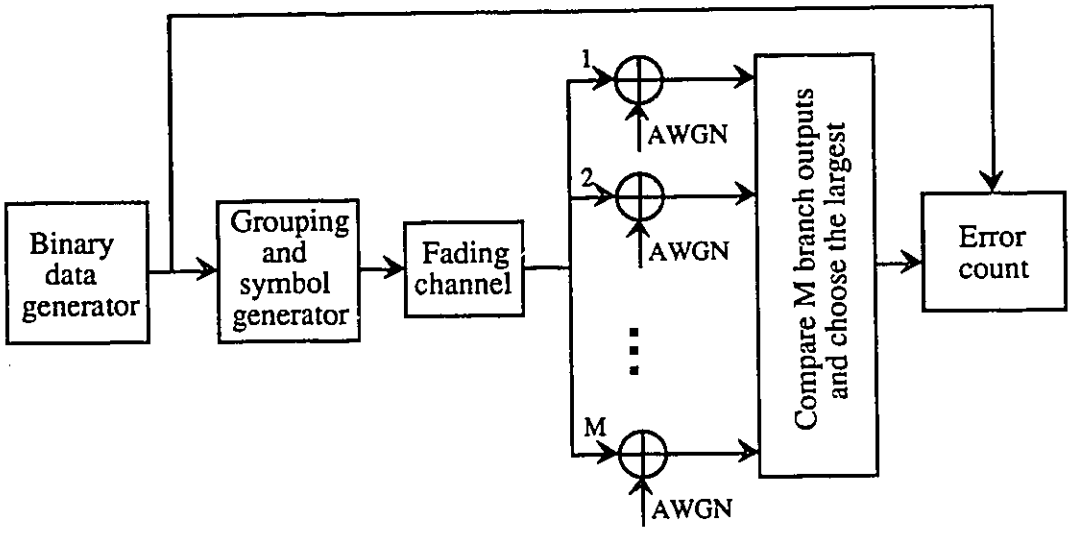

Figure 5.1 : Block diagram of a simulation model for MFSK.

Using this simulation model, we have performed a series of simulations for the noncoherent MFSK schemes over AWGN, Rayleigh and Rician fading channels. It is shown that the results agree with the standard analysis very well. This simple simulation model is efficient and useful to determine the BER performance in MFSK related systems. However, when one wants to study some frequency domain impairments such as frequency offset and amplifier nonlinearity, this model is not applicable.

5.2.2 Simulation Model for MFSK-OC/DS-CDMA

The model for MFSK-OC/DS-CDMA is developed from the one just discussed for MFSK. In the DS-CDMA system, one more interference contribution is from the MAI. A Gaussian approximation is used for this component.

The block diagram of the model is the same as that for MFSK shown in Fig. 5.1. The effect of the MAI is included in the AWGN. If M_c orthogonal codes are used, the number of branches in Fig. 5.1 is $M = M_f M_c$, corresponding to the $M_f M_c$ symbols. Assume the number of simultaneous users is K, among which one is the desired user. Then the number of interfering users is $(K-1)$. During each symbol interval, the $(K-1)$ interfering symbols randomly correspond to a set of tones from the M_f frequency tones. This is done in the program as follows. We generate $(K-1)$ random numbers r_i, $i = 1, 2, \cdots, K-1$, which are uniformly distributed in [0, 1]. Each random number determines a frequency tone by taking the integer part of $(M_f r_i + 1)$. The resultant integer is one of the numbers $[1, 2, \cdots, M_f]$, representing M_f frequency tones. Thus, by counting the $(K-1)$ random numbers, we can determine the number of interferers in each frequency tone. All the M_c branches with the same frequency tone have the same amount of MAI. In the analysis, we consider the MAI in an average way, that is, there are $(K-1)/M_f$ interferers in each frequency tone on the average. That consideration is a little optimistic. Our simulation will reveal the validity of the analysis.

Now we examine the Gaussian approximation for the MAI. In Fig. 5.1, the output from each of the M branches can be expressed as

$$U_i = S_i + I_i + \zeta = S_i + G_i, \qquad i = 1, 2, \cdots, M, \tag{5.1}$$

where S_i is the signal component, I_i is the MAI component, ζ is the noise component, and $G_i \triangleq I_i + \zeta$ is the equivalent noise component. During each symbol interval, if the jth symbol is transmitted, we have $S_j = 1$ and $S_i = 0$ $(i \neq j)$. The MAI component I_i may be different for each frequency tone, while the noise component ζ has the same variance for all the tones. For the simulation we need to find the equivalent noise variance $\sigma_G^2(i)$, $i = 1, 2, \cdots, M_f$, which may be different for different frequency tones. The symbol energy to noise spectral density ratio γ_s is given for each simulation

$$\gamma_s = \frac{E_s}{N_0} = \frac{1}{2\sigma_\zeta^2}, \tag{5.2}$$

where the symbol energy E_s is assumed to be 1. Thus, we have $\sigma_\zeta^2 = 1/2\gamma_s$. Assuming that the number of interferers is k_i in the ith branch, we have $\sum_{i=1}^{M_f} k_i = K - 1$.

Recalling that the equivalent symbol energy to the MAI ratio is $\gamma_{sm} = 3M_fN/[2(K-1)]$ for $(K-1)$ interferers in Section 3.4, the equivalent symbol energy to the MAI ratio in the ith tone can be written as

$$\gamma_{sm} = \frac{3M_fN}{2k_i}. \tag{5.3}$$

The variance of the MAI in the ith tone is

$$\sigma_I^2(i) = \frac{1}{2\gamma_{sm}} = \frac{k_i}{3M_fN}. \tag{5.4}$$

Thus the equivalent noise variance for the ith branch output is

$$\sigma_G^2(i) = \sigma_\zeta^2 + \sigma_I^2(i) = \frac{1}{2\gamma_s} + \frac{k_i}{3M_fN} \quad i = 1, 2, \cdots, M_f. \tag{5.5}$$

In the above equation, the equivalent noise variance is given for different frequency tones. But for each frequency tone, we still have M_c branches. In each of the M_c branches with the same frequency tone, the received signal is multiplied by a different PN sequence for despreading. We assume that the PN sequences are very well selected, so that the cross-correlation between each pair of PN sequences is very small. For an input noise component $n(t)$ and a PN sequence $a(t)$, the despreader output is

$$Q = \int_0^{T_s} n(t)a(t)\mathrm{d}t. \tag{5.6}$$

Since $\mathrm{E}\{n(t)\} = 0$ and $\sigma_n^2 = N_0/2$, we have $\mathrm{E}\{Q\} = 0$ and $\sigma_Q^2 = N_0T_s/2$. Considering two different branch outputs Q_1 and Q_2 in the M_c branches, we have

$$\begin{aligned} \mathrm{E}\{Q_1Q_2\} &= \mathrm{E}\left[\int_0^{T_s} n(t_1)a_1(t_1)\mathrm{d}t_1 \int_0^{T_s} n(t_1)a_2(t_2)\mathrm{d}t_2\right] \\ &= \int_0^{T_s}\int_0^{T_s} \mathrm{E}\{n(t_1)n(t_1)\}\mathrm{E}\{a_1(t_2)a_1(t_2)\}\mathrm{d}t_1\mathrm{d}t_2 = 0. \end{aligned} \tag{5.7}$$

In the above derivation, we have used the fact that $n(t)$ and $a(t)$ are independent and the assumption that every pair of PN sequences is uncorrelated. Thus the M_c branch noise component outputs with the same frequency tone are independent. But their noise variances are the same.

In summary, there are $M = M_fM_c$ branches in total in the receiver and every m_c branches have the same frequency tone. For any M_c branches with the same tone

where no desired signal is present, the M_c equivalent noise outputs are independent and have the same variance given by (5.5). For the M_c branches where the desired signal is present, one of the M_c branches contains the desired signal and the equivalent noise is also given by (5.5). The other $(M_c - 1)$ branches will experience one more interferer and their equivalent noise variance is modified to

$$\sigma_G^2 = \frac{1}{2\gamma_s} + \frac{k_i + 1}{3M_f N}. \tag{5.8}$$

5.3 Simulation Results for MFSK-OC/DS-CDMA

We simulated the BER performance over AWGN, Rayleigh and Rician fading channels. In all the simulations, the number of simultaneous users was chosen as 10, and the PN sequence length is 127. In Figs. 5.2–5.4, we give the simulation results for two MFSK-OC/DS-CDMA schemes: (1) $M_f = 2$, $M_c = 8$; (2) $M_f = 8$, $M_c = 2$. The corresponding analysis results are also shown for comparison. We see that they are in good agreement.

In Fig. 5.2, the BER performance of the two MFSK-OC/DS-CDMA schemes in an AWGN channel is shown. The system with $(M_f = 8, M_c = 2)$ is superior to that with $(M_f = 2, M_c = 8)$. Both of these schemes have the same parameter $M = M_f M_c$. Recall the results in Table 4.1 that the system with the same M have the same BER performance and also the same bandwidth efficiency. The seemingly contradiction can be resolved by pointing out the different condition given in Fig. 5.2. Firstly, the abscissa is marked by γ_b which is not including the effect of the MAI component. Secondly, since the PN sequence length is the same for both schemes, the one with a larger M_f has a wider bandwidth and gives a better performance. This is clear by recalling the equation $\gamma_{bm} = 3M_f N/[2\log_2(M_f M_p)(K-1)]$. The bandwidth efficiency of the two schemes will be the same.

In Fig. 5.3, the result is given for a Rician fading channel. The Rician parameter κ is chosen as 10 dB. For the difference between the two schemes, the same argument discussed above applies.

The system performance over a Rayleigh fading channel is given in Fig. 5.4. Under the given condition, the performance is pretty poor. We see an error floor in the

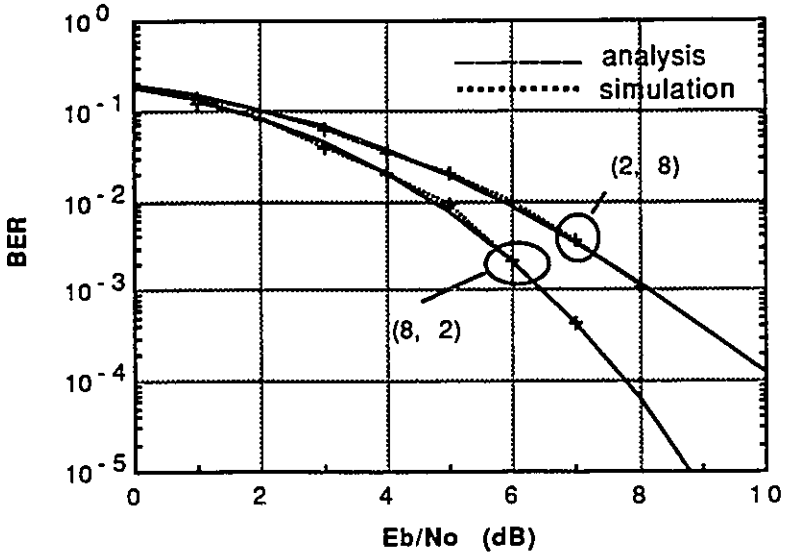

Figure 5.2 : BER performance of MFSK-OC/DS-CDMA over an AWGN channel: simulation vs. analysis; $N = 127$, $K = 10$. The index pair shown by the curves are (M_f, M_c).

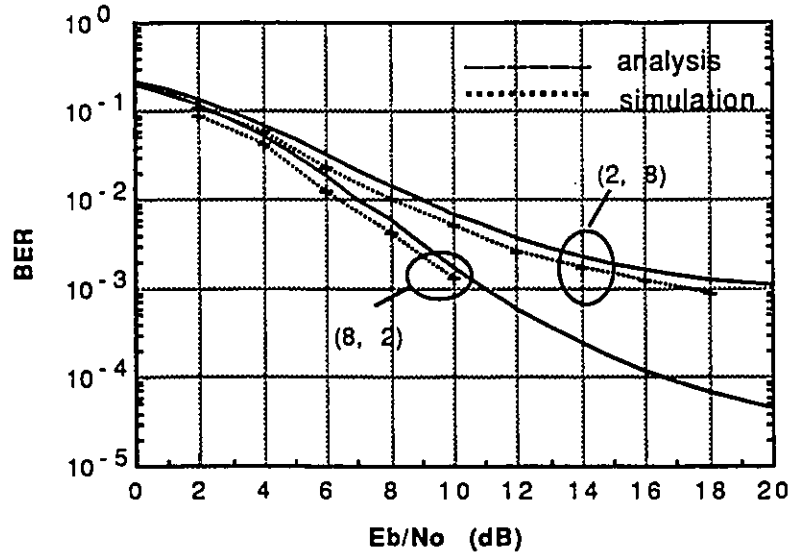

Figure 5.3 : BER performance of MFSK-CC/DS-CDMA over a Rician fading channel: simulation vs. analysis; $N = 127$, $K = 10$, $\kappa = 10$ dB. The index pair shown by the curves are (M_f, M_c).

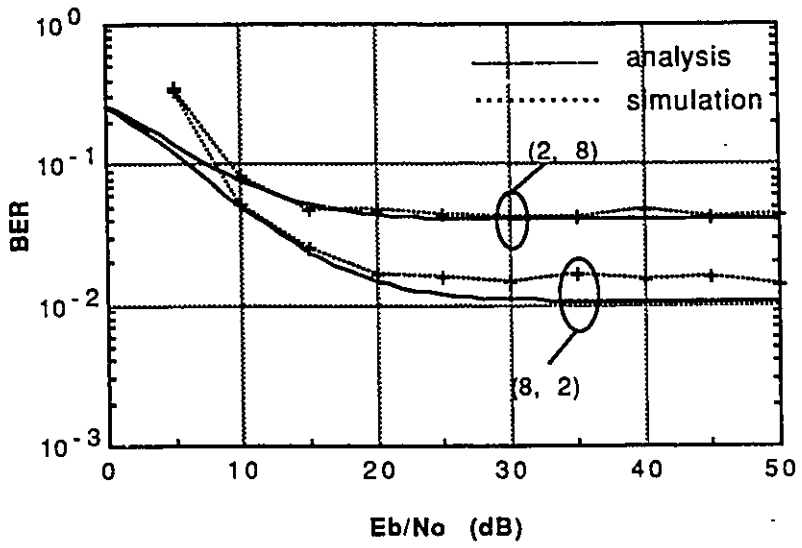

Figure 5.4 : BER performance of MFSK-OC/DS-CDMA over a Rayleigh fading channel: simulation vs. analysis; $N = 127$, $K = 10$. The index pair shown by the curves are (M_f, M_c).

curves, this is because of the MAI. Using the equation $\gamma_{bm} = 3M_f N/[2\log_2(M_f M_p)(K-1)]$ =, we have $\gamma_{bm} = 19.8$ dB for the system with $(M_f = 2, M_c = 8)$ and $\gamma_{bm} = 25.8$ dB for the system with $(M_f = 8, M_c = 2)$. The value of γ_b' is limited by γ_{bm}. Thus, the error floors for the two systems begin at about $\gamma_b = 19.8$ dB and 25.8 dB respectively.

5.4 Summary

In this chapter, we proposed a simulation model for the MFSK-OC/DS-CDMA system. We first gave a simple simulation model for the conventional noncoherent MFSK. Based on the simple model, and using Gaussian approximation for the MAI component, we built the CDMA system simulation model. Simulations have been carried out for AWGN, Rayleigh and Rician fading channels. The results agree well with the analysis. Since the MAI is considered as an equivalent additive Gaussian noise, the main purpose of the simulation is to verify the modulation scheme. In the analysis, the Gaussian approximation is considered as a contribution to the effective noise spectral density. However, due to the randomness of the MAI, the MAI is not equally

distributed in the M_f frequency tones during each symbol interval. Our simulation takes this into account. The results show that the analysis is valid.

Chapter 6

MFSK/DS-CDMA Employing Permutation Modulation

6.1 Introduction

In the conventional MFSK modulation scheme, one out of M frequency tones is transmitted per symbol interval to convey $\log_2 M$ bits of information. An extension of this modulation scheme is referred as FSK *permutation modulation* (PM) [88]-[90], in which a few frequency tones (say w) out of v are transmitted simultaneously per symbol interval to convey $\log_2 \begin{pmatrix} v \\ w \end{pmatrix}$ bits of information, where v is used to represent the total number of frequency tones for permutation modulation schemes in this chapter. Thus, MFSK modulation is a special case of permutation modulation (with $w = 1$ and $v = M$). Another modified permutation modulation scheme is referred as multi-tone FSK (MT-FSK) [91, 92], in which only a fraction of the $\begin{pmatrix} v \\ w \end{pmatrix}$ frequency tone combinations are selected, and thus a redundancy is introduced.

The permutation modulation was first proposed by Slepian [88]. Later the concept was developed from different aspects. A direct application of the concept is found in permutation codes used for FEC coding [88, 98, 99]. In [91], the MT-FSK scheme was introduced. It incorporates an implicit diversity in fading channels [91, 92]. An application of the permutation modulation to a FH-SS system is presented in [93] and [94]. Recently, the concept was used in a random multiple access system [95]. In this chapter, we apply the concept to a DS-CDMA system. The resultant system is referred as MT-FSK/DS-CDMA. This system uses MT-FSK as the modulation scheme.

Another permutation modulation scheme FSK-PM can be also used in a DS-CDMA system. Due to its nonefficiency in a fading channel, however, the corresponding DS-CDMA system is not considered in this thesis. In addition to the MT-FSK scheme, by making a simple selection of the available frequency tone combinations, we propose a new permutation modulation scheme, namely OMT-FSK/DS-CDMA where "O" stands for "orthogonal".

In narrowband systems, compared with MFSK with $v = M$, the FSK-PM scheme with $w > 1$ is more bandwidth efficient than power efficient. In a DS-CDMA system, since the bandwidth efficiency is directly related to the BER performance, a power efficient modulation scheme is preferred. The modified permutation modulation scheme, MT-FSK, is more power efficient especially in a fading channel, and thus can be attractive for certain applications.

The baseline signaling used in permutation modulation should be orthogonal; otherwise, the transmitted symbol cannot be detected efficiently. However, the permutation modulation is not only applicable to MFSK signaling, but also to other orthogonal signaling like the orthogonal codes discussed in Chapter 4. By introducing the orthogonal codes into the MT-FSK/DS-CDMA scheme, implementation complexity can be greatly reduced.

The contributions of this chapter are

(1) Applying the concept of permutation modulation to a DS-CDMA system, we propose a novel system, namely MT-FSK/DS-CDMA.

(2) By arranging the frequency tones in a different way, we propose a new permutation modulation, namely OMT-FSK. The corresponding DS-CDMA system is OMT-FSK/DS-CDMA.

(3) With the introduction of orthogonal codes to the MT-FSK/DS-CDMA system, implementation complexity can be greatly reduced.

(4) The system performance over AWGN and fading channels are evaluated. An analysis for the BER performance over a frequency non-selective slow Rician fading channel is presented.

(5) FEC coding is considered for the MT-FSK/DS-CDMA system.

(6) Computer simulation for the MT-FSK/DS-CDMA scheme is performed.

In Section 6.2, two permutation modulation schemes, FSK-PM and MT-FSK, are described. The system model for MT-FSK/DS-CDMA is discussed in Section 6.3. In Section 6.4, the performance of MT-FSK/DS-CDMA is analyzed over AWGN and fading channels. In Section 6.5, OMT-FSK/DS-CDMA is described. In Section 6.6, orthogonal codes are considered to reduce the implementation complexity of a MT-FSK/DS-CDMA system. FEC coding is considered for MT-FSK/DS-CDMA in Section 6.7. Computer simulation for the MT-FSK/DS-CDMA system is discussed in Section 6.8, and a summary is given in Section 6.9.

6.2 Permutation Modulation

In this section, we provide a basic description for the two permutation modulation schemes: FSK-PM and MT-FSK. Though the FSK-PM scheme will not be applied to a CDMA system in this thesis, it is briefly discussed here to aid the understanding of the permutation modulation concept.

6.2.1 FSK Permutation Modulation

FSK permutation modulation (FSK-PM) is specified by a pair of integer parameters (v, w), where v is the total number of frequency tones, and w is the number of frequency tones to be transmitted in one symbol interval. The total number of symbols is $\binom{v}{w}$ which contains $\log_2 \binom{v}{w}$ bits of information. The number $\binom{v}{w}$ may not be a integer power of two. If binary data is transmitted, a subset of $\binom{v}{w}$ symbols can be used. A nonbinary data transmission may be matched to an FSK-PM scheme perfectly. For example, the FSK-PM scheme with $v = 5$ and $w = 2$ contains 10 symbols and is well suited to decimal digits. For binary data transmission, however, 8 of the 10 symbols can be used, and each symbol contains 3 bits of information.

The transmitter contains v oscillators. In each symbol period, w frequency tones are selected according to the input data and combined for transmission. In the receiver, there are v parallel matched filters corresponding to the v frequency tones, as in a conventional MFSK receiver, and the w largest outputs are chosen as the decision. Noncoherent detection is usually employed.

The bandwidth efficiency of the FSK-PM is

$$\eta = \frac{1}{v} \log_2 \binom{v}{w}. \tag{6.1}$$

The BER performance in an AWGN channel is discussed in [89].

Compared to MFSK with parameter $v = M$, FSK-PM is more bandwidth efficient but less energy efficient. In MFSK as M increases the power efficiency increases while the bandwidth efficiency decreases. In the case of FSK-PM this tradeoff is not as straightforward and linear as for MFSK. As a result of this, some higher level FSK-PM schemes are more efficient in both bandwidth and energy than lower level MFSK schemes [89]. For example, compared to an MFSK scheme, an FSK-PM with parameters $v = 2M$ and $w = 2$ performs better in both bandwidth and energy considerations. We have the following argument to prove the above statement. Assuming that noncoherent detection is used, the bandwidth efficiency of MFSK is $\frac{\log_2 M}{M}$, while the bandwidth efficiency of FSK-PM is $\frac{1}{2M} \log_2 \binom{2M}{2}$. The latter is greater than the former for $M > 1$. For low symbol error rates, the probability of error is dominated by the SNR per frequency tone $\frac{E_t}{N_0}$, where E_t denotes the energy per tone. In the case of MFSK, $E_t = E_s$, and $\frac{E_t}{N_0} = \log_2 M \frac{E_b}{N_0}$. In the case of FSK-PM, we have $\frac{E_t}{N_0} = \frac{1}{w} \log_2 \binom{v}{w} \frac{E_b}{N_0}$. For a fixed bit energy to noise spectral density ratio $\frac{E_b}{N_0}$, it can be easily seen that $\frac{E_t}{N_0}$ of MFSK-PM with parameter $(2M, 2)$ is greater than that of MFSK for $M > 1$. Thus, in this example, FSK-PM achieves a greater bandwidth and energy efficiency than MFSK.

6.2.2 Multi-tone FSK

The FSK-PM scheme described above performs well in an AWGN channel. However, its performance is poor in fading channels. Another permutation modulation scheme,

multi-tone FSK, is discussed in [91].

As in the FSK-PM scheme, we still use v to denote the total number of frequency tones and w the number of selected transmit tones for a symbol. The total number of combinations for the transmit tones is $\begin{pmatrix} v \\ w \end{pmatrix}$. Each combination can be used to represent a symbol. However, only a small fraction of these combinations is used. Thus, a redundancy is introduced. The resultant symbol set can be equivalent to a block FEC code. The total number of frequency tones v is viewed as the code length. The number of selected tones w is viewed as the number of "1"s in each code word, also known as the Hamming weight. The number of the code words, i.e., the number of symbols is denoted as b. In finding b, we are concerned with a balanced incomplete block design (BIB design). The BIB design [96]-[99] is identified by five parameters (v, b, r, w, λ). Among the five parameters, three of them have been defined. For convenience, we list all the definitions as follows:

v: total number of frequency tones;

b: total number of distinct symbols;

r: number of symbols which contain a distinct tone;

w: number of selected tones per symbol;

λ: number of symbols which contain a distinct pair of tones.

In combinatorial theory [98], these five parameters are defined in more general terms. A more detailed explanation is given in Appendix F. The total number of frequency tones v is not necessarily an integer power of 2. For a simple case, the parameter r is chosen as unity. The resultant system is called Steiner MT-FSK. To help understanding the meaning of the five parameters, an example is given in Table 6.1 for the BIB design with parameters (7, 7, 3, 3, 1).

In this example, the total number of frequency tones (v) is 7 denoted respectively by f_1, f_2, f_3, f_4, f_5, f_6 and f_7. The total number of symbols (b) is 7. Each symbol contains 3 frequency tones, i.e., $w = 3$. For instance, the symbol-1 is formed by a summation of three frequency tones f_1, f_2 and f_4. The same frequency tone appears in 3 symbols ($r = 3$), and the same pair of frequency tones appear in only 1 symbol ($\lambda = 1$). For instance, the frequency tone f_1 appears in symbol-1, symbol-5 and symbol-7,

Table 6.1 : An example of BIB design with parameters (7, 7, 3, 3, 1).

symbols	selected frequency tones
1	f_1, f_2, f_4
2	f_2, f_3, f_5
3	f_3, f_4, f_6
4	f_4, f_5, f_7
5	f_5, f_6, f_1
6	f_6, f_7, f_2
7	f_7, f_1, f_3

and a pair of frequency tones f_1 and f_2 appears only in symbol-1. In this example, the total number of combinations for the transmit tones is $\begin{pmatrix} v \\ w \end{pmatrix} = \begin{pmatrix} 7 \\ 3 \end{pmatrix} = 35$, while the number of symbols is only 7, a fifth of 35. From a block code point of view, this example shows a (7,3) block code with a Hamming weight $w = 3$. Since two different symbols may contain the same tone, its minimum Hamming distance is $2(w-1) = 4$. Clearly, this is not a linear code in which the minimum Hamming distance is equal to the Hamming weight. Decoding techniques for these codes are discussed in [91]. For simple schemes, table-looking up methods can be employed. If a binary data stream is transmitted, k bits can be grouped to choose a symbol. In an MFSK scheme, we have $k = \log_2 M$. In the MT-FSK scheme, the parameter k satisfies the unequality $2^k \leq b$. In the example, k can be chosen as 2. As shown in Appendix F, the five parameters for a Steiner MT-FSK are not independent. In the following analysis, three parameters, (v, w, k), are used to express a specified Steiner MT-FSK scheme. A Steiner MT-FSK scheme is denoted as MT(v, w, k). The scheme shown in the above example is MT(7,3,2).

The implementation of the transmitter is simple. A mapper from input bits to symbols and w oscillators are needed. In each symbol interval, k bits input data is used to select w frequency tones according to the mapping rule. Then the w tones are combined linearly to form the transmit symbol. The receiver consists of a group of v matched filters followed by noncoherent detectors. The v outputs are properly grouped to form b decision variables. The largest is chosen as the decision.

The performance of the MT-FSK over AWGN and Rayleigh fading channels is given in [92]. The symbol error rate is

$$P_s(\gamma_b, w) \leq x_0 P_{2,0} + x_1 P_{2,1} \tag{6.2}$$

where

$$P_{2,0} = P_2(\gamma_b, w), \tag{6.3}$$

$$P_{2,1} = P_2(\gamma_b, w-1), \tag{6.4}$$

and x_0 and x_1 are given in (F.5) and (F.6). In an AWGN channel, the pairwise probability of error is

$$P_2(\gamma_b, L) = \frac{e^{-k\gamma_b/2}}{2^{2L-1}} \sum_{n=0}^{L-1} \frac{1}{n!} \left(\frac{k\gamma_b}{2}\right)^n \sum_{r=0}^{L-1-n} \binom{2L-1}{r}. \tag{6.5}$$

In a Rayleigh fading channel, the decision error probabilities are obtained as the average

$$P_2(\bar{\gamma}_b, L) = \int_0^\infty P_2(\gamma_b \rho^2, L) p(\rho) \mathrm{d}\rho, \tag{6.6}$$

where $p(\rho)$ is the Rayleigh distribution, and this expression is found as

$$P_2(\bar{\gamma}_b, L) = \left(\frac{1}{2+\bar{\gamma}_c}\right)^L \sum_{r=0}^{L-1} \binom{L-1+r}{r} \left(\frac{1+\bar{\gamma}_c}{2+\bar{\gamma}_c}\right)^r, \tag{6.7}$$

where $\bar{\gamma}_c = \bar{\gamma}_b' k/L$. The probability of bit error can be approximated by multiplying $P_s(\gamma_b, w)$ by a factor $2^{k-1}/(2^k - 1)$.

6.3 System Model

6.3.1 Transmitter Model

The implementation of MT-FSK/DS-CDMA is an extension of the corresponding narrowband system. The block diagram of the transmitter is shown in Fig. 6.1-(a). The input data is first FEC encoded. The FEC code may be nonbinary, and thus requires the input data to be grouped in blocks. The modulation is nonbinary. The number of bits per symbol k is determined by the MT-FSK scheme employed. It is desirable to choose a consistent coding scheme, i.e., a q-ary ($q = 2^k$) code. For

instance, dual-k code is a suitable choice. In each symbol period, according to the k input bits, the modulator chooses w frequency tones to transmit from a total of v tones. Each of the selected tones is multiplied by a PN sequence. For the time being, we assume that a single PN code is used. It will later be shown that multiple PN codes may be used to reduce the system complexity. The resultant signals are combined and transmitted; and the system is denoted as MT(v, w, k).

The baseband transmit signal for the ith user can be expressed as

$$u_i(t) = \sqrt{2P/w}\Psi(t)a_i(t)\sum_{j=1}^{w}\exp\left[j2\pi b_{i,j}(t)\Delta + j\theta_{i,j}(t)\right], \tag{6.8}$$

where P, $\Psi(t)$, $a_i(t)$ and Δ are as defined in Section 3.2. In (6.8), $b_{i,j}(t)$ is given as

$$b_{i,j}(t) = \sum_{l=-\infty}^{\infty} b_l^{i,j} P_{T_s}(t - jT_s), \tag{6.9}$$

where the symbol interval $T_s = T_b/k$, and $b_l^{i,j}$ takes the values $(-(v-1), -(v-3), \cdots, (v-1). \pm 1, \pm 3, \cdots, \pm(M-1)$. The phases $\theta_{i,j}(t)$ are introduced by the modulator. During a symbol interval, the phase $\theta_{i,j}(t)$ is assumed to be constant.

6.3.2 Receiver Model

The block diagram of the receiver for a single spreading code is shown in Fig. 6.1-(b). The receiver consists of v matched filters followed by b square-law combiners. The v matched filters correspond to the v frequency tones. PN sequence despreading is performed in each matched filter. The v noncoherently detected outputs are combined in b different ways to form b decision variables. These b combiner outputs are processed in the decision unit. For either uncoded case or for FEC coding with hard decision decoding, the largest one of the b outputs is selected as the detected output. For soft decision decoding, the b values from the combiner outputs are passed to the FEC decoder. For multiple spreading codes (say c), each matched filter will be replaced by c matched filters.

The received signal for the ith user can be expressed as

$$r_i(t) = \mathrm{Re}\{w_i(t)e^{j2\pi f_c t}\}, \tag{6.10}$$

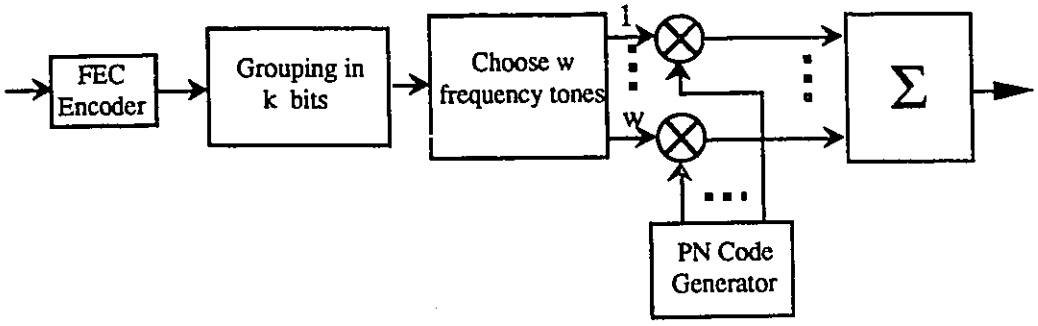

(a)

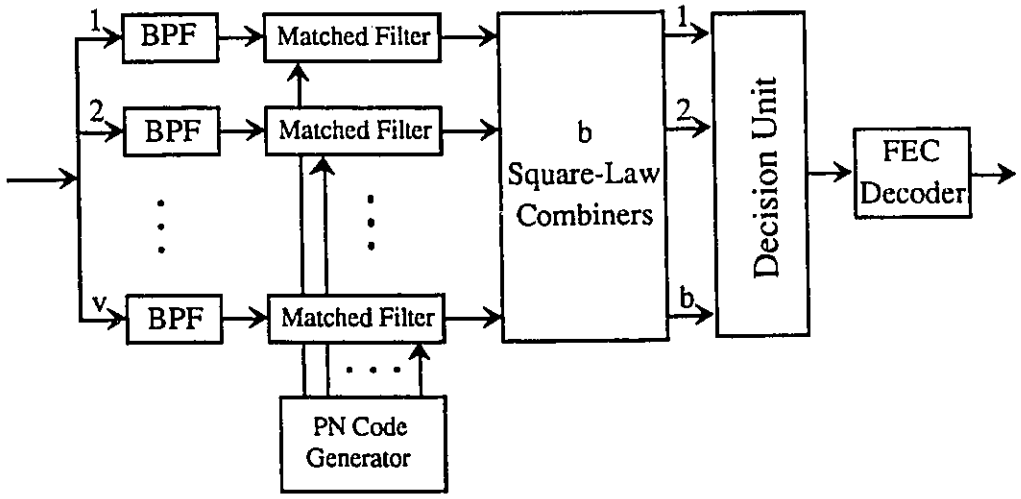

(b)

Figure 6.1 : Block diagram of MT-FSK/DS-CDMA. (a) Transmitter; (b) Receiver.

where $w_i(t)$ is the equivalent baseband signal given by

$$w_i(t) = \sum_{j=1}^{K} v_j(t) + n_i(t), \tag{6.11}$$

where $v_i(t)$ is the output of the fading channel for an input $u_i(t)$. For an AWGN channel, we have $v_i(t) = u_i(t)$. In (6.11), $n_i(t)$ is the equivalent lowpass additive Gaussian noise having a zero mean and a power spectral density N_0. In the v branch output, we have v decision variables defined as

$$U_m = \left| \int_0^{T_s} w_i(t) u_{i,m}(t) \mathrm{d}t \right| \quad m = 1, 2, \cdots, v. \tag{6.12}$$

6.4 Performance Analysis of MT-FSK/DS-CDMA

6.4.1 Bandwidth Efficiency

Assume γ_c' is the ratio of symbol energy in a frequency tone to the effective noise (AWGN plus MAI) spectral density. Since w tones are simultaneously transmitted, the symbol energy in each frequency tone is $\gamma_c' = \gamma_s'/w = k\gamma_b'/w$. Using the Gaussian approximation for the MAI, the effective noise power is $N_0 W + (K-1)E_s R_s$. The effective noise spectral density is

$$N_0' = \frac{N_0 W + (K-1)E_s R_s}{W} = N_0 + \frac{(K-1)E_s}{vN}. \tag{6.13}$$

We have

$$\gamma_s' = \frac{E_s}{N_0'} = \frac{\gamma_s}{1 + \frac{(K-1)\gamma_s}{vN}}, \tag{6.14}$$

and

$$\gamma_b' = \frac{\gamma_b}{1 + \frac{(K-1)\gamma_b k}{vN}}. \tag{6.15}$$

The above analysis assumes that the MAI from all users are independent Gaussian noise. By performing a detailed analysis as in Section 4.3.2 for MFSK-OC/DS-CDMA, (6.15) should be modified by

$$\gamma_b' = \frac{\gamma_b}{1 + \frac{2}{3}\frac{(K-1)\gamma_b k}{vN}}. \tag{6.16}$$

The term vN/k is equal to W/R_b. Thus, the bandwidth efficiency in b/s/Hz is

$$\eta = \frac{KR_b}{W} \simeq \frac{3}{2}\frac{\gamma_b - \gamma_b'}{\gamma_b\gamma_b'} \quad \text{(b/s/Hz)}. \tag{6.17}$$

This result is the same as that given in Chapter 3 and Chapter 4.

6.4.2 BER Performance

The BER performance of the MT-FSK over AWGN and Rayleigh fading channels is given in [92] and listed in (6.2) – (6.7) for narrowband system. The result can be modified for the CDMA system with the bit energy to effective noise spectral density ratio given by (6.15).

Now we are finding the performance of MT-FSK over Rician fading channels. We assume that all the frequency tones experience independent fading. A similar assumption was made in [92] for a Rayleigh fading channel. In each subchannel, the fading process is described by a Rician distribution given in (2.12). For the analysis, we first need to find the pairwise error probability. In an AWGN channel, the pairwise error probability is $P_2(\gamma_s', L)$ given in (6.5), where γ_s' is symbol energy to the effective noise spectral density ratio, and L is the number of tones in a symbol which are not common to the other symbol (if the pair of symbols have no common tone, then $L = w$). In a Rician fading channel, each frequency tone signal experiences a fading characterized by a Rician random variable ρ_i ($i = 1, \cdot, L$) with parameter s_1 and σ^2. Assume square-law combiner is used, the fading factor ρ is an addition of L Rician distributed random variables

$$\rho = \sqrt{\sum_{i=1}^{L} \rho_i^2}. \tag{6.18}$$

Thus, ρ has a generalized Rician distribution:

$$p(\rho) = \frac{\rho^L}{\sigma^2 s^{L-1}} \exp\left(-\frac{\rho^2 + s^2}{2\sigma^2}\right) I_{L-1}\left(\frac{\rho s}{\sigma^2}\right), \tag{6.19}$$

where $s^2 = \sum_{i=1}^{L} s_1^2$. The SNR per symbol at the receiver is

$$\gamma_s{}' = \gamma_c{}'\rho^2 = \gamma_c{}'\sum_{i=1}^{L} \rho_i^2. \tag{6.20}$$

The average SNR per symbol is

$$\bar{\gamma_s}' = \gamma_c' \mathrm{E}\{\sum_{i=1}^{L} \rho_i^2\} = \gamma_c' \sum_{i=1}^{L} \mathrm{E}\{\rho_i^2\} = L\bar{\gamma_c}'. \tag{6.21}$$

The pairwise error probability is

$$P_2(\bar{\gamma_b}', L) = \int_0^\infty P_2(\gamma_b', L) p(\rho) \mathrm{d}\rho, \tag{6.22}$$

where

$$\gamma_b' = \frac{\gamma_s'}{k} = \frac{\gamma_c' \rho^2}{k}. \tag{6.23}$$

Working on (6.22) gives the following result (see Appendix G):

$$P_2(\bar{\gamma_b}', L) = \frac{1}{2^{2L-1}(L-1)!\left(1+\frac{\bar{\gamma_c}'}{2(1+\kappa)}\right)^L} \exp\left[-\frac{L\kappa\bar{\gamma_c}' + 2(1+\kappa)L\kappa}{2(1+\kappa)+\bar{\gamma_c}'}\right] \sum_{n=0}^{L-1} \sum_{r=0}^{L-1-n} \frac{(L+n-1)!}{n!} \left[\frac{\bar{\gamma_c}'}{2(1+\kappa)+\bar{\gamma_c}'}\right]^n \binom{2L-1}{r} {}_1F_1\left(L+n, L; \frac{L\kappa}{1+\frac{\bar{\gamma_c}'}{2(1+\kappa)}}\right), \tag{6.24}$$

where ${}_1F_1(a, b; x)$ is the confluent hypergeometric function. This rather complex expression can be solved by using readily available software packages. We have solved (6.24) using *Mathematica* [100]. The results are presented in the next section.

The BER performance can be obtained from (6.2)–(6.4) with $P_2(\bar{\gamma_s}', L)$ given in (6.24).

6.4.3 Results and Discussions

We consider the performance in terms of the bit energy to effective noise spectral density ratio. The effect of MAI has been discussed is Section 3.5.

6.4.3.1 AWGN Channel

In Fig. 6.2, the BER performance of MT-FSK/DS-CDMA with $w = 4$ and various k and v is shown. The performance improves when the number of bits per symbol (k) and the total number of frequency tones (v) increase. This is similar to the behaviour of MFSK when M is increased. With the same number of frequency tones, the performance of MT-MFSK is worse than that of MFSK. In Fig. 6.3, the BER

performance of MT-FSK/DS-CDMA with the same k (=5) is shown. We see that the performance with larger w is a little worse. This can be explained as follows. With the same parameter k, the symbol energy is the same. For larger w, each transmitted tone contains smaller energy, and due to the noncoherent combining, the performance is degraded.

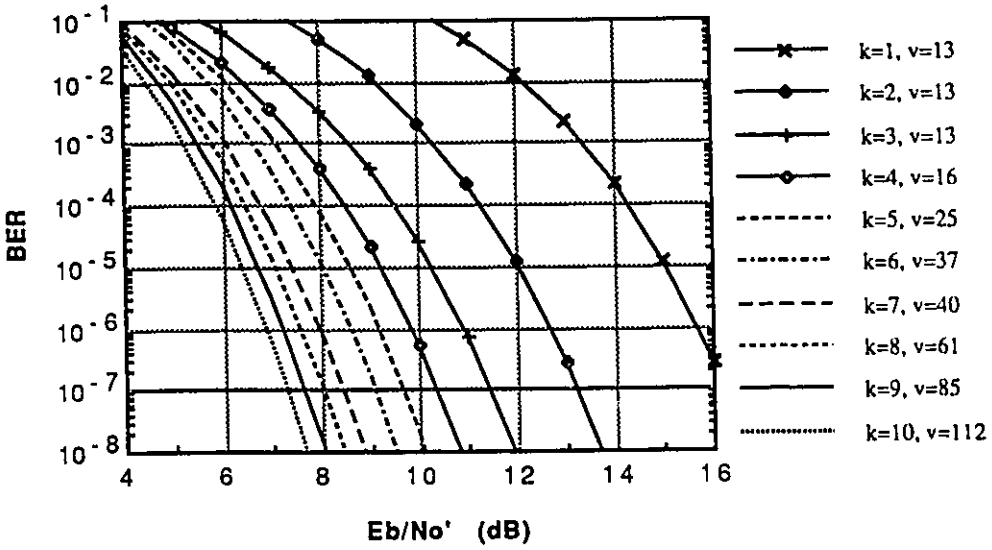

Figure 6.2 : BER performance of MT-FSK/DS-CDMA with $w = 4$ over an AWGN channel.

In Tables 6.2 and 6.3, we list the required bit energy to the effective noise spectral density ratio and the corresponding asymptotic bandwidth efficiency for a BER of 10^{-3} and 10^{-5} respectively.

6.4.3.2 Rayleigh Fading Channel

The BER performance of MT-FSK/DS-CDMA with $w = 4$ and various k and v is shown in Fig. 6.4. The BER performance of MT-FSK/DS-CDMA with the same k (=5) is shown in Fig. 6.5. The performance is better when w and k become larger. In this case, the parameter w is more important than k. It introduces an equivalent

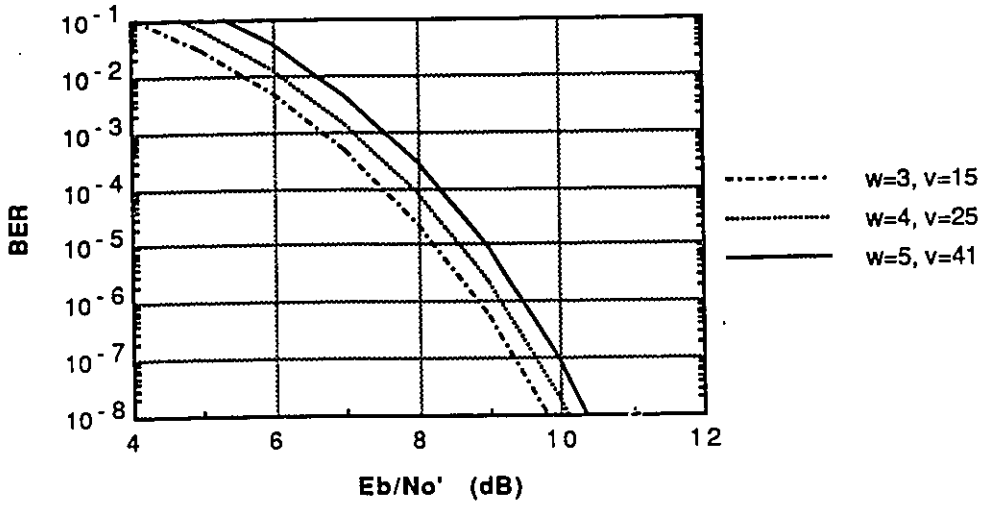

Figure 6.3 : BER performance of MT-FSK/DS-CDMA with $k = 5$ over an AWGN channel.

Table 6.2 : The required SNR per bit γ_b' (in dB) and asymptotic bandwidth efficiency (in b/s/Hz) for a BER of 10^{-3} for the MT-FSK/DS-CDMA.

v, w, k	γ_b'	η
(13, 4, 1)	13.4	0.07
(13, 4, 2)	10.4	0.14
(13, 4, 3)	8.6	0.21
(16, 4, 4)	7.6	0.26
(15, 3, 5)	6.5	0.34
(25, 4, 5)	7.1	0.29
(41, 5, 5)	7.6	0.26
(37, 4, 6)	6.7	0.32
(40, 4, 7)	6.1	0.37
(61, 4, 8)	5.8	0.39

Table 6.3 : The required SNR per bit γ_b' (in dB) and asymptotic bandwidth efficiency (in b/s/Hz) for a BER of 10^{-5} for the MT-FSK/DS-CDMA.

v, w, k	γ_b'	η
(13, 4, 1)	15.1	0.05
(13, 4, 2)	12.1	0.09
(13, 4, 3)	10.3	0.14
(16, 4, 4)	9.2	0.18
(15, 3, 5)	8.1	0.23
(25, 4, 5)	8.6	0.21
(41, 5, 5)	9.0	0.19
(37, 4, 6)	8.1	0.23
(40, 4, 7)	7.4	0.27
(61, 4, 8)	7.1	0.29

number $(w-1)$ of diversity paths. In a fading channel, increasing k and v causes very little performance benefit. Therefore it is not worthwhile using large number of frequency tones. Instead, larger w is preferred.

In Tables 6.4 and 6.5, we list the required bit energy to the effective noise spectral density ratio and corresponding bandwidth efficiency for BER of 10^{-3} and 10^{-5} respectively. Compared to MFSK/DS-CDMA system, it is observed that much larger bandwidth efficiency can be achieved, especially in fading channels.

6.4.3.3 Rician Fading Channel

The BER performance of MT-FSK/DS-CDMA over a Rician fading channel with $\kappa = 10$ dB is shown in Fig. 6.6. Three schemes, MT(15, 3, 5), MT(16, 4, 4) and MT(25, 4, 5), are illustrated. In choosing these three schemes, we want to examine the dependence of system performance on parameters w and k. We see that MT(25, 5, 4) and MT(15, 3, 5) do not have the big difference as in a Rayleigh fading channel. Comparing the scheme MT(25, 5, 4) with MT(16, 4, 4), the large difference is not seen as in an AWGN fading channel. So the system performance over a Rician fading channel ($\kappa = 10$ dB) does not have a strong dependence on either k or w. However, the performance improves when v increases. In Fig. 6.7, we take the scheme (15,3,5)

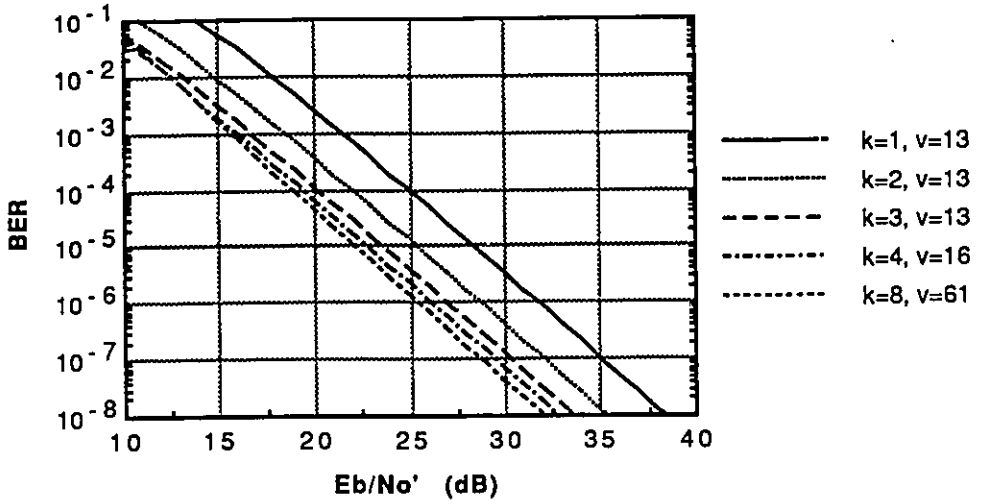

Figure 6.4 : BER performance of MT-FSK/DS-CDMA with $w = 4$ over a Rayleigh fading channel.

Table 6.4 : The required SNR per bit γ_b' (in dB) and asymptotic bandwidth efficiency (in b/s/Hz) for a BER of 10^{-3} for the MT-FSK/DS-CDMA in a Rayleigh fading channel.

v, k, w	γ_b'	η
(13, 4, 1)	21.5	0.011
(13, 4, 2)	18.5	0.021
(13, 4, 3)	16.7	0.032
(16, 4, 4)	15.9	0.039
(15, 3, 5)	19.3	0.018
(25, 4, 5)	15.9	0.039
(41, 5, 5)	14.4	0.054
(37, 4, 6)	15.9	0.039
(40, 4, 7)	15.4	0.043
(61, 4, 8)	15.6	0.041

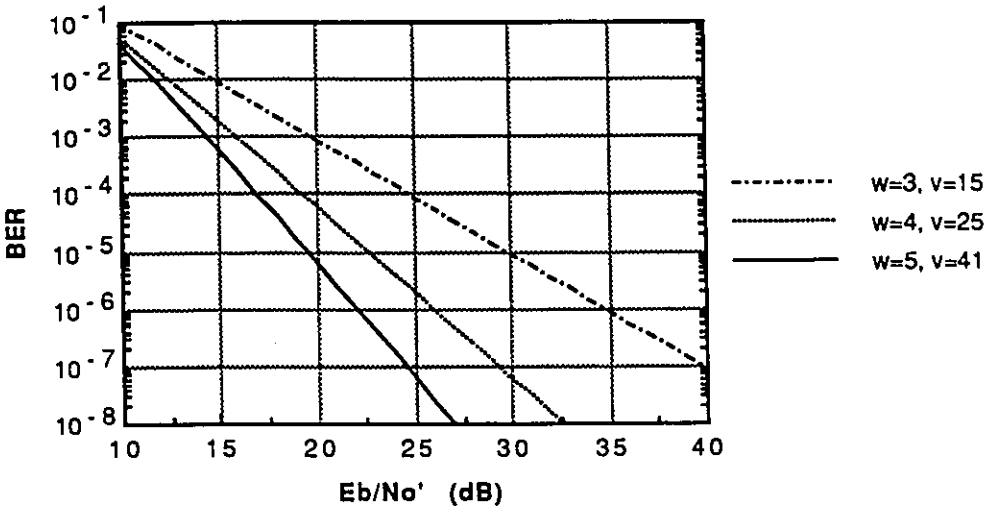

Figure 6.5 : BER performance of MT-FSK/DS-CDMA with $k = 5$ over a Rayleigh fading channel.

Table 6.5 : The required SNR per bit γ_b' (in dB) and asymptotic bandwidth efficiency (in b/s/Hz) for a BER of 10^{-5} for the MT-FSK/DS-CDMA in a Rayleigh fading channel.

v, k, w	γ_b'	η
(13, 4, 1)	28.3	0.0022
(13, 4, 2)	25.3	0.0044
(13, 4, 3)	23.5	0.0067
(16, 4, 4)	22.7	0.0081
(15, 3, 5)	29.3	0.0018
(25, 4, 5)	22.6	0.0082
(41, 5, 5)	19.5	0.0168
(37, 4, 6)	22.5	0.0084
(40, 4, 7)	22.0	0.0095
(61, 4, 8)	22.1	0.0092

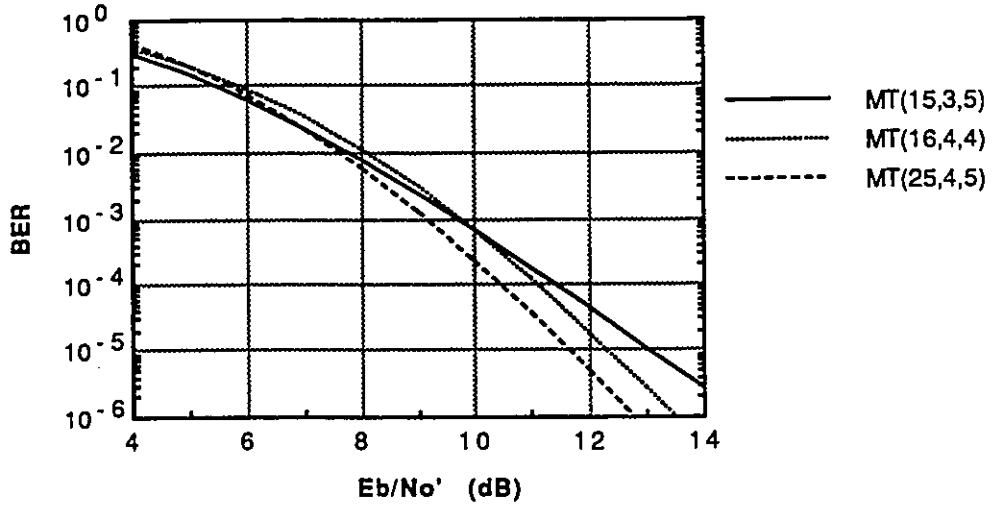

Figure 6.6 : BER performance of MT-FSK/DS-CDMA over a Rician fading channel with $\kappa = 10$ dB.

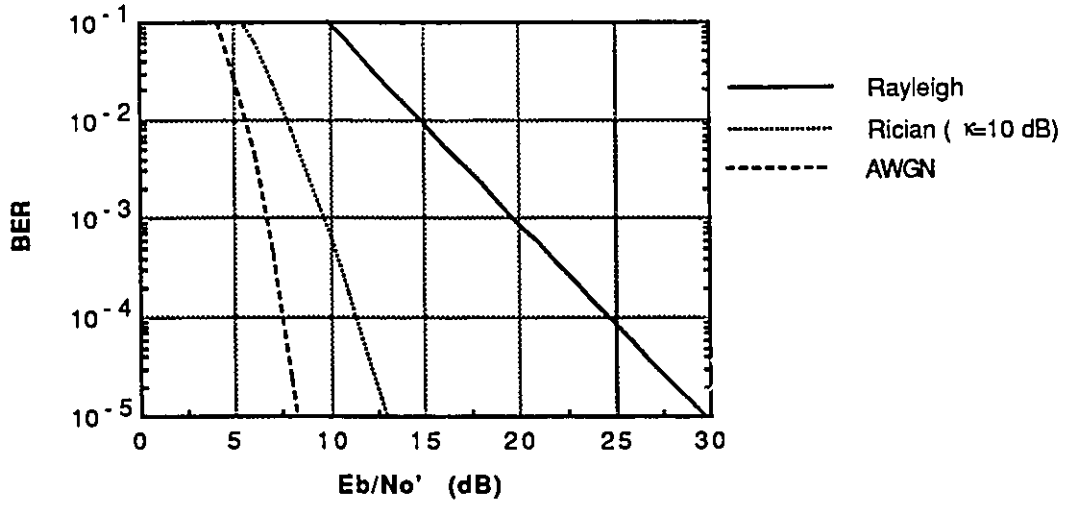

Figure 6.7 : BER performance of MT-FSK/DS-CDMA with MT(15, 3, 5) scheme in different channels.

as an example to show a comparison for the performance over a different channels. In this case, the behavior in a Rician fading is closer to that in an AWGN channel.

6.5 Performance Analysis of OMT-FSK/DS-CDMA

6.5.1 System Description

From the results of previous section, we see that the advantage of the MT-FSK/DS-CDMA lies in the implicit diversity in a fading channel. In an MT-FSK scheme, since two distinct symbols may contain the same tone, a diversity of order $w-1$ is obtained. If all the symbols are orthogonal to each other, we will expect a diversity of w. In this case, however, the number of choices of the symbols will be reduced. Thus, for a given parameter v, the number of information bits per symbol k will be smaller, and a performance degradation in an AWGN channel will occur. In this section, we discuss a new scheme by using a simple selection method for the frequency tone combinations. The resultant symbols will be orthogonal to each other. The system is called OMT-FSK/DS-CDMA, where O stands for orthogonal. The frequency selection rule is:

(1) The total number of frequency tones is v, each symbol contains w tones;

(2) Any two distinct symbols do not contain the same tone.

Thus, the scheme is specified by two parameters v and w. The total number of symbols is $b = v/w$ when w divides v. The transmitter and receiver structure are the same as that of MT-FSK/DS-CDMA except the frequency selection method. An example for $v = 16$ is given in Table 6.6.

Table 6.6 : An example of OMT-FSK with $v = 16$. b: the number of symbols; each symbol consists of w tones represented by integer numbers.

w	b	symbols
1	16	1, 2, $\cdots$,16 (16FSK)
2	8	(1,9), (2,10), (3,11), (4,12), (5,13), (6,14), (7,15), (8,16)
3	5	(1,6,11), (2,7,12), (3,8,13), (4,9,14), (5,10,15)
4	4	(1,5,9,13), (2,6,10,14), (3,7,11,15), (4,8,12,16)
8	2	(1,3,5,7,9,11,13), (2,4,6,8,10,12,14,16)

In this example, we try to make the frequency tone separation in each symbol as large as possible. By doing this way, frequency diversity can be obtained more easily. For $w = 3$, the total number of symbols is 5. The frequency tone 16 is never used. Thus, we would choose the number of frequency tones as a integer times of the weight w.

6.5.2 Performance Evaluation

The performance expression for the MT-FSK/DS-CDMA can be easily modified for the OMT-FSK/DS-CDMA scheme. Since the Hamming distance between every pair of the symbols is $2w$, the symbol error rate is bounded by

$$P_s(\gamma_b, w, v) \leq x P_{\gamma_b, w}, \tag{6.25}$$

where $P_{\gamma_b,w}$ is given in (6.5), (6.7) and (6.24) for AWGN, Rayleigh and Rician channels respectively, and x is the total number of symbols minus one

$$x = \left(\frac{v}{w} - 1\right). \tag{6.26}$$

In Fig. 6.8, the BER performance of OMT-FSK/DS-CDMA over an AWGN channel is shown for $v = 16$ and $w = 1$, 2, 4 and 8. When $w = 1$, the system reduces to the MFSK/DS-CDMA system with $M = v$. For comparison, the MT-FSK/DS-CDMA with schemes MT(16, 4, 4) and MT(15, 3, 5) are also given. For the OMT-FSK scheme, a larger value of w results in a worse BER performance. So in an AWGN channel, the proposed scheme is not preferred. In Fig. 6.9, the performance of the same systems over a Rayleigh fading channel is shown. Our conclusion for an AWGN channel is reversed. The worst scheme ($w = 8$) in a AWGN channel is now the best one. This is an interesting result. The reason is the large diversity introduced by the new scheme. In Fig. 6.10, performance of a few schemes over both AWGN and Rayleigh fading channels is shown. The quite different behavior of the OMT-FSK scheme in the two different channels can be seen clearly. In this figure, the worst scheme ($w = 4$) in an AWGN channel is the best scheme in a Rayleigh fading channel. In a mobile environment which shows a Rayleigh behavior, our proposed scheme will obtain a best performance in a worst channel situation.

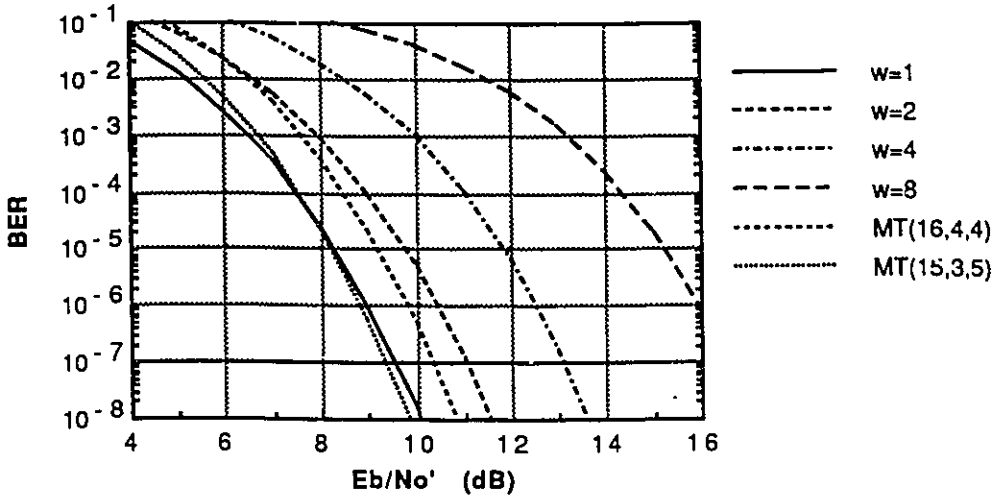

Figure 6.8 : BER performance of OMT-FSK/DS-CDMA ($v = 16$) over an AWGN channel.

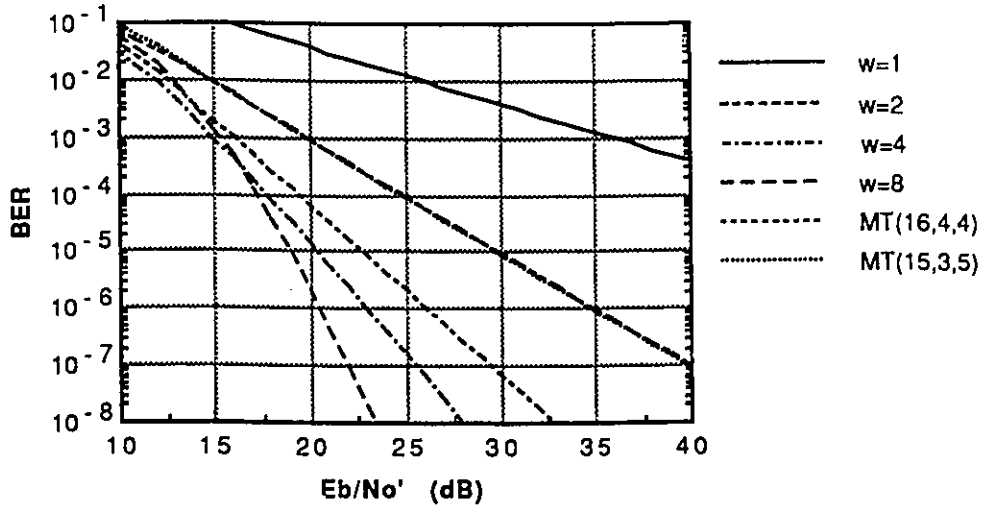

Figure 6.9 : BER performance of OMT-FSK/DS-CDMA ($v = 16$) over a Rayleigh fading channel.

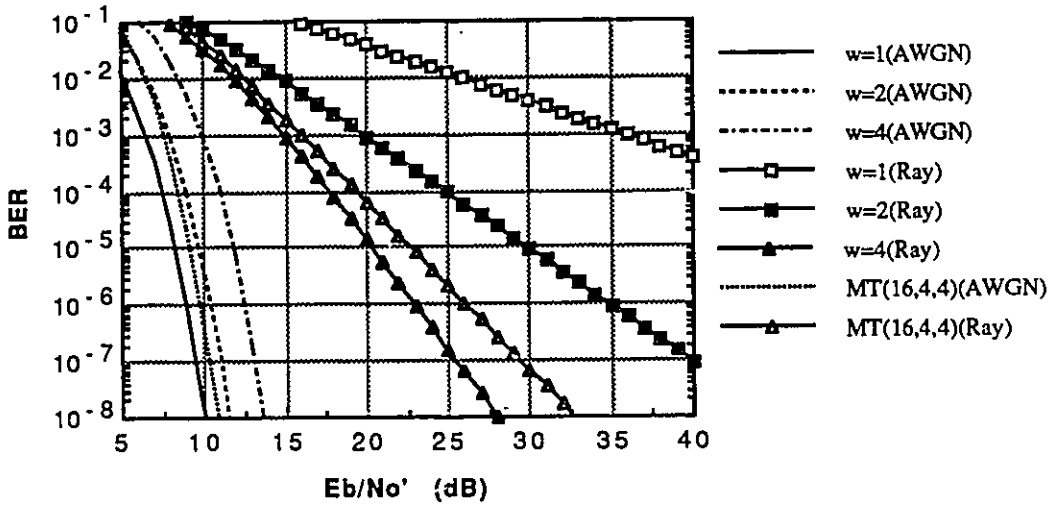

Figure 6.10 : Comparison for the BER performance of OMT-FSK/DS-CDMA over AWGN and Rayleigh fading channels.

As an example, we consider a possible cellular radio channel. Assuming that the multipath spread is 3 microseconds, the coherence bandwidth is about 333 kHz. Let the data rate be 10 kb/s. If using the OMT-FSK/DS-CDMA with $v = 16$ and $w = 4$, the symbol rate is $\frac{10}{\log_2(16/4)} = 5$ ksymbols/sec. Using a PN sequence of length 63, we obtain the PN chip rate as $R_c = NR_s = 315$ kHz, which is smaller than the coherence bandwidth. Thus, for each frequency tone, the spread signal experiences flat fading. In the system, since any two different tones (for instance, tone 1 and tone 5 in the symbol (1,5,9,13)) have a frequency spacing more than $3R_c = 945$ kHz which is larger than the coherence bandwidth, then the two tones fade independently and a diversity can be achieved. This example is only conceptual. From this example, however, we see that with a judicious selection of permutation modulation parameters and transmitted waveforms, the fading can be viewed as flat for each frequency tone and independent for the w simultaneously transmitting tones. Thus, a frequency diversity can be realized.

6.6 Complexity Reduction Using Orthogonal Codes

The performance of MT-FSK/DS-CDMA and OMT-FSK/DS-CDMA depends much on the number of information bits per symbol k in an AWGN channel and on the number of tones per symbol w in a fading channel. To achieve either a large k or w, the total number of frequency tones v should be large. A large value of v, however, means a high complexity. A possible way of reducing the complexity is by using orthogonal spreading codes. In Fig. 6.1-(a), we initially assumed that during each symbol transmission, the w selected frequency tones are multiplied by a single PN sequence. Now, if two or more PN sequences are utilized, we will have many more choices for the symbol representation. We assume that c orthogonal PN codes are used, all of them being orthogonal to each other, and the total number of frequency tones is v_c. For the MT-FSK/DS-CDMA scheme with $c = 1$, the relationship among parameters b, w and v for $\lambda = 1$ is (see Appendix F)

$$b = \frac{v_1(v_1 - 1)}{w(w-1)}. \tag{6.27}$$

Using c orthogonal codes, the total number of orthogonal signals is cv_c. To accommodate the same number of bits per symbol k, a sufficient condition is

$$\frac{cv_c(cv_c - 1)}{w(w-1)} - v_c \binom{c}{2} \geq 2^k. \tag{6.28}$$

In the above equation, the term $\binom{c}{2}$ represents the number of symbols which contain the same two tones with different PN codes. If this case is not excluded, the expected diversity cannot be obtained. Since each pair of elements occurs together only once ($\lambda = 1$), the number of pairs of elements occurring together for each tone is $\binom{c}{2}$. Thus the total number of such pairs is $v_c \binom{c}{2}$. Solving the above equation, the number of frequency tones v_c using c orthogonal codes can be expressed in terms of c as

$$v_c = \frac{\left[c + w(w-1)\binom{c}{2}\right] + \sqrt{\left[c + w(w-1)\binom{c}{2}\right]^2 + 4c^2w(w-1)2^k}}{2c^2}. \tag{6.29}$$

The number of frequency tones for $c = 2, 3$ and 4 are compared with single PN code as shown in Table 6.7. The number of frequency tones is reduced significantly by using orthogonal codes. For large number of frequency tones, the amount of reduction tends to be c times of v_1. Thus the complexity is much reduced, because the frequency synthesizer required for the frequency tone generation in both transmitter and receiver becomes simpler. Furthermore, the number of bandpass filters in both transmitter and receiver is reduced. Although the number of matched filters in the receiver will be cv_c which is the same number as in a single PN code case, the matched filtering can possibly be performed in software.

Table 6.7 : Relationship between the number of frequency tones v_c and the number of orthogonal codes c.

(k, w)	v_1	v_2	v_3	v_4
(3, 3)	9	5	4	4
(3, 4)	13	7	7	6
(3, 5)	21	10	9	9
(4, 4)	16	9	8	7
(5, 4)	25	12	10	8
(10, 4)	112	58	40	32
(10, 5)	145	75	52	40

6.7 FEC Coded MT-FSK/DS-CDMA

It was shown in the previous sections that the MT-FSK/DS-CDMA scheme introduces implicit diversity in a fading environment. It is also well known that FEC coding is a form of diversity in a fading situation. Thus, applying FEC coding to the MT-FSK/DS-CDMA will result in an effective concatenated diversity. Since the modulation scheme is nonbinary, we only considered nonbinary codes. For hard decision decoding, the performance is characterized by the symbol error rate of the uncoded system. For soft decision decoding, the performance analysis in a fading channel given in Appendix E can be used if the transmitted symbols are orthogonal to each

other. For the MT-FSK/DS-CDMA, however, the symbols are partially orthogonal. Recall that in an MT-FSK/DS-CDMA system, any two symbols are either orthogonal (having no common tone) or overlap in only one frequency tone. In Appendix E, we see that the coded system performance is determined by the pairwise error probability. In the MT-FSK/DS-CDMA system, the pairwise error probability can be upper bounded by the error probability of the symbols which have one common tone. This pairwise error probability can be approximated by $P_{2,1}$ given in (6.4) with γ_b replaced by γ_s. The pairwise probability of error $P_2(\gamma_s, L)$ is given by (6.5) in an AWGN channel, by (6.7) in a Rayleigh fading channel, and by (6.24) in a Rician fading channel. The performance of the coded system using soft decision decoding can be obtained from (E.14) and (E.16).

First we give the performance using hard decision decoding of Reed-Solomon codes. The performance of MT(16, 4, 4) scheme using RS codes is shown in Fig. 6.11 for an AWGN channel. The code length is 15. With the error correcting capability $t = 1$ and 2, a half dB coding gain is obtained for a BER of 10^{-3} and one dB is obtained for a BER of 10^{-5}. At this range, there is no big difference for different error correcting capabilities t.

For the MT(15, 3, 5) scheme as given in Fig. 6.12, since the uncoded scheme is better than MT(16, 4, 4) scheme, the coded system is even better. Corresponding to the parameter k, the code length is 31. The error correcting ability is stronger.

The same schemes and codes are examined for a Rayleigh fading channel as shown in Fig. 6.13 and Fig. 6.14. In this case, the coded scheme for MT(16, 4, 4) gives a better performance. However, this attributes to the larger diversity offered by the MT(16, 4, 4) signal. We see that the coding gain in MT(15, 3, 5) scheme is much larger.

In Fig. 6.15, we give the system performance over a Rayleigh fading channel using dual-k codes. Compared with the RS codes, a much better performance is obtained. This is due to the advantage of soft decision decoding. In a Rayleigh fading channel, in addition to the diversity introduced by the MT-FSK/DS-CDMA scheme, FEC coding further improves the performance.

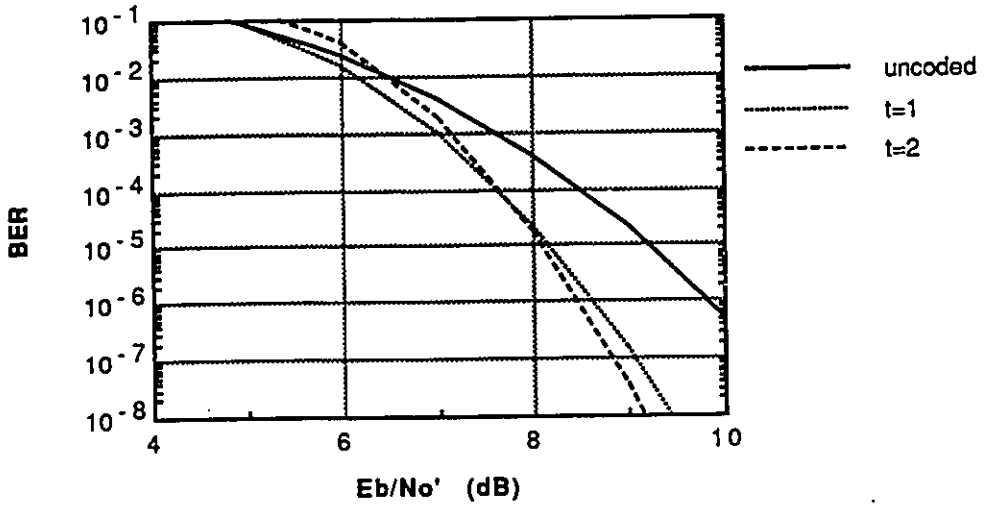

Figure 6.11 : BER performance for the MT-FSK/DS-CDMA (15, 4, 4) scheme over an AWGN channel using RS codes.

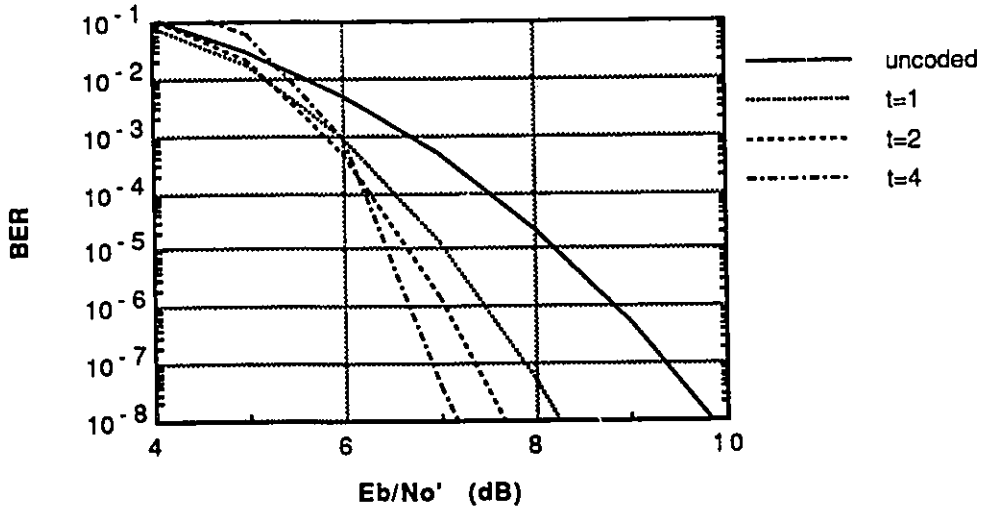

Figure 6.12 : BER performance for the MT(15, 3, 5) scheme over an AWGN channel using RS codes.

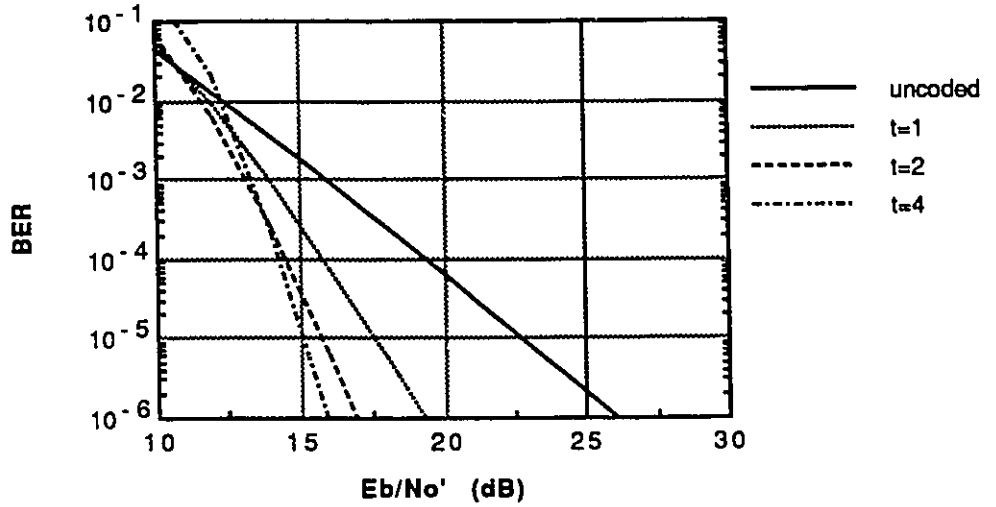

Figure 6.13 : BER performance for the MT(16, 4, 4) scheme over a Rayleigh fading channel using RS codes.

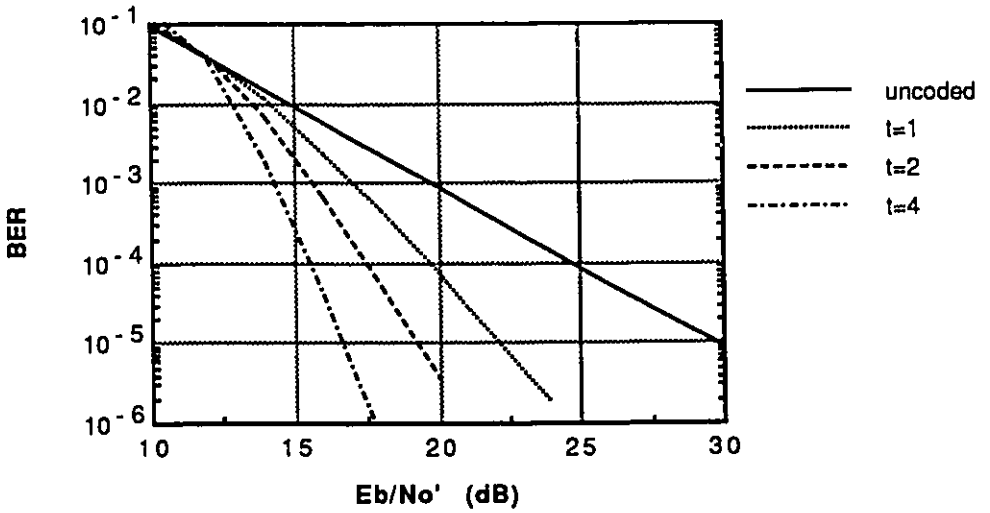

Figure 6.14 : BER performance for the MT(15, 3, 5) scheme over a Rayleigh fading channel using RS codes.

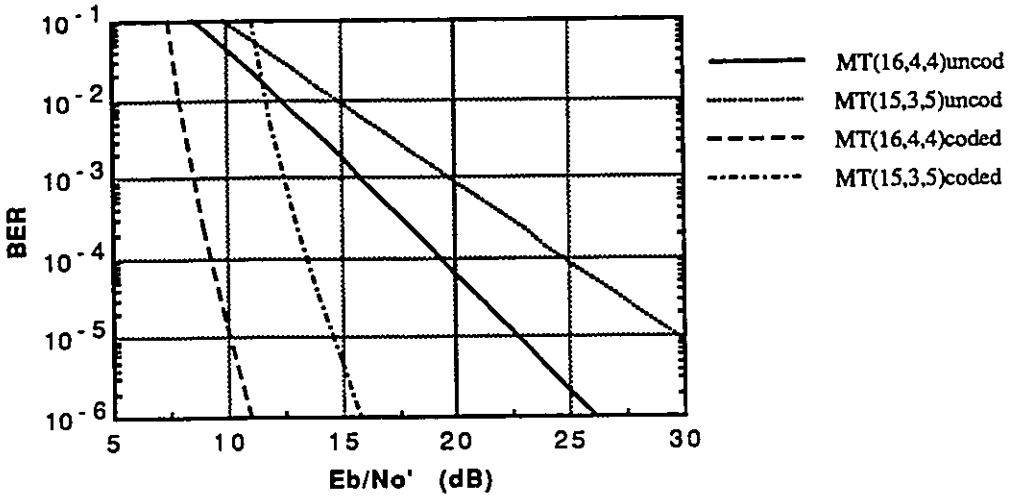

Figure 6.15 : BER performance for the MT(15, 3, 5) and MT(16, 4, 4) schemes over a Rayleigh fading channel using dual-k codes.

6.8 Simulation of MT-FSK/DS-CDMA

The simulation of the MT-FSK/DS-CDMA is based on the MFSK simulation model described in Chapter 5. For a given scheme, the correspondence between the input data and the transmitted frequency tones can be easily set up. For instance, a table look-up can be use for this mapping. The channel is divided into v independent subchannels. The w simultaneously transmitted frequency tones pass through w independent or correlated subchannels. In the receiver, the v detected outputs are square-law combined to form b decision variables. The largest of the b decision variables is chosen as the final output. When making the decision, a table look-up decoding method can be used.

For the simulation, the MAI is not considered. The symbol error rate is found for a given γ_b. So it is purely a narrowband system simulation. The simulation results for the MT(15,3,5) scheme in an AWGN and Rayleigh fading channels are shown in Fig. 6.16.

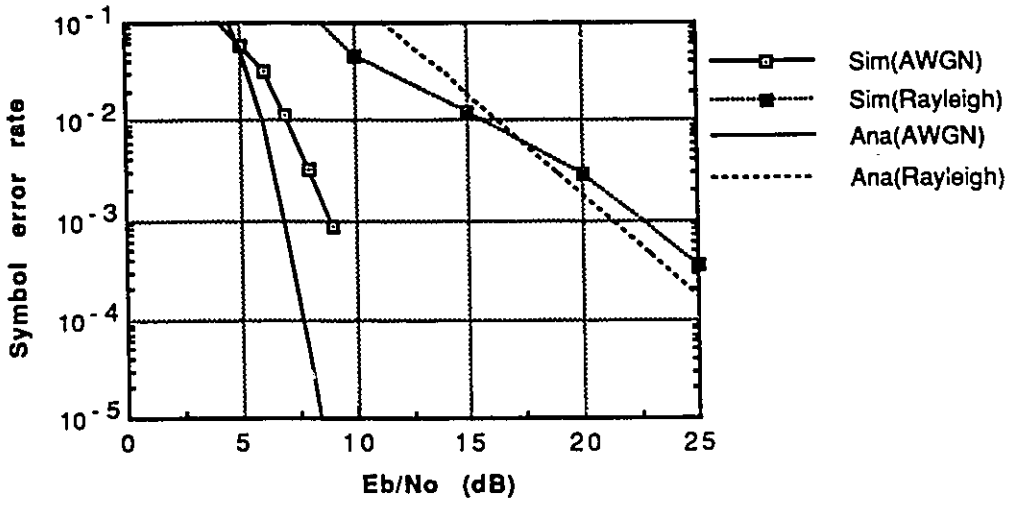

Figure 6.16 : Simulation of the symbol error rate for the MT(15,3,5) scheme over AWGN and Rayleigh fading channels.

6.9 Summary

In this chapter, we applied the concept of permutation modulation to the DS-CDMA system. The resultant system MT-FSK/DS-CDMA was evaluated over AWGN, Rayleigh and Rician fading channels. In the CDMA system, the bandwidth efficiency is only slightly increased by increasing v and k, since the performance is dominated by the required bit energy to the effective noise spectral density ratio. There is a great difference between the performance over AWGN and over Rayleigh fading channels. In an AWGN channel, the performance depends much on the parameters v and k; while in a Rayleigh fading channel, it depends more on the parameter w, which introduces $w-1$ order diversity. In a frequency selective fading channel, by properly choosing the parameters of the MT-FSK or OMT-FSK schemes, diversity advantage can be fully utilized.

The implementation complexity of the MT-FSK/DS-CDMA is proportional to the parameters v and w. We proposed the OMT-FSK/DS-CDMA scheme to reduce the

complexity. We analyzed the reduction factor of the parameters v. FEC coding has been considered for the performance improvement. A simulation for a MT-FSK/DS-CDMA scheme has also been discussed.

Chapter 7

Conclusions and Suggestions for Future Research

7.1 Conclusions

In this thesis, we studied three system concepts for the DS-CDMA applications. Under each concept, we developed specific schemes. The performance of the proposed schemes were analyzed over AWGN and fading channels. FEC coding was also considered. To confirm the analysis, Monte Carlo simulations were conducted for selected schemes. In this section, we summarize the main contributions of each proposed system and make comparisons among various DS-CDMA schemes.

For the system performance, the main focus is on the BER performance and the bandwidth efficiency. In a DS-CDMA system, power and bandwidth efficiencies are closely related. The bandwidth efficiency is determined by the required bit energy to the effective noise spectral density ratio. In the extreme case when the bit energy to the Gaussian noise spectral density ratio is very large, the asymptotic bandwidth efficiency is inversely proportional to the bit energy to effective noise spectral density ratio. Thus, finding a bandwidth efficient system is equivalent to finding an energy efficient system. If a modulation scheme is energy efficient and can be used in direct-sequence spread spectrum, then the resultant DS-CDMA system will be bandwidth efficient. This is a fundamental guideline for designing bandwidth efficient DS-CDMA schemes.

The first system concept which was discussed in Chapter 3 is the application

of combined modulation schemes in a DS-CDMA application. Under this concept, we proposed MFSK-MPSK/DS-CDMA and MFSK-DMPSK/DS-CDMA schemes. In fact, this system concept may find more general applications. The MFSK-OC/DS-CDMA scheme can be viewed as a DS-CDMA system using the combination of MFSK and orthogonal code modulation. The orthogonal code concept can be also combined with MFSK-MPSK/DS-CDMA and MT-FSK/DS-CDMA. In general, the three independent systems discussed in three chapters can be combined to form a new system. The basic goal of this combination is to obtain a powerful modulation scheme.

The second concept which was discussed in Chapter 4 is orthogonal coding. Orthogonal codes have already been studied in the literature, but not for a MFSK/DS-CDMA system. In this thesis it is shown that by using orthogonal codes the number of frequency tones of an MFSK/DS-CDMA system can be reduced, yielding a system with less complexity. Furthermore, the analyses performed show that the condition of ideal code orthogonality can be partially relaxed without causing adverse effects. Thus, quasi-orthogonal codes can be used in practical applications. It is found in this thesis that the orthogonal coding concept has many significant applications in both performance improvement and complexity reduction in DS-CDMA system.

The third system concept discussed in Chapter 6 is the application of permutation of modulation to a DS-CDMA system. By using the MT-FSK scheme, we proposed the MT-FSK/DS-CDMA. In a fading channel, this system introduces an implicit diversity, and thus is robust in a mobile environment. By using a simple frequency tone selection rule by which all the symbols are orthogonal to each other, we further proposed a novel scheme, namely OMT-FSK/DS-CDMA. By using the concept of orthogonal coding, the implementation complexity is greatly reduced.

In all the proposed schemes, noncoherent MFSK is used as the basic signalling scheme. In fact, all the three proposed systems (MFSK-MPSK/DS-CDMA, MFSK-OC/DS-CDMA and MT-FSK/DS-CDMA) treat MFSK/DS-CDMA as a special case. The reason lies in the power efficiency of MFSK. Based on this condition, all the system concepts can be properly combined.

In Table 7.1, the asymptotic bandwidth efficiency of some selected schemes over an AWGN channel at BER of 10^{-3} and 10^{-5} is given. For a fair comparison, we choose

a number of frequency tones around 16. The conventional DS-CDMA schemes using BPSK, DBPSK and MFSK are also listed in the table as references. At a BER of 10^{-3} without FEC coding, the MFSK-MPSK scheme with $M_f = 16$ and $M_p = 4$ achieves the best performance. The asymptotic bandwidth efficiency is 0.56 b/s/Hz. The 16FSK-DBPSK is in the second place with the asymptotic bandwidth efficiency of 0.46 b/s/Hz. At a BER of 10^{-5}, the two values are reduced to 0.35 b/s/Hz and 0.29 b/s/Hz respectively. Other uncoded schemes are slightly worse. Three FEC coded examples are also given in the table. Due to the advantage of soft decision decoding, the MT-FSK(16, 4, 4) using dual-4 code achieves bandwidth efficiencies of 0.81 b/s/Hz and 0.7 b/s/Hz for a BER of 10^{-3} and 10^{-5} respectively.

Table 7.1 : The required SNR per bit and the asymptotic bandwidth efficiency of various schemes over an AWGN channel. The entry is γ_b'/η_∞, with γ_b' in dB and η_∞ in b/s/Hz.

DS-CDMA schemes	BER=10^{-3}	BER=10^{-5}
BPSK	6.8/0.31	9.6/0.16
DBPSK	7.9/0.24	10.4/0.14
16FSK	6.0/0.38	8.0/0.24
16FSK-4PSK	4.3/0.56	6.3/0.35
16FSK-DBPSK	5.1/0.46	7.1/0.29
16FSK-OC($M_c = 2$)	5.4/0.43	7.3/0.28
MT-FSK (16,4,4)	7.6/0.26	9.2/0.18
MT-FSK (15,3,5)	6.5/0.34	8.1/0.23
OMT-FSK (16,4)	10.0/0.15	11.8/0.10
16FSK-DBPSK, RS(n=31, t=4)	4.3/0.56	5.3/0.44
MT-FSK (16,4,4), RS(n=15, t=2)	7.2/0.29	8.1/0.23
MT-FSK (16,4,4), dual-4	2.7/0.81	3.3/0.70

In Table 7.2, the same schemes are considered over a Rician fading channel with $\kappa = 10$ dB. At a BER of 10^{-3}, the 16FSK-4PSK gives the best result. However, the difference among various schemes is very small. At a BER of 10^{-5}, due to the diversity gain, the MT(16,4,4) scheme performs the best. For coded case, MT-FSK(16, 4, 4) using dual-4 code gives the best performance.

The performance over a Rayleigh fading channel is shown in Table 7.3. In this

Table 7.2 : The required SNR per bit and the asymptotic bandwidth efficiency of various schemes over a Rician fading channel (κ = 10 dB). The entry is γ_b'/η_∞, with γ_b' in dB and η_∞ in b/s/Hz.

DS-CDMA schemes	BER=10^{-3}	BER=10^{-5}
BPSK	10.2/0.14	17.4/0.027
DBPSK	11.2/0.11	18.8/0.020
16FSK	9.9/0.15	17.6/0.026
16FSK-4PSK	12.1/0.095	21.5/0.011
16FSK-DBPSK	8.9/0.19	16.4/0.034
16FSK-OC ($M_c = 2$)	9.2/0.18	17.4/0.027
MT-FSK (16,4,4)	10.0/0.15	13.0/0.075
MT-FSK (15,3,5)	10.0/0.15	14.0/0.060
OMT-FSK (16,4)	10.5/0.13	13.1/0.073
16FSK-DBPSK, RS(n=31, t=4)	7.4/0.27	14.0/0.060
MT-FSK (16,4,4), RS(n=15, t=2)	9.1/0.18	10.3/0.14
MT-FSK (16,4,4), dual-4	7.3/0.28	8.7/0.20

Table 7.3 : The required SNR per bit and the asymptotic bandwidtl. efficiency of various schemes over a Rayleigh fading channel. The entry is γ_b'/η_∞, with γ_b' in dB and η_∞ in b/s/Hz.

DS-CDMA scheme	BER=10^{-3}	BER=10^{-5}
BPSK	24.0/0.0060	44.0/0.00006
DBPSK	27.0/0.0030	47.0/0.00003
16FSK	26.5/0.0034	46.5/0.00003
16FSK-4PSK	33.1/0.0007	53.3/0.000007
16FSK-DBPSK	25.9/0.0037	45.9/0.00004
16FSK-OC($M_c = 2$)	23.2/0.0072	43.2/0.00007
MT-FSK (16,4,4)	15.9/0.039	22.7/0.0081
MT-FSK (15,3,5)	19.3/0.018	29.3/0.0018
OMT-FSK (16,4)	15.0/0.047	20.2/0.014
16FSK-DBPSK, RS(n=31, t=4)	14.0/0.060	18.8/0.020
MT-FSK (16,4,4), RS(n=15, t=2)	13.1/0.073	15.7/0.040
MT-FSK (16,4,4), dual-4	9.1/0.18	11.2/0.11

case, all the uncoded schemes perform very poorly. The permutation modulation schemes, due to their implicit diversity, achieve a better performance. Among the three permutation modulation schemes, the OMT-FSK(16,4) has a equivalent diversity of 4 and thus performs the best. At a BER of 10^{-3}, however, the asymptotic bandwidth efficiency is only 0.047 b/s/Hz. By employing FEC coding, the performance is improved significantly. The best scheme is the MT-FSK(16,4,4) using dual-k codes with soft decision decoding. At a BER of 10^{-3}, an efficiency of 0.18 b/s/Hz is achieved. Thus, in a Rayleigh fading environment, the combination of FEC coding and the permutation modulation schemes offers a powerful system.

7.2 Suggestions for Future Research

The suggestions for future research are listed below.

- A system which judiciously combines the three systems studied in this thesis is expected to be more powerful. Furthermore, other modulation schemes may also be considered jointly with the systems proposed in this thesis. The orthogonal codes may be beneficial in keeping the complexity of the combined system at a manageable level. The analysis of such systems, including the modem and codec structures may be fruitful.

- We have a great interests in applying the proposed schemes discussed in this thesis to practical mobile satellite and/or cellular radio systems. In that case, system structure, channel situation and implementation should be more strictly examined. For this consideration, MT-FSK/DS-CDMA and OMT-FSK/DS-CDMA are highly recommended.

- In chapter 3, we proposed the MFSK-DPSK/DS-CDMA. Furthermore, multiple symbol differential detection (MSDD) [101, 102, 102] can be applied. The MSDD is more powerful than the conventional one, and can be considered as one of the combining component in a DS-CDMA system. However, in either the MFSK-DPSK/DS-CDMA or the proposed new scheme, FEC decoding uses

only hard decision decoding which results in a worse performance than soft decision decoding. Whether soft decision decoding is feasible in this case remains to be answered.

- In the DS-CDMA applications, FEC is a very important means to enhance the system performance. For the multi-ary CDMA systems, more powerful nonbinary coding techniques (e.g., using concatenated codes) can be employed to further increase the system bandwidth efficiency.

- In MFSK-OC/DS-CDMA system, the application of the orthogonal codes is limited by the cross-correlation consideration. Polyphase sequences can be employed to extend this limitation.

- We assumed a perfect power control in this thesis. In a practical situation, however, the power control is a critical issue. An accuracy of ± 1.5 dB is reported to be implementable [103]. In order to work in a practical environment, the proposed system can be analyzed in a non-perfect power control situation.

Appendix A

Performance of DPSK and MFSK over a Frequency Non-selective Slow Rician Fading Channel

In this thesis, we need the BER expressions of DPSK and MFSK in several places. In this appendix, the BER expressions of DPSK and MFSK over a frequency non-selective slow Rician fading channel are reviewed. For clarification, a simple derivation is presented.

In the receiver, the received signal can be expressed as

$$r = s\rho + n \tag{A.1}$$

where ρ represents fading, whose pdf is given by (2.12). The BER performance of DPSK over an AWGN channel is

$$p_b(\rho) = \frac{1}{2}e^{-\gamma_b\rho^2}, \tag{A.2}$$

where ρ is a constant value representing the channel attenuation. In a Rician fading channel, the BER can be obtained by averaging $p(\rho)$ over the Rician fading variable

ρ. We have

$$\begin{aligned} P_{\text{DPSK}} &= \int_0^\infty p_b(\rho)p(\rho)\mathrm{d}\rho \\ &= \int_0^\infty \tfrac{\rho}{2\sigma^2}\exp[-\tfrac{\rho^2+2\sigma^2\gamma_b\rho^2+s^2}{2\sigma^2}]I_0\left(\tfrac{\rho s}{\sigma^2}\right)\mathrm{d}\rho \\ &= \int_0^\infty \tfrac{\rho}{2\sigma^2}\exp[-\tfrac{\rho^2+s_1^2-s_1^2}{2\sigma_1^2}-\tfrac{s^2}{2\sigma^2}]I_0\left(\tfrac{\rho s_1}{\sigma_1^2}\right)\mathrm{d}\rho \\ &= \tfrac{\sigma_1^2}{2\sigma^2}\exp[-\tfrac{s^2}{2\sigma^2}+\tfrac{s_1^2}{2\sigma_1^2}]\int_0^\infty \tfrac{\rho}{\sigma_1^2}\exp[-\tfrac{\rho^2+s_1^2}{2\sigma_1^2}]I_0\left(\tfrac{\rho s_1}{\sigma_1^2}\right)\mathrm{d}\rho \\ &= \tfrac{\sigma_1^2}{2\sigma^2}\exp[-\tfrac{s^2}{2\sigma^2}+\tfrac{s_1^2}{2\sigma_1^2}]. \end{aligned} \tag{A.3}$$

In the above equation, $p(\rho)$ is given in (2.12), and

$$\sigma_1^2 \triangleq \frac{\sigma^2}{1+2\gamma_b\sigma^2}, \tag{A.4}$$

$$s_1 \triangleq \frac{\sigma_1^2 s}{\sigma^2} = \frac{s}{1+2\gamma_b\sigma^2}. \tag{A.5}$$

By comparing (2.12) and (2.13), we have

$$\sigma^2 = \frac{1}{2(1+\kappa)}, \tag{A.6}$$

and

$$s^2 = \frac{\kappa}{1+\kappa}. \tag{A.7}$$

Substituting the results into (A.3), we have

$$P_{\text{DPSK}} = \frac{1+\kappa}{2\bar{\gamma}_b+2(1+\kappa)}\exp\left[-\frac{\kappa\bar{\gamma}_b}{\bar{\gamma}_b+(1+\kappa)}\right], \tag{A.8}$$

where $\bar{\gamma}_b = \gamma_b \mathrm{E}\{\rho^2\}$.

The symbol error rate of MFSK over an AWGN channel is

$$p_s(\rho) = \sum_{n=1}^{M-1}(-1)^{n+1}\binom{M-1}{n}\frac{1}{n+1}\exp\left[-\frac{n\gamma_s\rho^2}{n+1}\right]. \tag{A.9}$$

By similar derivation as for DPSK, one obtains the symbol error rate of noncoherent MFSK over Rician fading channel as

$$P_{\text{MFSK}} = \sum_{n=1}^{M-1}(-1)^{n+1}\binom{M-1}{n}\frac{1+\kappa}{n\bar{\gamma}_s+(n+1)(1+\kappa)}\exp\left[-\frac{\kappa n\bar{\gamma}_s}{n\bar{\gamma}_s+(n+1)(1+\kappa)}\right]. \tag{A.10}$$

For coherent PSK, there is no close form for the BER performance over Rician fading channel. The BER performance can be expressed as

$$P_{\text{PSK}} = \int_0^\infty \frac{1}{2}\text{erfc}\left(\sqrt{\gamma_b\rho^2}\right) 2\rho(1+\kappa)\exp[-\kappa-\rho^2(1+\kappa)] I_0\left(2\rho\sqrt{\kappa(1+\kappa)}\right) \mathrm{d}\rho. \quad \text{(A.11)}$$

An upper bound is [70]

$$P_{\text{PSK}} \leq \frac{1+\kappa}{1+\kappa+\bar{\gamma}_b}\exp\left(-\frac{\kappa\bar{\gamma}_b}{1+\kappa+\bar{\gamma}_b}\right). \quad \text{(A.12)}$$

Appendix B

Gaussian Approximations for the MAI

In this thesis, asynchronous CDMA systems using random signature sequences are considered. For the performance analysis, the MAI component is approximated as a Gaussian noise. In literature, there are two Gaussian approximations for the MAI in a BPSK/DS-CDMA system. The first one is proposed by Pursley [41] and called standard Gaussian approximation. Under this approximation, the bit error rate of BPSK/DS-CDMA is expressed as

$$P_b = Q\left(\sqrt{2\gamma_b'}\right) \tag{B.1}$$

where γ_b' is simply approximated by

$$\gamma_b' = \left[(\gamma_b)^{-1} + \left(\frac{3N}{2(K-1)}\right)^{-1}\right]^{-1}. \tag{B.2}$$

This approximation is simple and accurate for large K, but becomes optimistic when K is small. An improved Gaussian approximation with good accuracy is presented in [43-45] which is expressed as

$$\begin{aligned} P_b \simeq\ & \tfrac{2}{3}Q\left[\left(\tfrac{K-1}{3N} + \tfrac{N_0}{2E_b}\right)^{-1/2}\right] + \tfrac{1}{6}Q\left[\left(\tfrac{(K-1)(N/3)+\sqrt{3}\sigma}{N^2} + \tfrac{N_0}{2E_b}\right)^{-1/2}\right] \\ & + \tfrac{1}{6}Q\left[\left(\tfrac{(K-1)(N/3)-\sqrt{3}\sigma}{N^2} + \tfrac{N_0}{2E_b}\right)^{-1/2}\right], \end{aligned} \tag{B.3}$$

where

$$\sigma^2 = (K-1)\left[N^2\frac{23}{360} + N\left(\frac{1}{20} + \frac{K-2}{36}\right) - \frac{1}{20} - \frac{K-2}{36}\right]. \tag{B.4}$$

It was shown in [43] that the improved Gaussian approximation is located in between the upper and lower bound BER curves. However, this improved Gaussian approximation is more complex. Whenever possible, the standard Gaussian approximation is preferred. Now we explore the effectiveness of the standard Gaussian approximation in our analyses.

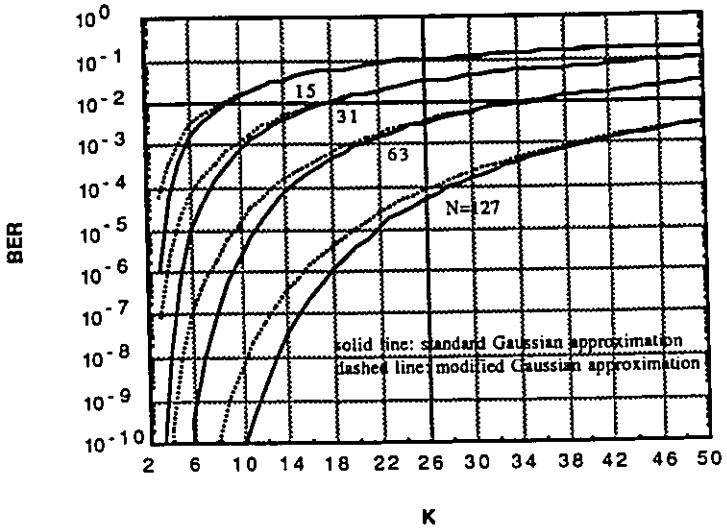

Figure B.1 : Comparison of standard and modified Gaussian approximations for PSK/DS-CDMA with $E_b/N_0 = 100$ dB.

In Fig. B.1 and Fig. B.2, the BER performance of PSK/DS-CDMA is plotted using two Gaussian approximations for $E_b/N_0 = 100$ dB and $E_b/N_0 = 10$ dB respectively. In these figures, the BER performance obtained by improved Gaussian approximation is used as a reference. In Fig. B.1, E_b/N_0 is very large, the BER is dominated by the MAI. For small values of K, the standard Gaussian approximation gives optimistic results. For large values of K, the two approximations agree with each other well. We also notice that the two approximations match better for small values of N than for large values of N. However, one should note that for a large value of N, greater number of simultaneous transmissions can be accommodated.

In Fig. B.2, the BER is dominated by E_b/N_0. There is not much difference between

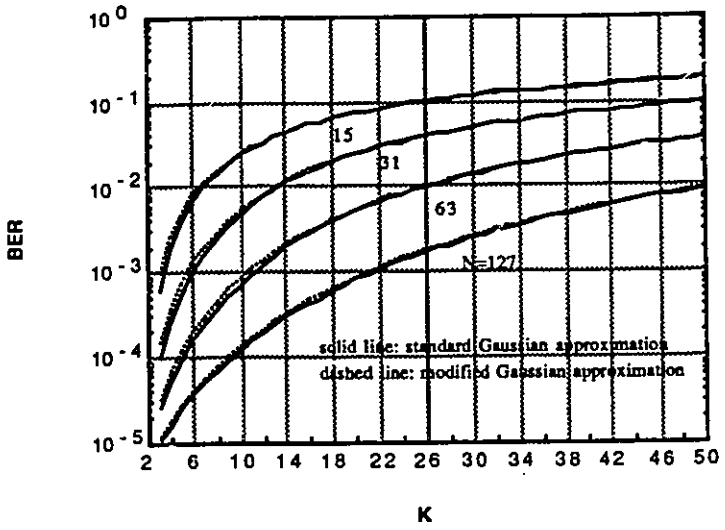

Figure B.2 : Comparison of standard and modified Gaussian approximations for PSK/DS-CDMA with $E_b/N_0 = 10$ dB.

the two approximations.

Table B.1 : Comparison of two Gaussian approximations for $E_b/N_0 = 100$ dB.

	$K = 5$	$K = 10$	$K = 15$	$K = 20$	$K = 25$	$K = 30$
$N = 15$	0.693	0.107	0.011	0-.009	-0.013	-0.014
$N = 31$	0.958	0.405	0.139	0.050	0.017	0.004
$N = 63$	1.000	0.829	0.458	0.235	0.126	0.070
$N = 127$	1.000	0.993	0.870	0.630	0.420	0.278

In Tables B.1 and B.2, we list the relative error of using the standard Gaussian approximation for $E_b/N_0 = 100$ dB and $E_b/N_0 = 10$ dB respectively. The relative error is defined as

$$\epsilon = \frac{P_e(\text{imp}) - P_e(\text{std})}{P_e(\text{mod})}, \tag{B.5}$$

where $P_e(\text{imp})$ is the BER performance obtained using improved Gaussian approximation, and $P_e(\text{std})$ is the BER performance obtained using standard Gaussian ap-

Table B.2 : Comparison of two Gaussian approximations for E_b/N_0 = 10 dB.

	$K=5$	$K=10$	$K=15$	$K=20$	$K=25$	$K=30$
$N=15$	0.207	0.034	-0.002	-0.010	-0.012	-0.012
$N=31$	0.261	0.100	0.039	0.014	0.003	-0.002
$N=63$	0.213	0.138	0.082	0.049	0.030	0.018
$N=127$	0.116	0.115	0.092	0.071	0.054	0.041

proximation. In these tables, the negative values mean that the P_e(std) is larger than P_e(imp). In Table B.1, the relative error for $N = 15$, $K = 10$ is 0.1 which is acceptable. For large N, the relative error becomes large. For $N = 127$, in order for the error to be less than 0.3 (still a good approximation), the value of K needs to be larger than 30. We can make an estimation of the efficiency for this case. Using (2.10), we have

$$\eta = \frac{KR_b}{W} = \frac{K}{N} = \frac{30}{127} \simeq 0.24 \quad \text{b/s/Hz.} \tag{B.6}$$

Thus, if a bandwidth efficiency of 0.24 can be achieved, the relative error of using the standard Gaussian approximation is less than 0.3.

In Table B.2, all the relative errors are very small. This is because of the small E_b/N_0.

From the above discussion, we see that the standard Gaussian approximation gives a few tenths of relative errors for moderate values of bandwidth efficiency. For practical situations when E_b/N_0 is not infinite, the standard Gaussian approximation is accurate even for small K. Thus, it is valid to use the simple standard Gaussian approximation in this thesis. Although the discussion is for the PSK/DS-CDMA system, it is valid for other DS-CDMA systems using MFSK modulations due to the similar derivation for the BER performance.

Appendix C

Derivation for the Variance of the MAI Component

In Chapter 4, a detailed analysis is performed for the MFSK-OC/DS-CDMA system. In this appendix, an expression for the variance of the MAI component is derived.

The MAI from the kth user ($k \neq i$) is

$$\begin{aligned}
I_k &= \int_0^{T_s} u^{(k)}_{m_f^{(k)},m_c^{(k)}}(t-\tau_k)u^{(i)*}_{m_f^{(i)},m_c^{(i)}}(t)dt \\
&= \int_0^{T_s} \sqrt{2P}\Psi(t-\tau_k)a_{k,m_c^{(k)}}(t-\tau_k)\exp[j2\pi d_{k,m_f^{(k)}}(t-\tau_k)\Delta + j\theta_k(t-\tau_k)] \\
&\quad \sqrt{2P}\Psi(t)a_{i,m_c^{(i)}}(t)\exp[j2\pi d_{i,m_f^{(i)}}\Delta]\mathrm{d}t \\
&= 2P\int_0^{\tau_k} \Psi(t-\tau_k)a_{k,m_c^{(k)}}(t-\tau_k)\exp[j2\pi d^{(1)}_{k,m_f^{(k)}}(t-\tau_k)\Delta + j\theta_k(t-\tau_{k_1})] \\
&\quad \Psi(t)a_{i,m_c^{(i)}}(t)\exp[j2\pi d_{i,m_f^{(i)}}\Delta]\mathrm{d}t \\
&\quad +2P\int_{\tau_k}^{T_s} \Psi(t-\tau_k)a_{k,m_c^{(k)}}(t-\tau_k)\exp[j2\pi d^{(2)}_{k,m_f^{(k)}}(t-\tau_k)\Delta + j\theta_{k_2}(t-\tau_k)] \\
&\quad \Psi(t)a_{i,m_c^{(i)}}(t)\exp[j2\pi d_{i,m_f^{(i)}}\Delta]\mathrm{d}t \\
&= 2P\int_0^{\tau_k} \delta(d^{(1)}_{k,m_f^{(k)}}, d_{i,m_f^{(i)}})e^{j\theta_{k_1}}\Psi(t-\tau_k)a_{k,m_c^{(k)}}(t-\tau_k)\Psi(t)a_{i,m_c^{(i)}}(t)\mathrm{d}t \\
&\quad +2P\int_{\tau_k}^{T_s} \delta(d^{(2)}_{k,m_f^{(k)}}, d_{i,m_f^{(i)}})e^{j\theta_{k_2}}\Psi(t-\tau_k)a_{k,m_c^{(k)}}(t-\tau_k)\Psi(t)a_{i,m_c^{(i)}}(t)\mathrm{d}t \\
&= 2P\delta(d^{(1)}_{k,m_f}, d_{i,m_f^{(i)}})e^{j\theta_{k_1}}R_{k,i}(\tau_k) + 2P\delta(d^{(2)}_{k,m_f^{(k)}}, d_{i,m_f^{(i)}})e^{j\theta_{k_2}}\hat{R}_{k,i}(\tau_k).
\end{aligned} \tag{C.1}$$

The division of the integral into two parts can be visualized in Fig. C.1.

In the above equation, the continuous-time partial crosscorrelation function $R_{k,i}$ and $\hat{R}_{k,i}$ are given in terms of the discrete aperiodic crosscorrelation function $C_{k,i}$ for

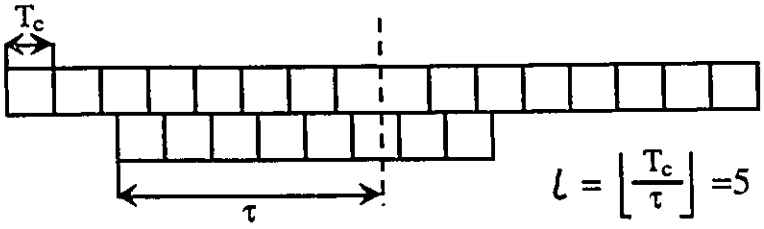

Figure C.1 : Illustration of the correlation between two PN codes.

the kth and the ith sequences by [33]

$$R_{k,i}(\tau) = C_{k,i}(l-N)\hat{R}_\psi(\tau - lT_c) + C_{k,i}(l+1-N)R_\psi(\tau - lT_c) \tag{C.2}$$

and

$$\hat{R}_{k,i}(\tau) = C_{k,i}(l)\hat{R}_\psi(\tau - lT_c) + C_{k,i}(l+1)R_\psi(\tau - lT_c) \tag{C.3}$$

respectively, where $l = \lfloor \tau/T_c \rfloor$ (the integer part of τ/T_c), and $R_\psi(s)$ and $\hat{R}_\psi(s)$ (the partial autocorrelation functions of the chip waveform) are defined as $\hat{R}_\psi(s) = \int_s^{T_c} \psi(t)\psi(t-s)\mathrm{d}t$ and $R_\psi(s) = \hat{R}_\psi(T_c - s)$. The discrete aperiodic crosscorrelation function $C_{k,i}$ is defined by

$$C_{k,i}(l) = \begin{cases} \sum_{j=0}^{L-1-l} a_j^{(k)} a_{j+l}^{(i)}, & 0 \le l \le L-1, \\ \sum_{j=0}^{L-1+l} a_j^{(k)} a_{j-l}^{(i)}, & 1-L \le l \le 0, \\ 0, & |l| \ge L. \end{cases} \tag{C.4}$$

From symmetry and randomness of the PN sequences, I_k has a zero mean. Its

variance is [30]

$$\begin{aligned}
\sigma_I^2 &= \mathrm{E}\{I_k^2\} \\
&= \mathrm{E}\{(2E_sT_s^{-1})^2[\delta(d^{(1)}_{k,m_f^{(k)}}, d_{i,m_f^{(i)}})e^{j\theta_{k_1}}R_{k,i}(\tau_k) + \delta(d^{(2)}_{k,m_f^{(k)}}, d_{i,m_f^{(i)}})e^{j\theta_{k_2}}\hat{R}_{k,i}(\tau_k)] \\
&\quad [\delta(d^{(1)}_{k,m_f^{(k)}}, d_{i,m_f^{(i)}})e^{j\theta_{k_1}}R_{k,i}(\tau_k) + \delta(d^{(2)}_{k,m_f^{(i)}}, d_{i,m_f^{(i)}})e^{j\theta_{k_2}}\hat{R}_{k,i}(\tau_k)]^*\} \\
&= (2E_sT_s^{-1})^2\mathrm{E}[\delta(d^{(1)}_{k,m_f^{(k)}}, d_{i,m_f^{(i)}})R^2(\tau_k) + \delta(d^{(2)}_{k,m_f^{(k)}}, d_{i,m_f^{(i)}})\hat{R}^2(\tau_k) \\
&\quad +\delta(d^{(1)}_{k,m_f^{(k)}}, d_{i,m_f^{(i)}})\delta(d^{(2)}_{k,m_f^{(k)}}, d_{i,m_f^{(i)}})R(\tau_k)\hat{R}(\tau_k)(e^{j(\theta_{k_1}-\theta_{k_2})} + e^{-j(\theta_{k_1}-\theta_{k_2})})] \\
&= (2E_sT_s^{-1})^2\mathrm{E}[\tfrac{1}{M_f}R^2(\tau_k) + \tfrac{1}{M_f}\hat{R}^2(\tau_k) + \tfrac{1}{M_f^2}R(\tau_k)\hat{R}(\tau_k)e^{j\theta_{1,2}}] \\
&= (2E_sT_s^{-1})^2\tfrac{1}{M_fT_s}\int_0^{T_s}[R^2 + \hat{R}^2 + \tfrac{2}{M_f}R\hat{R}]d\tau.
\end{aligned} \tag{C.5}$$

In the above equation, the expectation is over $m_f^{(k)}$, θ_{k_1}, θ_{k_2}, and τ. Using the result of [30]

$$\mathrm{E}\{C_{k,i}(l)C_{k,i}(m)\} = \begin{cases} N-|l| & l=m, \\ 0 & l\neq m, \end{cases} \tag{C.6}$$

one has

$$\begin{aligned}
\int_0^{T_s} R^2(\tau)\mathrm{d}\tau &= \int_0^{T_s}[C(l-N)\hat{R}_\Psi(\tau-lT_s) + C(l+1-N)R_\Psi(\tau-lT_s)]^2\mathrm{d}\tau \\
&= \int_0^{T_s}[C^2(l-N)\hat{R}_\Psi^2(\tau-lT_s) + C^2(l+1-N)R_\Psi^2(\tau-lT_s) \\
&\quad +2C(l-N)C(l+1-N)\hat{R}_\Psi(\tau-lT_s)R_\Psi(\tau-lT_s)]\mathrm{d}\tau \\
&= \sum_{l=0}^{N-1}C^2(l-N)\int_0^{T_c}\hat{R}_\Psi^2(\tau)\mathrm{d}\tau + \sum_{l=0}^{N-1}C^2(l+1-N)\int_0^{T_c}R_\Psi^2(\tau)\mathrm{d}\tau \\
&= \tfrac{T_c^3}{3}\left[\sum_{l=0}^{N-1}C^2(l-N) + \sum_{l=0}^{N-1}C^2(l+1-N)\right] \\
&= \tfrac{T_c^3}{3}\left[\sum_{l=0}^{N-1}l + \sum_{l=0}^{N-1}(l+1)\right] \\
&= \tfrac{T_c^3}{3}\left[\tfrac{l(l-1)}{2} + \tfrac{l(l+1)}{2}\right] \\
&= \tfrac{N^2T_c^3}{6}.
\end{aligned} \tag{C.7}$$

Similarly we have

$$\int_0^{T_s}\hat{R}^2(\tau)\mathrm{d}\tau = \frac{N^2T_c^3}{6}, \tag{C.8}$$

and

$$\int_0^{T_s}R(\tau)\hat{R}(\tau)\mathrm{d}\tau = 0. \tag{C.9}$$

Then

$$E\{I_k^2\} = (2E_s T^{-1})^2 \frac{1}{M_f} T_s \left(2\frac{N^2 T_c^3}{6}\right) = \frac{(2E_s)^2}{3M_f N}. \tag{C.10}$$

In the above derivation, a rectangular chip waveform is assumed, and thus $\int_0^{T_c} \hat{R}_\Psi^2(\tau)\mathrm{d}\tau = \int_0^{T_c} R_\Psi^2(\tau)\mathrm{d}\tau = T_c^3/3$.

Appendix D

An Alternative Analysis Method for MFSK/DS-CDMA System

In Section 4.3.2, a detailed analysis for the probability of error of MFSK-OC/DS-CDMA systems is presented. For the case of ideal orthogonal codes, the result is the same as for MFSK/DS-CDMA systems. In the analysis, the MAI component is approximated as a Gaussian random variable. By finding the variance of this random variable, the variance of the effective noise (thermal noise plus MAI) can be obtained. Then the following analysis is similar to that of MFSK modulation scheme. In finding the variance of the MAI, the formal variance taking operation is performed, and the signal phase $(0 - 2\pi)$, time delay $(0 - T_c)$, and the PN chips $(0 - N)$ are averaged.

An alternative analysis for MFSK/DS-CDMA system is given by Ha [32]. The MAI is also considered as Gaussian noise. Ha mentioned that MAI components can be made to approximate white noise by properly choosing the spacing between adjacent frequency tones Δf and the chip rate R_c. We have $\Delta f = \rho R_c$. The selection of parameter ρ is done such that the signal spectrum is nearly flat. In an example given in [32], ρ is chosen as $22/15 \simeq 1.47$. The total bandwidth is $W = (M-1) + 2R_c$.

Since an individual frequency tone from an interfering user is spread twice by two different asynchronous PN sequences at the receiver, the power spectral density of the interfering signal is determined by the convolution of the densities of the two PN sequences. This density at frequency f_j is [32]

$$S_j(f) = \frac{PR_c}{4R_c^2 + \pi^2(f - f_j)^2}, \tag{D.1}$$

where $P = E_b R_b$ is carrier power. Since there are $(K-1)$ interferering users, each transmitting any of the M symbols with equal probability, the total power spectral density of $(K-1)$ interfering users plus AWGN of density $N_0/2$ is

$$S(f) = \frac{N_0}{2} + \frac{kPR_c}{M} \sum_{j=1}^{M} \frac{1}{4R_c^2 + \pi^2 (f - f_j)^2}. \tag{D.2}$$

The effective noise density at frequency f_i is

$$N_{oi} = N_o + \frac{2(K-1)E_b R_b R_c}{M} \sum_{j=1}^{M} \frac{1}{4R_p^2 + (\pi \Delta f)^2 (i-j)^2}. \tag{D.3}$$

Based on the above results, we did further analysis in [71]. By averaging N_{oi} the noise density is obtained as:

$$N_o' = N_o + \frac{2(K-1)E_b R_b R_c}{M^2} \sum_{i=1}^{M} \sum_{j=1}^{M} \frac{1}{4R_c^2 + (\pi \Delta f)^2 (i-j)^2}. \tag{D.4}$$

The required bit energy to noise density ratio is:

$$\frac{E_b}{N_o'} = \frac{\frac{E_b}{N_o}}{1 + \frac{E_b}{N_o} \frac{K-1}{W/\rho R_b} \sigma(M, \rho)} \tag{D.5}$$

where

$$\sigma(M, \rho) \triangleq \frac{W}{\rho R_b} \frac{2R_b R_p}{M^2} \sum_{i=1}^{M} \sum_{j=1}^{M} \frac{1}{4R_p^2 + (\pi \Delta f)^2 (i-j)^2}, \tag{D.6}$$

Since $\Delta f = \rho R_c$, and $W = M \Delta f = M \rho R_c$, one obtains:

$$\sigma(M, \rho) = \frac{2}{M} \sum_{i=1}^{M} \sum_{j=1}^{M} \frac{1}{4 + (\pi \rho)^2 (i-j)^2}. \tag{D.7}$$

The number of simultaneous users is:

$$K = \frac{W}{R_b} \frac{\frac{E_b}{N_o} - \frac{E_b}{N_o'}}{\rho \frac{E_b}{N_o} \frac{E_b}{N_o'} \sigma(M, \rho)} + 1 \simeq \frac{W}{R_b} \frac{\frac{E_b}{N_o} - \frac{E_b}{N_o'}}{\rho \frac{E_b}{N_o} \frac{E_b}{N_o'} \sigma(M, \rho)} \quad (\text{for } K \gg 1). \tag{D.8}$$

The system capacity is:

$$\eta = \frac{KR_b}{W} = \frac{\frac{E_b}{N_o} - \frac{E_b}{N_o'}}{\rho \frac{E_b}{N_o} \frac{E_b}{N_o'} \sigma(M, \rho)} \quad (\text{b/s/Hz}). \tag{D.9}$$

The parameter $\sigma(M,\rho)$ is a function of M and ρ, and is tabulated in Table 3 for M=8, 16 and 32 and $\rho = 1.5$. The asymptotic capacity is

$$\eta_\infty = \frac{1}{\rho E_b/N_0' \sigma(M,\rho)}. \tag{D.10}$$

The asymptotic capacity η_∞ for MFSK/DS-CDMA as a function of BER is given in Table 4.

Table D.1 : Parameter $\sigma(M,\rho)$ as a function of M for $\rho = 1.5$.

M	8	16	32
$\sigma(M,\rho)$	0.69	0.72	0.74

Table D.2 : Asymptotic capacity η_∞ (in b/s/Hz) as a function of BER for MFSK/DS-CDMA.

BER	10^{-3}	10^{-5}
M=8	0.197	0.114
M=16	0.233	0.143
M=32	0.260	0.172

Comparing (D.9) with (4.34), we see that these two expressions are similar. The coefficient $1/(\rho\sigma(M,\rho))$ in (D.9) has a value of 1, which is smaller than the coefficient 1.5 in (4.34). However, in (D.9), the effect of filter and spectrum shaping has been included, while in (4.34), an ideal filter was assumed. If choosing a raise cosine filter with $\alpha = 1.5$, the same results would be expected.

Appendix E

Probability of Error of Nonbinary Codes for Orthogonal Nonbinary Modulation Schemes over Fading Channels

In this section, we give the derivation of the performance of nonbinary FEC coding over fading channels. The results were referred to in Chapters 4 and 6.

In an M-ary orthogonal modulation system, the equivalent lowpass transmitted signal is $u_m(t)$, $m = 1, 2, \cdots, M$. The equivalent lowpass received signal is

$$r_m(t) = \alpha_m e^{-j\phi_m} u_m(t) + z(t), \quad m = 1, 2, \cdots, M, \tag{E.1}$$

where the attenuation factor α_m and the phase shift ϕ_m are introduced in the channel, and $z(t)$ is the equivalent lowpass noise. The optimum noncoherent demodulator computes the decision variable

$$y_m = \left| \int_0^T r_m(t) u_m(t) \mathrm{d}t \right|, \quad m = 1, 2, \cdots, M. \tag{E.2}$$

Assuming that $u_1(t)$ is transmitted, then

$$y_1 = \left| 2\alpha_1 E_s + N_1 \right|, \tag{E.3}$$

and

$$y_m = \left| N_m \right|, \quad m \neq 1. \tag{E.4}$$

We have

$$\mathrm{E}\{y_1\} = 2\alpha_1 E_s, \tag{E.5}$$

$$\mathrm{E}\{y_m\} = 0, \quad m \neq 1, \tag{E.6}$$

and

$$\sigma_m^2 = \mathrm{Var}\{y_m\} = 2E_s N_0, \quad m = 1, 2, \cdots, M. \tag{E.7}$$

Block Codes

First consider soft decision decoding. For noncoherent detector, square-law combining is used. For an $(n,\ k)$ M-ary code, there are q^k $(q = \log_2(M))$ code words. The corresponding q^k decision variables are

$$U_i = \sum_{j=1}^{n} \left[\delta(c_{ij}, 0)y_{0j}^2 + \cdots + \delta(c_{ij}, M-1)y_{(M-1)j}^2\right], \quad i = 1,\ 2,\ \cdots,\ q^k. \tag{E.8}$$

where $c_{ij} \in [0,\ 1,\ \cdots,\ M-1]$ is the jth code symbol of the ith code word, and y_{lj} $(l = c_{ij})$ is the receiver output corresponding to c_{ij}.

Assume that an all "0" code word C_1 is transmitted. The corresponding decision variable is given by (E.8) with $c_{1j} = 0$ for all j. The pairwise error probability, i.e., the probability that a decision is made in favor of the mth code word $(m \neq 1)$ is

$$P_2 = P\{U_m > U_1\} = P\{U_1 - U_m < 0\} = P\left\{\sum_{j=1}^{w_m}\left(y_{0j}^2 - y_{c_{mj},j}^2\right) < 0\right\}, \tag{E.9}$$

where w_m is the number of symbols in which C_1 and C_m differ (Hamming distance in binary case), and $c_{mj} \in [1, 2, \cdots, M-1]$. We have $\mathrm{E}\{y_{l,j}\} = 2E_s\rho$ and $\sigma_{y_{l,j}}^2 = 2E_s N_0$ for $j = 1, \cdots, w_m$. From the above expression, P_2 is equal to the probability of error for square-law combining of binary orthogonal FSK with w_m-order diversity [75]

$$\begin{aligned} P_2(m) = &\ p^{w_m} \sum_{k=1}^{w_m - 1} \binom{w_m - 1 + k}{k} (1-p)^k \\ \leq &\ p^{w_m} \sum_{k=1}^{w_m - 1} \binom{w_m - 1 + k}{k} = \binom{2w_m - 1}{w_m} p^{w_m}, \end{aligned} \tag{E.10}$$

where p is the pairwise symbol error probability for the uncoded system.

The probability of symbol error is bounded as

$$P_M \leq \sum_{m=2}^{q^k} P_2(m) \leq \frac{1}{(2+\bar{\gamma}_s)^{w_m}} \sum_{m=2}^{q^k} \left(\begin{array}{c} 2w_m - 1 \\ w_m \end{array} \right). \tag{E.11}$$

The bit error probability is

$$P_b = \frac{2^{k-1}}{2^k - 1} P_s. \tag{E.12}$$

For hard decision decoding, the probability of error in this case is

$$P_s = \frac{1}{n} \sum_{i=t+1}^{n} i \left(\begin{array}{c} n \\ i \end{array} \right) p^i (1-p)^{n-i}, \tag{E.13}$$

where t is the error correcting ability of the code, and p is probability of error of uncoded system.

Convolutional Codes

We assume that all "0" code sequence is transmitted as a reference. Corresponding to another possible sequence with distance d (from the reference sequence), the pairwise probability of error is similar to the block code case

$$P_2(d) = p^d \sum_{k=1}^{d-1} \left(\begin{array}{c} d-1+k \\ k \end{array} \right) (1-p)^k, \tag{E.14}$$

where p pairwise symbol probability of error for the uncoded system. The distance property can be found from the transfer function $T(X, D)$

$$\left. \frac{dT(X,D)}{dX} \right|_{X=1} = \sum_{d=1}^{\infty} \beta_d D^d. \tag{E.15}$$

The probability of symbol error is upper bounded by

$$P_s \leq \sum_{d=d_{free}}^{\infty} \beta_d P_2(d). \tag{E.16}$$

The probability of bit error is given by (E.12).

For hard decision decoding, (E.16) holds. The pairwise probability of error is

$$P_2 = \begin{cases} \displaystyle\sum_{k=(d+1)/2}^{d} \left(\begin{array}{c} d \\ k \end{array} \right) p^k (1-p)^{d-k}, & (d \text{ even}), \\ \displaystyle\sum_{k=d/2-1}^{d} \left(\begin{array}{c} d \\ k \end{array} \right) p^k (1-p)^{d-k}, & (d \text{ odd}). \end{cases} \tag{E.17}$$

In the equation, p is given by (4.77) with the average symbol energy to equivalent noise spectral density ratio given in (4.74). Again the bit error probability is given by (E.12).

Appendix F

Incomplete Balanced Block Design

In combinatorial theory [98], one important problem is concerned with the arrangements of objects into a specified number of sets based on some specified rules. This is called *incidence system* or *tactical configuration.* The *incomplete balanced block design* (BIB design) is a special kind of incidence system. It is identified by five parameters (v, b, r, w, λ)[1].

The definition of the BIB design is [98]

> "A BIB design is an arrangement of v distinct objects into b blocks such that each block contains exactly w distinct objects, each object occurs in exactly r different blocks, and every pair of distinct objects occurs together in exactly λ blocks."

There are two elementary relations among these parameters,

$$bw = vr; \tag{F.1}$$

$$\lambda(v-1) = r(w-1). \tag{F.2}$$

The first counts the total number of incidences in two ways, each of b blocks containing w objects and each of v objects being contained in r blocks. The second counts the occurrences of pairs containing a particular object a_1. The object a_1 occurs in r

[1]In textbooks, the conventional expression of the five parameters is (v, b, r, k, λ). In Chapter 5, k is chosen as the number of information bits per symbol. So we use w for k in the five parameters, as is done in [92].

blocks, and in each of these is a pair with the $w-1$ remaining objects, while on the other hand, a_1 is paired λ times with each of the remaining $v-1$ objects.

An example is given below for (7, 7, 3, 3, 1):

block-1: 1, 2, 4

block-2: 2, 3, 5

block-3: 3, 4, 6

block-4: 4, 5, 7

block-5: 5, 6, 1

block-6: 6, 7, 2

block-7: 7, 1, 3

In the MT-FSK scheme, we refer to the object as a frequency tone, and the block as a selection of w frequency tones. Only $\lambda = 1$ is considered. From (F.1) and (F.2), b and r can be found as

$$b = \lambda \frac{v(v-1)}{w(w-1)} = \frac{v(v-1)}{w(w-1)}; \tag{F.3}$$

$$r = \lambda \frac{v-1}{w-1} = \frac{v-1}{w-1}. \tag{F.4}$$

If two blocks have no common object, they are orthogonal. For any block B, the whole set of blocks can be partitioned into 3 disjoint subsets,

- B,
- $X_0(B)$, containing all orthogonal blocks to B,
- $X_1(B)$, containing all non-orthogonal blocks to B (intersecting to B on a single object).

The number of blocks in the subsets $X_0(B)$ and $X_1(B)$ are given by

$$x_1 = w(r-1) = \frac{w}{w-1}(v-w); \tag{F.5}$$

$$x_0 = w(r-1) = b - x_1 - 1. \tag{F.6}$$

Appendix G

Derivation of the Probability of Error for MT-FSK over a Rician Fading Channel

In [92], the performance of MT-FSK scheme over AWGN and Rayleigh fading channels are derived. In this appendix, we derive the performance over a Rician fading channel. As mentioned in Chapter 6, the channel is assumed to be frequency selective, but each frequency tone experiences independent flat fading.

As discussed in Section 6.4, the pairwise error probability is

$$P_2(\bar{\gamma}_s', L) = \int_0^\infty P_2(\gamma_s', L) p(\rho) \mathrm{d}\rho, \tag{G.1}$$

where $P_2(\gamma_s', L)$ is the pairwise error probability in an AWGN channel given in (6.5)

$$P_2(\gamma_b', L) = \frac{e^{-\gamma_c' \rho^2/2}}{2^{2L-1}} \sum_{n=0}^{L-1} \frac{1}{n!} \left(\frac{\gamma_c' \rho^2}{2} \right)^n \sum_{r=0}^{L-1-n} \binom{2L-1}{r}, \tag{G.2}$$

and ρ has a generalized Rician the distribution ofgeneralized

$$p(\rho) = \frac{\rho^L}{\sigma^2 s^{L-1}} \exp\left(-\frac{\rho^2 + s^2}{2\sigma^2} \right) I_{L-1}\left(\frac{\rho s}{\sigma^2} \right). \tag{G.3}$$

In (G.2), we have replaced $k\gamma_b'$ with $\bar{\gamma_c}'\rho^2$. In general, we have

$$\gamma_c' = \gamma_{c1}' \rho_i^2, \tag{G.4}$$

where we use γ_{c1}' for the unfaded signal energy per channel to noise ratio. Then

$$\bar{\gamma_c}' = \gamma_{c1}' \mathrm{E}\{\rho_i^2\}. \tag{G.5}$$

For the Rician distribution, we have $\mathrm{E}\{\rho_i^2\} = s^2 + 2\sigma^2$ [75]. Substituting s^2 and σ^2 from (A.6) and (A.7), we have $\mathrm{E}\{\rho_i^2\} = 1$. Thus, $\bar{\gamma_c}' = \gamma_{c1}'$, and $k\gamma_b' = \bar{\gamma_c}'\rho^2$.

The equation (G.1) is expanded as

$$\begin{aligned} P_2(\bar{\gamma_b}', L) &= \frac{1}{2^{2L-1}} \sum_{n=0}^{L-1} \frac{1}{n!} \sum_{r=0}^{L-1-n} \binom{2L-1}{r} \int_0^\infty e^{-\bar{\gamma_c}'\rho^2/2} \left(\frac{\bar{\gamma_c}'\rho^2}{2}\right) p(\rho) \mathrm{d}\rho \\ &\triangleq \frac{1}{2^{2L-1}} \sum_{n=0}^{L-1} \frac{1}{n!} \sum_{r=0}^{L-1-n} \binom{2L-1}{r} \mathcal{I}. \end{aligned} \tag{G.6}$$

The term c is evaluated below

$$\begin{aligned} \mathcal{I} &= \left(\frac{\bar{\gamma_c}'}{2}\right)^n \int_0^\infty e^{-\bar{\gamma_c}'\rho^2/2} \rho^{2n} \frac{\rho^L}{\sigma^2 s^{L-1}} \exp\left(-\frac{\rho^2+s^2}{2\sigma^2}\right) I_{L-1}\left(\frac{\rho s}{\sigma^2}\right) \mathrm{d}\rho \\ &= \left(\frac{\bar{\gamma_c}'}{2}\right)^n \int_0^\infty \rho^{2n} \frac{\rho^L}{\sigma^2 s^{L-1}} \exp\left(-\frac{\rho^2(1+\sigma^2\bar{\gamma_c}')+s^2}{2\sigma^2}\right) I_{L-1}\left(\frac{\rho s}{\sigma^2}\right) \mathrm{d}\rho. \end{aligned} \tag{G.7}$$

By defining the following variables

$$\sigma_1^2 \triangleq \frac{\sigma^2}{1+\sigma^2\bar{\gamma_c}'}, \tag{G.8}$$

$$s_1 \triangleq \frac{\sigma_1^2}{\sigma^2} s = \frac{s}{1+\sigma^2\bar{\gamma_c}'}, \tag{G.9}$$

$\mathcal{I}$ becomes

$$\begin{aligned} \mathcal{I} &= \left(\frac{\bar{\gamma_c}'}{2}\right)^n \exp\left(-\frac{s^2}{2\sigma^2} + \frac{s_1^2}{2\sigma_1^2}\right) \int_0^\infty \rho^{2n} \frac{\rho^L}{\sigma^2 s^{L-1}} \exp\left(-\frac{\rho^2+s_1^2}{2\sigma_1^2}\right) I_{L-1}\left(\frac{\rho s_1}{\sigma_1^2}\right) \mathrm{d}\rho \\ &= \left(\frac{\bar{\gamma_c}'}{2}\right)^n \exp\left(-\frac{s^2}{2\sigma^2} + \frac{s_1^2}{2\sigma_1^2}\right) \frac{\sigma_1^2 s_1^{L-1}}{\sigma^2 s^{L-1}} \int_0^\infty \rho^{2n} \frac{\rho^L}{\sigma_1^2 s_1^{L-1}} \exp\left(-\frac{\rho^2+s_1^2}{2\sigma_1^2}\right) I_{L-1}\left(\frac{\rho s_1}{\sigma_1^2}\right) \mathrm{d}\rho \\ &= \left(\frac{\bar{\gamma_c}'}{2}\right)^n \exp\left[-\frac{s^2}{2\sigma^2}\left(1 - \frac{1}{1+\sigma^2\bar{\gamma_c}'}\right)\right] \frac{1}{(1+\sigma^2\bar{\gamma_c}')^L} \mathrm{E}\{\rho^{2n}\}, \end{aligned} \tag{G.10}$$

where $\mathrm{E}\{\rho^{2n}\}$ is the $2n$th moment of ρ given by [75]

$$\mathrm{E}\{\rho^{2n}\} = (2\sigma^2)^n \exp\left(-\frac{s_1^2}{2\sigma_1^2}\right) \frac{(L+n-1)!}{(L-1)!} \, {}_1F_1\left(L+n, L; \frac{s_1^2}{2\sigma_1^2}\right). \tag{G.11}$$

The confluent hypergeometric function ${}_1F_1(a, b; x)$ is given by

$${}_1F_1\left(L+n, L; \frac{s_1^2}{2\sigma_1^2}\right) = \sum_{k=0}^{\infty} \frac{(L+n+k-1)!(L-1)!}{(L+n-1)!(L+k-1)!k!} \left(\frac{s_1^2}{2\sigma_1^2}\right)^k. \tag{G.12}$$

This function can be evaluated using some available computer programs.

Using (A.6) and (A.7), the pairwise probability of error can be expressed in term of Rician parameter κ:

$$P_2(\bar{\gamma_b}', L) = \frac{1}{2^{2L-1}(L-1)!\left(1+\frac{\bar{\gamma_c}'}{2(1+\kappa)}\right)^L} \exp\left[-\frac{L\kappa\bar{\gamma_c}'+2(1+\kappa)L\kappa}{2(1+\kappa)+\bar{\gamma_c}'}\right] \sum_{n=0}^{L-1}\sum_{r=0}^{L-1-n} \frac{(L+n-1)!}{n!}\left[\frac{\bar{\gamma_c}'}{2(1+\kappa)+\bar{\gamma_c}'}\right]^n \binom{2L-1}{r} {}_1F_1\left(L+n, L; \frac{L\kappa}{1+\frac{\bar{\gamma_c}'}{2(1+\kappa)}}\right). \quad \text{(G.13)}$$

Bibliography

[1] K.G. Johannsen, "Code division multiple access versus frequency division multiple access capacity in mobile satellite communication," *IEEE Trans. Veh. Technol.*, vol. VT-39, pp. 17-26, Feb. 1990.

[2] K.S. Gilhousen, I.M. Jacobs, R. Padovani, and L.A. Weaver, Jr., "Increased capacity using CDMA for mobile satellite communication," *IEEE J. Select. Areas Commun.*, vol. SAC-8, pp.503-5144, May 1990.

[3] A. Yongaçoğlu, R.G. Lyons, and B.A. Mazur, "Comparison of FDMA and CDMA for second generation land-mobile satellite communications," in *Proc. of the second Int. Mobile Satellite Conf.*, Ottawa, Canada, June 1990, pp. 639-644.

[4] W.C.Y. Lee, "Overview of cellular CDMA," *IEEE Trans. Veh. Technol.*, vol. VT-40, pp. 291-302, May 1991.

[5] K.S. Gilhousen, I.M. Jacobs, R. Padovani, A.J. Viterbi, L.A. Weaver, Jr., and C.E. Wheatley, "On the capacity of a cellular CDMA system," *IEEE Trans. Veh. Technol.*, vol. VT-40, pp. 303-312, May 1991.

[6] K. Raith and J. Uddenfeldt, "Capacity of digital cellular TDMA systems," *IEEE Trans. Veh. Technol.*, vol. VT-40, pp. 323-332, May 1991.

[7] D.J. Goodman, "Second generation wireless information networks," *IEEE Trans. Veh. Technol.*, vol. VT-40, pp. 366-374, May 1991.

[8] ——, "Cellular packet communications," *IEEE Trans. Commun.*, vol. COM-38, pp. 1272-1280, Aug. 1990.

[9] R. Steele, "Deploying personal communication networks," *IEEE Commun. Mag.*, vol. 28, pp. 12-15, Sept. 1990.

[10] D.C. Cox, "Personal communications – a viewpoint," *IEEE Commun. Mag.*, vol. 28, p. 8-22, Nov. 1990.

[11] ——, "A radio system proposal for widespread low-power tetherless communication," *IEEE Trans. Commun.*, vol. COM-39, pp. 324-335, Feb. 1991.

[12] A.J. Viterbi, "Wireless digital communication: a view based on three lessons learned," *IEEE Commun. Mag.*, vol. 29, pp. 33-36, Sept. 1991.

[13] R.L. Pickholtz, L.B. Milstein, and D.L. Schilling, "Spread spectrum for mobile communications," *IEEE Trans. Veh. Technol.*, vol. VT-40, pp. 313-322, May 1991.

[14] D.L. Schilling, L.B. Milstein, R.L. Pickholtz, M. Kullback, and F. Miller, "Spread spectrum for commercial communications," *IEEE Commun. Mag.*, vol. 29, pp. 66-79, Apr. 1991.

[15] *Special Report on WARC'92. IEEE Spectrum*, Feb. 1992.

[16] *Special Issue on Telecommunications Regulation. IEEE Commun. Mag.*, vol. 30, June 1992.

[17] A. Polydoros, "Physical, link-access and topological aspects on slotted-ALOHA packet-Switched, code-division random-access networks," in *Proc. of Spread Spectrum Workshop*, Montebello, Canada, May 1991. pp. 3.1.11-3.1.3.

[18] A. Polydoros and J. Silvester, "Slotted random access spread-spectrum networks: an analytical framework," *IEEE J. Select. Areas Commun.*, vol. SAC-5, pp. 989-1002, July 1987.

[19] M.B. Pursley, "The role of spread spectrum in packet radio networks," *Proceedings of the IEEE*, vol. 75, pp. 116-134, Jan. 1987.

[20] A.J. Viterbi, *Principles of Coherent Communication.* New York: McGraw-Hill, 1966.

[21] K.S. Shanmugam, *Digital and Analog Communication Systems.* New York: John Wiley & Sons, 1979.

[22] C.A. French and W.A. Gardner, "Spread-spectrum despreading without the code," *IEEE Trans. Commun.*, vol. COM-34, pp. 404-407, April 1986.

[23] M.K. Simon, J.K. Omura, R.A. Scholtz, and B.K. Levitt, *Spread Spectrum Communications*, Volume I, II, III. Rockville, MD: Computer Sciences, 1985.

[24] G.L. Turin, "Introduction to spread-spectrum antimultipath techniques and their application to urban digital radio," *Proc. IEEE*, vol.68, pp. 328-353, Mar. 1980.

[25] C. D'Amours, J. Wang, A. Yongaçoğlu and M. Moher, "Differential and pilot symbol-aided detection of DS-CDMA in frequency-selective Rayleigh fading channels," 16th Biennial Symposium on Communications, Kingston, Canada, May 27-29, 1992.

[26] A.J. Viterbi, "Spread spectrum communications – myths and realities," *IEEE Commun. Mag.*, vol. 17, pp. 11-18, May 1979.

[27] E. A. Geraniotis, "Performance of coherent direct-sequence spread-spectrum communications over specular multipath fading channels," *IEEE Trans. Commun.*, vol. COM-33, pp. 502-508, June 1985.

[28] E. A. Geraniotis, "Performance of noncoherent direct-sequence spread-spectrum communications over specular multipath fading channels,". *IEEE Trans. Commun.*, vol. COM-34, pp. 219-226, Mar. 1986.

[29] B. Sanderford, Jr., "New market emerge as PCN reduces wireless link costs," *IEEE Commun. Mag.*, vol. 30, pp. 28-32, June 1992.

[30] E. A. Geraniotis, "Performance of Noncoherent Direct Sequence Direct-Sequence Multiple-Access Communications," *IEEE J. Select. Areas Commun.*, vol. SAC-3, pp. 687-694, Sept. 1985.

[31] E. A. Geraniotis, "Direct-Sequence Spread-Spectrum Multiple-Access Communications over Nonselective and Frequency-Selective Rician Fading Channels," *IEEE Trans. Commun.*, vol. COM-34, pp. 756-764, Aug. 1986.

[32] T.T. Ha, *Digital Satellite Communications*. New York: Macmillan, 1986.

[33] E. A. Geraniotis and M. B. Pursley, "Error Probability for Direct-sequence Spread-spectrum Multiple-Access Communication—Part II: Approximations," *IEEE Trans. Commun.*, vol. COM-30, pp. 985-995, May 1982.

[34] E. A. Geraniotis and B. Ghaffari, "Performance of binary and quaternary direct-sequence spread-spectrum multiple-access with random signature sequences," *IEEE Trans. Commun.*, vol. COM-39, pp. 713-724, May 1991.

[35] K. Yao, "Error probability of asynchronous spread spectrum multiple access communication systems," *IEEE Trans. Commun.*, vol. COM-25, pp. 803-809, Aug. 1977.

[36] D. Laforgia, A. Luvision, and V. Zinalelli, "Bit error rate evaluation for spread-spectrum multiple-access systems," *IEEE Trans. Commun.*, vol. COM-32, pp. 660-669, June 1984.

[37] M. Kavehrad, "Performance of nondiversity receivers for spread-spectrum in indoor wireless communications," *Bell Syst. Tech. J.*, vol. 64, pp. 1181-1211, July-Aug. 1985.

[38] M. B. Pursley, D.V. Sarwate, and W.E. Stark, "Error probability for direct-sequence spread-spectrum multiple-access communications – Part I: upper and lower bounds," *IEEE Trans. Commun.*, vol. COM-30, pp. 975-984, May 1982.

[39] L.S. Lehnert and M. B. Pursley, "Error probability for binary direct-sequence spread-spectrum multiple-access communications with random signature sequences," *IEEE Trans. Commun.*, vol. COM-35, pp. 87-98, Jan. 1987.

[40] N. Nazari and R.E. Ziemer, "Computationally efficient bounds for the performance of direct-sequence spread-spectrum multiple-access communications systems in jamming environments," *IEEE Trans. Commun.*, vol. COM-36, pp. 577-587, May 1987.

[41] M. B. Pursley, "Performance Evaluation for Phase-Coded Spread-Spectrum Multiple-Access Communication—Part I: System Analysis," *IEEE Trans. Commun.*, vol. COM-25, pp. 795-799, August 1977.

[42] A.J. Viterbi, "When Not to Spread Spectrum – a Sequel," *IEEE Commun. Mag.*, vol. 23, pp. 12-17, April 1985.

[43] R.K. Morrow, Jr. and J.S. Lehnert, "Bit-to-bit error dependence in slotted DS/SSMA packet systems with random signature sequences," *IEEE Trans. Commun.*, vol. COM-37, pp. 1052-1061, Oct. 1989.

[44] R.K. Morrow, Jr. and J.S. Lehnert, "Packet throughput in slotted ALOHA DS/SSMA radio systems with random signature sequences," *IEEE Trans. Commun.*, vol. COM-40, pp. 1223-1230, July 1992.

[45] J.M. Holtzman, "A simple method to calculate spread-spectrum multiple-access error probabilities," *IEEE Trans. Commun.*, vol. COM-40, pp. 461-464, March 1992.

[46] M. Kavehrad and P.J. McLane, "Performance of low-complexity channel coding and diversity for spread spectrum in indoor, wireless communications," *Bell Syst. Tech. J.*, vol. 64, pp. 1927-1965, Oct. 1985.

[47] D.V. Sarwate and M.B. Pursley, "Correlation properties of pseudorandom and related sequences," *Proc. IEEE*, vol.68, pp. 593-605, May 1980.

[48] D.J. Torrieri, "Performance of direct-sequence systems with long pseudonoise sequences," *IEEE J. Select. Areas Commun.*, vol. SAC-10, pp. 770-781, May 1992.

[49] D.C Chu, "Polyphase codes with good periodic correlation properties," *IEEE Trans. Inform. Theory*, vol. IT-18, pp. 531-532, July, 1972.

[50] R.L. Frank and S. Zadoff, "Phase shift codes with good periodic correlation properties," *IEEE Trans. Inform. Theory*, vol. IT-8, pp. 381-382, 1962.

[51] D.V. Sarwate, "Bounds on crosscorrelation and autocorrelation of sequences," *IEEE Trans. Inform. Theory*, vol. IT-25, pp. 720-724, Nov. 1979.

[52] A.W. Lam and F.M. Ozluturk, "Performance bounds for DS/SSMA communications with complex signature sequences," *IEEE Trans. Commun.*, vol. COM-40, pp. 1607-1614, Oct. 1992.

[53] R.S. Lunayach, "Performance of a direct sequence spread-spectrum system with long period and short period code sequences," *IEEE Trans. Commun.*, vol. COM-31, pp. 412-419, Mar. 1983.

[54] R.E. Ziemer and R.L. Peterson, *Digital communications and Spread Spectrum Systems*, New York: Macmillan Publishing Company, 1985.

[55] J.S. Lehnert, "Serial MSK spread-spectrum multiple-access communications," *IEEE Trans. Commun.*, vol. COM-40, pp. 1119-1127, June 1992.

[56] M.B. Pursley and H.F.A. Roefs, "Numerical evaluation of correlation parameters for optical phase of binary shift-register sequences," *IEEE Trans. Commun.*, vol. COM-27, pp. 1597-1604, Oct. 1979.

[57] B. Aazhang, B-P Paris, and G.C. Orsak, "Neural networks for multiuser detection in CDMA communications," *IEEE Trans. Commun.*, vol. COM-40, pp. 1212-1222, July 1992.

[58] M. Schwartz, *Telecommunication Networks: Protocols, Modeling and Analysis*, Addison-Wesley Publishing Company, Reading, MA, USA, 1987.

[59] W. Stallings, *Data and Computer Communications*, Macmillan Publishing Company, New York, USA, 1988.

[60] D.H. Davis and S.A. Gronemeyer, "Performance of slotted ALOHA random access with delay capture and randomized time of arrival," *IEEE Trans. Commun.*, vol. COM-28, pp. 703-710, May 1980.

[61] D. Raychaudhuri, "Performance analysis of random access packet switched code division multiple access systems," *IEEE Trans. Commun.*, vol. COM-29, pp. 895-901, June 1981.

[62] E.S. Sousa and J.A. Silvester, "Spreading code protocols for distributed spread spectrum packet radio networks," *IEEE Trans. Commun.*, vol. COM-36, pp. 272-281, May 1988.

[63] J.S. Storey and F.A. Tobagi, "Throughput performance of an unslotted direct sequence SSMA packet radio network," *IEEE Trans. Commun.*, vol. COM-37, pp. 814-823, Aug. 1989.

[64] J.N. Daigle, "Throughput in asynchronous CDMA systems," in *Proc. of INFOCOM.* 1987, pp. 1079-1089.

[65] M. Schwartz, *Information Transmission, Modulation and Noise*, third ed., McGraw-Hill Book Company, New York, 1980.

[66] K. Feher, *Digital Communications - Satellite/Earth Station Engineering*, Prentice-Hall Inc., Englewood Cliffs, USA, 1985.

[67] A.A.M. Saleh and R.A. Valenzuela, "A statistical model for indoor multipath propagation," *IEEE J. Select. Areas Commun.*, vol. SAC-5, pp. 138-146, Feb. 1987.

[68] T.S Rappaport and C.D. McGillem, "UFH fading in factories," *IEEE J. Select. Areas Commun.*, vol. SAC-7 pp. 40-48, Jan. 1989.

[69] T.S Rappaport, "Characterization of UFH multipath radio channels in factories building," *IEEE Trans. Antennas Propagat., vol.* 37, pp. 1058-1069, Aug. 1989.

[70] E. Biglieri, D. Divsalar, P.J. McLane and M.K. Simon, *Introduction to Trellis-Coded Modulation with Applications*, New York: Macmillan Publishing Company, 1991.

[71] J. Wang and A. Yongaçoğlu, "Capacity comparison between direct sequence PSK and MFSK spread spectrum systems in CDMA applications," in *Proc. 4th Canadian Conf. Electrical and Computer Eng.*, Quebec, Canada, Sept. 1991, pp. 53.51-4.

[72] ——, "Capacity evaluation and code acquisition consideration for MFSK/DS-SS systems," The 9th International Conference on Digital Satellite Communications, Copenhagen, Denmark, May 18-22, 1992.

[73] J. Wang and A. Yongaçoğlu, "MFSK modulated PSK direct sequence CDMA," 16th Biennial Symposium on Communications, Kingston, Canada, May 27-29, 1992.

[74] A. Papoulis, "Probability, Random Variables, and Stochastic Processes," New York: McGraw-Hill Book Company, 1984.

[75] J.G. Proakis, *Digital Communications*. McGraw-Hill, New York, 1989.

[76] M.K. Simon and A. Polydoros, "Coherent detection of frequency-hopped quadrature modulation in the presence of jamming – Part I: QPSK and QASK modulations," *IEEE Trans. Commun.*, vol. COM-29, pp. 1644-1660, Nov. 1981.

[77] J.M. Wozencraft and I.M. Jacobs, *Principles of Communication Engineering*. John Wiley & Sons, Inc., New York, 1965.

[78] R.W. Lucky, J. Salz and E.J. Weldon, *Principles of Data Communications*, New York: McGraw-Hill, 1968.

[79] S. Stein, *Communication System and techniques, Part III*, New York: McGraw-Hill, 1966.

[80] A.J. Viterbi, "Very low rate convolutional codes for maximum theoretical performance of spread-spectrum multiple-access channels," *IEEE J. Select. Areas Commun.*, vol. SAC-8, pp. 641-649, May 1990.

[81] K.H. Li and L.B. Milsyein, "On the optimum processing gain of a block-coded direct-sequence spread-spectrum system," *IEEE J. Select. Areas Commun.*, vol. SAC-7, pp. 618-626, May 1989.

[82] G.C. Clark and J.B. Cain, *Error Correcting Coding for Digital Communications.* New York: Plenum Press, 1981.

[83] W.E. Ryan and S.G. Wilson, "Two classes of convolutional codes over GF(q) for q-ary orthogonal signaling," *IEEE Trans. Commun.*, vol. COM-39, pp. 30-39, Jan. 1991.

[84] S. Lin and D.J. Costello, Jr., *Error Control Coding.* Englewood Cliffs, New Jersey: Prentice-Hall, 1983.

[85] P.K. Enge and D.V. Sarwate, "Spread-spectrum multiple-access performance of orthogonal codes: linear receivers," *IEEE Trans. Commun.*, vol. COM-35, pp. 1309-1319, Dec. 1987.

[86] K. Pahlavan and M. Chase, "Spread-spectrum multiple-access performance of orthogonal codes for indoor radio communications," *IEEE Trans. Commun.*, vol. COM-38, pp. 574-577, May 1990.

[87] A. Vardy and Y. Be'ery, "Bit-level soft-decision decoding of Reed-Solomon codes," *IEEE Trans. Commun.*, vol. COM-39, pp. 440-444, Mar. 1991.

[88] D. Slepian, "Permutation Modulation," *Proc. IEEE*, vol.53, pp. 228-236, Mar. 1965.

[89] H. L. Schneider, "Data transmission with FSK permutation modulation," *Bell Syst. Tech. J.*, vol. 47, pp. 1131-1138, July-Aug. 1969.

[90] E. Biglieri, V. Castellani and M. Pent, "Waveform transmission with permutation modulation," *Electron. Lett.*, vol. 5, pp. 149-151, Apr. 3, 1969.

[91] J.F. Pieper, J.G. Proakis, R.R. Reed and J.K Wolf, "Design of efficient coding and modulation for a Rayleigh fading channel," *IEEE Trans. Inform. Theory*, vol. IT-24, pp. 457-468, July 1978.

[92] G. E. Atkin and H. P. Corrales, "An efficient modulation/coding scheme for MFSK systems on bandwidth constrained channels," *IEEE J. Select. Areas Commun.*, vol. SAC-7, No. 9, pp. 1396-1401, Dec. 1989.

[93] ——, "Performance analysis of a multiple tone FH/MFSK spread spectrum system," *IEEE Tech. Conf. Tactical Commun.*, Fort Wayne, IN, May 1988, pp. 284-289.

[94] ——, "Performance analysis of a non-orthogonal FH/MFSK system under partial band interference," *Adv. Commun., Contr. Conf.*, Baton Rouge, LA, Oct. 1988, pp. 40-53.

[95] T.M.P. Percival, R. Boreli, R.A.Z. Simington. D.K. Kwan, and S. Reisenfeld, "A new combined modulation and multiple access scheme for VSATS," The 9th International Conference on Digital Satellite Communications, Copenhagen, Denmark, May 18-22, 1992, pp. 399-406.

[96] M. Hall, Jr., *Combinatorial Theory*. New York: Join Wiley & Son, 1986.

[97] I.F. Blake and R.C. Mullin, *The Mathematical Theory of Coding*. New York: Academic Press, 1975.

[98] F.G. McWilliams and N.J. Sloane, *The Theory of Error Correcting Codes*. Amsterdam: North-HollandPublishing Company, 1977.

[99] C. Heegard, H.E. dePedro and J.K Wolf, "Permutation codes for the Gaussian broadcast channel with two receivers," *IEEE Trans. Inform. Theory*, vol. IT-24, pp. 569-578, Sep. 1978.

[100] Stephen Wolfram, *Mathematica - A System for Doing Mathematics by Computer*. Redwood City: Addison-Wesley Publishing Company, 1988.

[101] D. Divsalar and M.K. Simon, "Multiple-symbol differential detection of MPSK," *IEEE Trans. Commun.*, vol. COM-38, Mar. 1990, pp. 300-308.

[102] D. Makrakis, A. Yongaçoğlu, and K. Feher, "Novel receiver structure for systems using differential detection," *IEEE Trans. Veh. Technol.*, vol. VT-36, May 1987, pp. 71-77.

[103] A.J. Viterbi, "Modulation and coding performance of the power-controlled direct-sequence CDMA cellular channel," in *Proc. of Spread Spectrum Workshop*, p. 1.1.1. Montebello, Canada, May 1991.